CARDIAC STRUCTURE AND MECHANISMS OF FIBRILLATION

by

Nathan Angel

A dissertation submitted to the faculty of
The University of Utah
in partial fulfillment of the requirements for the degree of

Doctor of Philosophy

Department of Bioengineering

The University of Utah

May 2016

The University of Utah Graduate School

STATEMENT OF DISSERTATION APPROVAL

The dissertation of **Nathan Angel**

has been approved by the following supervisory committee members:

Ravi Ranjan	, Chair	**January 4, 2016** Date Approved
Derek James Dosdall	, Member	**January 4, 2016** Date Approved
Robert S. MacLeod	, Member	**January 8, 2016** Date Approved
Frank Sachse	, Member	**January 5, 2016** Date Approved
Alexey V. Zaitsev	, Member	**January 5, 2016** Date Approved

and by **Patrick A. Tresco** , Chair/Dean of

the Department/College/School of **Bioengineering**

and by David B. Kieda, Dean of The Graduate School.

ABSTRACT

Fibrillation is defined as turbulent cardiac electrical activity and results in the inability of the myocardium to contract. When fibrillation occurs in the ventricles, it is known as ventricular fibrillation (VF). The consequence of VF is sudden death unless treated immediately. Fibrillation can also occur in the atria and is known as atrial fibrillation (AF). The consequences of atrial fibrillation (AF) are less immediate; however, it leads to increased risk of stroke. Despite the impact of fibrillatory arrhythmias, there are many gaps in our mechanistic knowledge of these arrhythmias. The purpose of this dissertation is to study through several projects how different cardiac substrates help initiate and/or sustain fibrillation.

The first project examined several properties of the ventricular conduction system during VF. The conduction system coordinates excitation and consequently coordinates the contraction of the ventricles. Despite the conduction system's unique structure, its role in VF remains unclear. We examined the proximal conduction system and found that it develops a more rapid activation rate than the ventricular myocardium during prolonged VF, and may be driving the arrhythmia.

The second and third projects examined the effects of fibrosis on electrical conduction to initiate and/or sustain AF. Despite fibrosis being associated with AF, it is still unknown whether it is a byproduct of an underlying heart disease and does not in itself promote AF, or if it affects the organization of conduction during fibrillation to promote AF. In the second project we studied the effect of fibrosis on conduction following different types of triggers. We found that fibrosis causes transverse conduction slowing following premature stimulation, which makes AF more likely to initiate. As AF persists, single episodes of AF last longer before the patient transitions into normal sinus rhythm, and in some cases AF can become permanent. The third project examined why some patients may never transition from AF to normal sinus rhythm. Specifically, this project found that regions of dense fibrosis anchor high-frequency activation that may be driving the arrhythmia. These studies showed that fibrosis causes conduction changes that make AF more likely to initiate and to be sustained.

CONTENTS

ACKNOWLEDGMENTS

I would like to thank all those who have assisted me in this work, in particular my primary advisors Ravi Ranjan and Derek Dosdall, Both of whom have offered great assistance with my projects and have given me opportunities to grow. I thank Dr. Derek Dosdall for taking me on as a PhD student when I first started. I thank Ravi Ranjan for agreeing to mentor me as a PhD student even after I had completed half of my PhD progress. In addition, I would like to thank all of the students and postdocs who have helped me through my graduate experience, including Josh Blauer, Josh Silveragel, Dr. Li Li, and Dr. Jungling Huo. In addition, I would like to thank the professors who have served on my doctoral program: Dr. Ranjan, Dr. Dosdall, Dr. MacLeod, Dr. Sachse, and Dr. Zaitsev. All of my committee members have given me much support and advice, which have helped me to achieve my goals of higher education.

I would also like to thank Dr. Kholmovski for his assistance with the magnetic resonance imaging. I would like to thank Layne Norlund, Orvelin Roman, and Jose Reyes for excellent technical animal support. I would also like to thank the faculty and staff of the Nora Eccles Harrison Cardiovascular Research and Training Institute (CVRTI) for allowing us to use their facilities and recording equipment to conduct studies.

Most importantly, I would like to thank my family, especially my wife Danielle, for their support and encouragement.

CHAPTER 1

INTRODUCTION

A guiding principle in physiology is that structure dictates function. This principle can be expanded to state that the function of a system cannot be completely understood until the structure is known. Cardiac electrophysiology follows this same paradigm and leads to an understanding of how different cell and tissue types within the heart have different functions, an example of which is the first examination of the heart with electron microscopy. These early studies found structural differences between cell types in the heart. Specifically, it was found that there existed a working myocardium and conductive tissue [1]. These cell types were then examined with various electrical measurements and it was found that the conductive tissue can have more rapid conduction velocities than the myocardium, and the conductive tissue has autorhythmicity, or pacemaker function [1]. Under physiological conditions, cardiac conduction is due to the formation and coordinated propagation of electrical impulses through cardiac cells. Arrhythmias are broadly referred to as disorders in cardiac impulse formation and/or impulse propagation [2]. The concept that structure dictates function has been well characterized for normal electrophysiology conditions. However, much is still unknown about the relationship between these different cells and structures in the heart, which we define as the cardiac substrate, and mechanisms of arrhythmia. The purpose of this dissertation is to utilize the structure function principle to examine the relationship between cardiac substrate and mechanisms of how arrhythmias initiate and become sustained.

The goal of understanding the relationship between structure and function with mechanisms of arrhythmia is not novel; however, the implementation has many unique challenges. Uncovering the relationship between structure and function in arrhythmia entails the development of novel imaging and electrical recording techniques as well as the development of methodology to bridge these two domains. Specifically, this dissertation has been made possible by recent advancements in noninvasive imaging, electrical recoding equipment, and signal processing techniques.

1.1 Background

Understanding the relationship between cardiac substrate and mechanisms of arrhythmia is a topic of great interest and study in cardiac electrophysiology, primarily because arrhythmia can lead to failure of the cardiovascular system [3, 4]. The focus of this dissertation is fibrillation, the most severe arrhythmia, which is defined as turbulent cardiac electrical activity whereby propagation of electrical waves through the heart is disrupted, with consequent production of wavelets, high frequency rotating waves, and inability of the myocardium to contract [5]. When fibrillation occurs in the ventricles it is known as ventricular fibrillation (VF). The consequence of VF is sudden death unless treated immediately [6]. Fibrillation can also occur in the atria and is known as atrial fibrillation (AF). The consequences of atrial fibrillation (AF) are less immediate, however it also leads to decreased life expectancy, quality of life and increased risk of stroke [7–10]. Despite the huge impact of fibrillatory arrhythmias, there are many gaps in our mechanistic knowledge of arrhythmias, and especially fibrillation, as well as many technical challenges to studying them.

Fibrillation is thought to initiate and be sustained due to alterations in normal cardiac impulse formation and impulse conduction [2]; however, much is still unknown about the role of specific substrates beyond the myocardium in causing these alterations to cardiac impulses. Most canonical theories of fibrillation (which is discussed in detail in Chapters 3.1 and 3.2) state that abnormalities in cardiac conduction within the myocardium are responsible for the turbulent electrical activity that is characteristic of fibrillation. However, great mechanistic leaps in our understanding of arrhythmia have occurred from examining the cardiac substrate beyond the myocardium. The ventricular conduction system has been shown to initiate VF with abnormal impulse formation [11, 12]. In addition, many reports suggest that the conduction system may be critical in sustaining prolonged VF [13–15]. Structures beyond the myocardium have also been shown to be critical for initiating and sustaining AF. Haissaguerre et al. found that the pulmonary veins in the left atrium are prone to ectopic activity to initiate AF [16]. Furthermore, reports have found that a fibrotic substrate during AF may cause decreased coupling between myocardial cells to increase AF stability [17]. This dissertation builds on these and other reports to suggest that the cardiac substrate may, at least in part, explain the observed electrical organizations of fibrillation. In three aims we tested the general hypothesis that specific detectable substrate abnormalities beyond the working myocardium are responsible for the initiation and organization of cardiac impulses in fibrillation. This hypothesis was tested

using multiple methods to discriminate different cardiac substrates including electrogram morphology from different forms of abnormal substrates, microscopy of histology, and novel magnetic resonance imaging (MRI) methods. The electrophysiological properties of the heart were then measured and compared directly with features of the cardiac substrate.

In the first aim of this dissertation we examined whether the proximal ventricular conduction system may facilitate sustained VF. The ventricular conduction system coordinates excitation and consequently coordinates the contraction of the ventricles. Cardiac impulse propagation begins at the sinoatrial (SA) node in the right atrium and conducts to the atrioventricular (AV) node. The ventricular conduction system is then excited by the AV node. The ventricular conduction system electrically connects the AV node to the ventricular myocardium (VM) and consists of specialized conduction cells that conduct rapidly, but do not have contractile function. One component of this system that is located at the distal end of the AV node is called the Bundle of His or His Bundle, the distal end of which is known as the Purkinje system. The His/Purkinje system consists of a network of electrically coupled cells, and is the only connection from the atria to the VM. The terminal Purkinje is one structure beyond the myocardium that has been implicated in sustaining VF, however it is unclear whether the His Bundle is involved in sustaining VF as well. The first aim of this dissertation was to determine whether the proximal ventricular conduction system may be a driver of prolonged VF.

1.1.1 Specific Aims

Aim 1 of this dissertation is to characterize how the activation rate and conduction velocity of the proximal conduction system change during the time course of VF. The hypothesis of this aim was that the proximal ventricular conduction system is a driving force during the time course of VF, and that it is not being passively driven by the VM. Most studies of VF measure only signals from the VM because canonical theories of fibrillation suggest that the VM alone can sustain the arrhythmia, which is likely true during early VF. However, growing evidence suggests that the ventricular conduction system may be critical for sustaining prolonged VF [14]. This difference in early and prolonged VF is due to many cellular changes that occur during VF that alter the electrophysiology of the heart [18,19]. Specifically, it is thought that the distal Purkinje system develops a more rapid activation rate than the VM during prolonged VF. However, it is unknown whether this activity is exclusive to the distal regions of the ventricular conduction system or whether it occurs in the proximal ventricular conduction system as well. In this aim we overcame previous

challenges to studying the ventricular conduction system, which included signals being of low amplitude, often being masked by larger ventricular signals, and having mostly unknown characteristics during VF. We overcame these challenges by applying novel signal processing techniques to directly measure the electrical activity from the ventricular conduction system.

Fibrillation in the ventricles has many similarities to fibrillation in the atria, but a primary difference between the arrhythmias is that VF is an acute arrhythmia and AF can be chronic. VF lasts only from seconds to minutes before it's either treated, becomes fatal, or very rarely self terminates. Fibrillation in the atria is not immediately fatal, and therefore this arrhythmia can persist for years, causing many electrical and structural changes to the cardiac substrate. AF has also been shown to be progressive, starting out as short lasting (paroxysmal) episodes, but eventually the arrhythmia becomes persistent or even permanent [20]. As AF progresses, it is associated with the development of a nonconductive tissue within the atrial substrate as a result of fibrosis. It is known that fibrotic tissue density increases as AF progresses and that more fibrosis is associated with a worse prognosis [21, 22]. Despite fibrosis being associated with AF, it is still unknown whether fibrosis is a byproduct of an underlying heart disease, and does not in itself promote sustained AF, or if it affects the organization of conduction during fibrillation to promote sustained AF. The next two aims in this dissertation examine how fibrotic tissue relates to conduction changes and whether fibrosis can cause increased incidence and maintenance of AF.

Past studies have found that increased levels of fibrotic tissue may increase stability of AF, allowing individual episodes to last longer; however, the mechanism is unknown and controversial [23, 24]. What is less known is whether fibrotic tissue causes conduction changes that increase the likelihood of AF onset. Although potentially similar, it is important to recognize that the mechanisms by which AF is sustained may be very different from the mechanisms that cause it to initiate. For example, for fibrillation to initiate, there must be a trigger, such as a premature atrial contraction (PAC), and the cardiac tissue must have a response that is different from normal sinus conduction to initiate the arrhythmia. A further subtlety is the differentiation between sustained and nonsustained arrhythmia that may be directly related to the cardiac substrate. Healthy hearts, i.e., hearts without a history of AF, may transiently be able to sustain AF; however, these hearts usually cannot sustain AF for longer than a few tens of seconds. In various rapid atrial paced animal models of AF it has been shown to take over one month of pacing before this arrhythmia sustains [25]. Furthermore, when AF first becomes sustained in these animal models, it is

characterized by lower activation frequencies and less turbulent electrical activity than in hearts that have experienced AF for longer durations [26, 27]. These studies suggest that healthy hearts may have compensatory mechanisms that do not allow the heart to maintain the rapid activation rate necessary to sustain the arrhythmia for longer periods of time. However, in hearts with a history of AF, the compensatory mechanisms may fail due to the presence of a fibrotic substrate, which may cause anatomical slowing or even block of conduction, to sustain the arrhythmia [24, 26, 28]. In aim 2 we examined how the structure of fibrosis relates to the onset of AF.

Aim 2 is to determine how local fibrotic tissue architecture and densities in chronic AF relate to conduction changes that facilitate reentrant activity. The hypothesis of this aim was that specific architectures of fibrotic myocardium cause conduction slowing and/or block, thus facilitating the initiation of sustained AF. Fibrotic tissue is nonconductive and therefore it likely slows conduction; however, certain architectures of fibrotic myocardium may have a more pronounced effect than others. Understanding whether certain architectures of fibrotic myocardium slow conduction is of critical importance, because slowed conduction is necessary for initiating fibrillation in all major mechanistic theories of this arrhythmia. Past reports suggest that overall fibrosis density may not be as important as the fibrotic structure for causing conduction disruptions [29, 30]. For example, a heart with large patches of fibrotic tissue may be more arrhythmogenic than a heart with homogenous diffuse fibrotic tissue [31]. Other groups have expanded on this finding to show qualitatively that large fibrotic strands may cause conduction slowing [32]. This aim built and expanded on these past reports by quantitatively measuring the structure of fibrotic myocardium and comparing this structure to conduction velocity [33]. The goal of this aim was to distinguish between diffuse fibrosis and patches or strands of fibrosis and relate the findings to arrhythmogenesis.

A major question about AF is whether specific regions of the atria are critical to sustaining the arrhythmia. Most of this research has been done by examining high-density cardiac electrical recordings to locate regions of stable high-frequency activation during persistent AF [34, 35]. There is some evidence that targeting therapy at these driving sites can result in long-term freedom from AF [36]. This evidence suggests that these local regions of high-frequency activation may be driving the entire fibrillatory behavior in the atria, and the rest of the atria may be a passive bystander subject to the high-frequency activation. There is some evidence for the spatiotemporal stability of these driving sites over the time course of AF [34, 35]. This spatiotemporal stability suggests a stable substrate,

which may anchor these driving sites to particular locations. Aim 3 examined whether fibrosis is the anchor for high-frequency activating driving sites during AF. Fibrosis is a good candidate because it is implicated in conduction slowing and block, which may be critical for formations of rapid reentrant activity [33,37,38].

Aim 3 is to evaluate the relationship between fibrotic myocardium determined by magnetic resonance imaging and local drivers of persistent AF. The hypothesis of this aim was that regions of high fibrosis create sites of rapid activations to sustain fibrillation. When AF is induced in hearts without a history of AF, it is characterized by a slow, global activation rate and broad, organized wavefronts. However, AF in hearts with a history of sustaining the arrhythmia is different, and is characterized by a much faster global activation rate and more disorganized wavefronts [26]. This disorganization of wavefronts is thought to make the arrhythmias more likely to be sustained for longer episodes [39]. Fibrosis has been implicated in causing dissociation of conduction during AF, but it is unclear whether it also may anchor regions of rapid high-frequency activity [28, 40]. A possible mechanism of how fibrosis may anchor sites of rapid high-frequency activation is that it may cause conduction slowing or block to break up broad more organized wavefronts into many disorganized wavefronts, which would result in discrete regions of rapid activation rates near regions of fibrosis. This aim combined many techniques that are traditionally used to examine the cardiac substrate and cardiac conduction in isolation, including whole-chamber electrical mapping of the atrium as well as both MRI and pathological quantification of fibrotic myocardium. By combining these techniques, a holistic examination of both cardiac substrate and organization of fibrillation could be made to link the spatial organization of fibrotic myocardium with regions that are driving AF.

In summary, the three aims to this dissertation are:

- Aim 1: Characterize how the activation rate and conduction velocity of the proximal conduction system change during the time course of VF.
- Aim 2: Determine how local fibrotic tissue architecture and densities in chronic AF relate to conduction changes that facilitate reentrant activity.
- Aim 3: Evaluate the relationship between fibrotic myocardium determined by magnetic resonance imaging and local drivers of persistent AF.

Although these aims use different substrate investigation and electrical recording techniques, they share the common feature of examining conduction properties from an identified cardiac substrate. The results of the research driven by these aims showed that although

fibrillation is characterized by turbulent cardiac activity, that it is not completely stochastic. Specifically, the results showed that the cardiac substrate can manifest in specific electrophysiology properties that relate to the initialization and maintenance of fibrillation. These aims were completed using animal models of fibrillation. Possible future research would be to determine whether the findings and conclusions of these aims will translate to improving our understanding of human fibrillation.

1.2 Organization of Dissertation by Chapter

This dissertation is organized into eight chapters. Chapter 2 provides an overview of cardiac electrophysiology from the cellular to whole-tissue levels under normal physiological conditions. Chapter 3 provides an overview of cardiac electrophysiology during arrhythmia, focusing on the known and proposed mechanisms of cardiac fibrillation. Chapter 4 explains the challenges and the methodology of the imagining and electrical recoding techniques used to compare cardiac structure and function. Chapter 5 presents a published manuscript in *PLOS One*, which examines conduction properties of the ventricular conduction system during prolonged ventricular fibrillation. Chapter 6 presents a published manuscript in the *Journal of Cardiac Electrophysiology* that examines the conduction properties of atrial fibrotic tissue, and how these properties relate to the initiation of atrial fibrillation. Chapter 7 presents a manuscript which examines the relationship between fibrosis and high-frequency activation sites within the atrium during atrial fibrillation. Chapter 8 concludes the dissertation by discussing the research presented and by outlining future research projects.

CHAPTER 2

CARDIAC ELECTROPYHSIOLOGY OVERVIEW

Cardiac heart disease is the most common cause of morbidity and mortality in the world [10]. Cardiac heart diseases often results in arrhythmia [2, 10]. Due to the impact of arrhythmia, cardiac electrophysiology has been studied extensively by physicians, mathematicians, and engineers. These studies have resulted in many tools to examine cardiac electrophysiology from the subcellular level all the way to whole-heart. This chapter will begin by providing a background on the subcellular components that allow for excitability in cardiac cells. Then the chapter will detail the mechanisms of excitability of single cardiac cells and cell-to-cell coupling, and conclude with the organization of whole-heart conduction.

2.1 Generation of Electrical Potential in Cardiac Cells

Many cells can generate an electric current following exposure to an electric field. These cells are classified as excitable. Examples of excitable cells are neurons, which generate current for communication with other cells, as well as muscle cells, which generate current not only for communication but also for generation of a contraction force. Excitability in cells comes from two mechanisms. The first is the presence of a nonzero resting membrane potential and the second is the presence of gated ion channels. This section will detail the components of cardiac cell excitability.

2.1.1 The Sarcolemma

A 4-6 nm lipid bilayer, which is partially hydrophobic, surrounds cardiac cells and does not allow ions or many molecules to freely enter the cell. Water can diffuse through specific membrane transport proteins, known as aquaporins. Water is a dipolar molecule with a positive charge on hydrogen and a negative charge on oxygen. Electrostatic forces cause positively charged ions (cations) to attract to oxygen in water, and the negatively

charged ions (anions) to attract to hydrogen. For an ion to break away from water and pass through the membrane of a cell, it would require a large amount of energy. Due to the the chemical composition of the lipid bilayer, it is impenetrable to the ions surrounded by water molecules. However, the plasma membrane of all cells, including cardiac cells, is made up of proteins that can form complex structures. One of these protein structures can conduct ions across the sarcolemma and is known as an ion channel. The ion channels of particular importance to cardiac cells have the characteristics of selectivity and rectification. Fig. 2.1 shows a simple schematic of the sarcolemma.

The property of selectivity refers to the ion channel's selective permeability to specific ions [41]. The ions of primary interest to cardiac cells are Na^+, Ca^{2+}, and K^+, and diverse ion channels transport these ions. A large portion of the selectivity of an ion channel is determined by the size of the ion it is meant to conduct. Smaller ions have a more localized charge than larger ions, due to the larger ions having a decreased charge density. Water is attracted to ions due to electrostatic interactions; therefore, smaller ions bind water molecules strongly whereas larger ions bind water molecules weakly relative to the strength of water-water interactions [42]. The process of water surrounding an ion is known as hydration. The hydration of an ion depends upon its size; the more hydrated an ion, the larger the radius of the hydrated shell. For ions to conduct through an ion channel they must be dehydrated so that they can conduct through the selectivity filter, which separates the intracellular and extracellular spaces of a cell [43]. Ion channels undergo different state changes as a result of the arrangement of the amino acids that form the channel. This process is known as a conformational change. The three types of states are open, closed, and inactive. The open state is when a conformational change occurs that increases the lumen size and positioning polar amino acids to optimize ion conductance through the channel. The closed state is when ions cannot conduct through the channel. The inactive state is a state after open during which ions cannot conduct through the channel. Not all types of channels exhibit all conformational states; for instance, some channels only have open and closed states. Ion channels transition between states dependent on the kinetics of the channel, which may depend on time, voltage, stretch, phosphorylation, or the presence of a ligand.

The ion channel property of rectification refers to the nonlinear current voltage characteristics, or the conductance of the channel [41]. If ion channels did not have rectification, the magnitude of current flow would be equal for the same absolute value of the electrochemical potential. However, for most ion channels the magnitude of current flow also depends on the

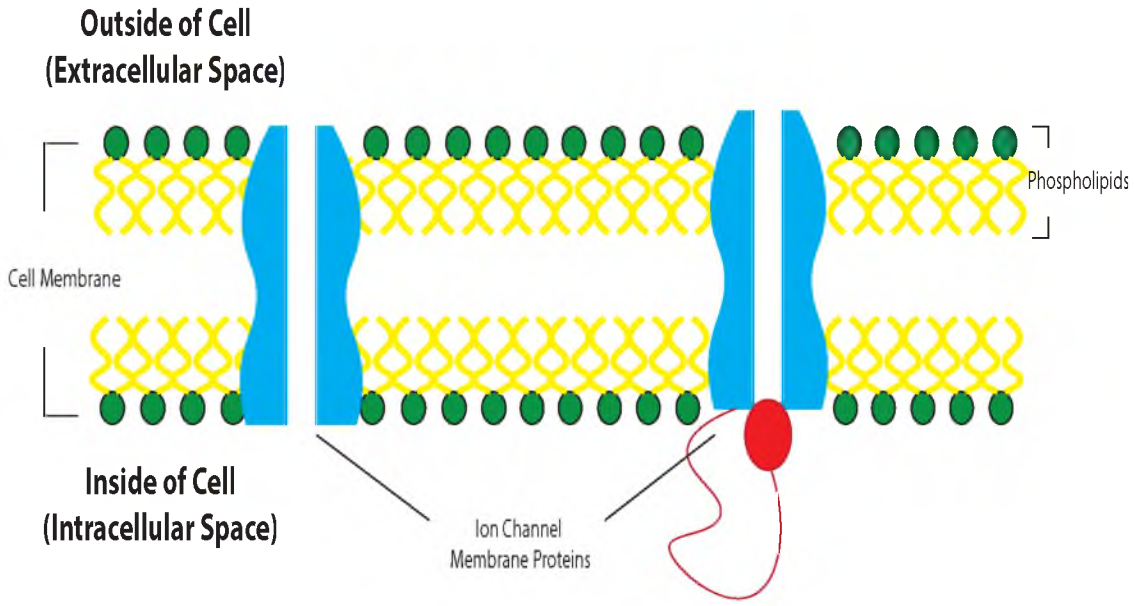

Fig. 2.1: **Schematic of sarcolemma**. Cardiac cells are surrounded by a phospholipid bilayer. The phospholipids of the bilayer are arranged where the hydrophilic heads, shown in green, are exposed to water, and the hydrophobic tails, shown in yellow, are pointed towards each other. The bilayer creates an intracellular and extracellular space. Embedded in the sarcolemma are proteins such as ion channels.

direction of ion movement into or out of the cells [41]. Rectification is thought to manifest due to several mechanisms, including conformational changes in ion channels, blocking of open channels by other internal ions that cannot travel through the ion channel, and other ion concentration gradients [44]. Some channels exhibit outward rectification, such as the delayed rectification K^+ channel, which has large outward conductance for a depolarized cell, but little to no conductance when the cell is repolarized [44]. Other channels can exhibit inward rectifying, such as the inward rectifying K^+, which has a large conductance for membrane potentials below -75mV, but has low conductance for higher membrane potentials [45].

2.1.2 Mechanisms of a Cellular Electrical Potential

Each ionic species has an equilibrium potential, known as the Nernst potential, which is a result of the diffusion and electrostatic gradients in a cell. Consider the case for a cell permeable only to K^+ ions; the resting membrane potential would be the K^+ Nernst potential, because K^+ ions would conduct across the membrane until the electrochemical driving forces (diffusive and electrostatic) on the ions are in equilibrium. Once in equilibrium, there would be no driving force, and therefore no net movement of K^+ ions, which would result in a steady state membrane potential. For example, Na^+, K^+ and Ca^{2+} ions each have their own Nernst potential. Once the membrane potential reaches an ion Nernst potential, there is no more electrochemical driving force for the ion, and there will be no more net movement of the specific ion. The Nernst potential for a specific ion, E_x, may be calculated using the Nernst equation as follows:

$$E_x = \frac{RT}{zF} \ln \frac{[X]_o}{[X]_i} \tag{2.1}$$

where $[X]_o$ and $[X]_i$ are the concentration of the ionic species inside and outside the membrane, T is temperature of the environment, and z is the valance of the ion. The constants in the equation are the gas constant, R, and Faradays constant, F.

The Nernst potential takes into account driving forces as a result of both diffusion and electrostatic gradients for an ionic species. K^+, Na^+, and Cl^- ions are not in equal concentration on either side of the cell membrane. As a result, K^+, Na^+ and Cl^- all have different Nernst potentials. The resting membrane potential will not equal the Nernst potential for K^+, Na^+, and Cl^-, but instead be a weighted average of all the membrane permeability ions. To calculate the resting membrane potential, the Goldman equation may be used. The Goldman equation takes into account all ionic species to which the

membrane is permeable. The Goldman equation for a cardiac membrane permeable to only K^+, Na^+ and Cl^- is shown as follows:

$$E = \frac{RT}{F} \ln \frac{P_{Na}[Na^+]_o + P_K[K^+]_o + P_{Cl}[Cl^-]_i}{P_{Na}[Na^+]_i + P_K[K^+]_i + P_{Cl}[Cl^-]_o} \tag{2.2}$$

where P_X is the permeability of the membrane to ion X. The larger the permeability of the ion, the more ions influence resting membrane potential. The Goldman equation shown in Eqn. 2.2 is for only three ions, but this equation can be expanded to account for any number of membrane-permeable ions. Concentrations of the primary ions in cardiac cells at rest are shown in Table 2.1.

2.1.3 Action Potentials

The relative concentration of ionic species across a cardiac cell's membrane determines the transmembrane potential. As a result of both diffusive and electrostatic driving forces cardiac cells have a negative resting membrane potential with respect to the extracellular space. In response to an electric field, cardiac cells can generate a current, which is the cellular property known as excitability. The excitability of cardiac cells is caused by changes in conductivity of voltage-gated ion channels, which allows the flux of ionic species. The flux of ionic species results in changes in the membrane potential. This process is called an action potential. The time course of an action potential is separated into four phases, which is based on the opening of specific ion channels [46]. The first phase, Phase 0, is the characteristic upstroke of the action potential. This phase is caused primarily by fast-acting Na^+ channels in contractile cells. During this phase, Na^+ channels undergo a conformational change from closed to open. Na^+ ions are then free to conduct into the cell, down both a concentration and electrostatic gradient, which causes the membrane potential to increase towards the Na^+ Nernst potential. Due to the kinetics of the Na^+ channels, these channels go into an inactive state rapidly (within 1-2ms). Phase 1 is the initial depolarization, which is caused by transient outward K^+ current, which in turn causes the

Table 2.1: Concentration of primary ions in cardiac cells at rest.

Ion	Intracellular concentration(mM)	Extracellular concentration(mM)
K^+	130-140	4
Na^+	7-8	140
Ca^{2+}	10^{-4}	1.2

transmembrane potential to trend towards the K^+ Nernst potential. Phase 2 is the extension of the action potential, which is caused by an outward K^+ current and intracellular release of Ca^{2+} from the sarcoplasmic. Phase 3 is mediated primarily by K^+ channels, I_{Kr} and I_{Ks}. The inward-rectifying K^+ current, I_{Kir}, activates later in Phase 3. This K^+ current is primarily responsible for the resting membrane potential. Phase 4 differs between cells, depending on whether the cell can generate an action potential without exposure to an external electric field. Cells with this property are said to have automaticity. Phase 4 in these cells is composed of the funny current, I_f, which is primarily Na^+ and K^+. In cells without automaticity, Phase 4 is rest, and a major current in this phase is I_{Kir}. In response to an electric field, ion channels can change their conductance, which is both time and voltage dependent. This dynamic change in conductance allows cells to generate an action potential. An example action potential is shown in Fig. 2.2.

After an action potential has been generated, there is an absolute refractory period until another action potential can occur. This absolute refractory period is caused by Na^+ channels not being able to transition to an open state, regardless of membrane potential. The Na^+ channels need to come out of inactivation before another action potential can occur. Na^+ channels come out of inactivation by experiencing a negative potential for a prolonged period of time [18]. Cells have a resting membrane potential of approximately -70mV, which is near the K^+ Nernst potential. The refractory period partially acts as a deterrent for arrhythmia formation. Generally, the refractory period of the tissue is longer than what it takes for an entire chamber to activate. The refractory period ensures that during normal electrophysiology conditions, all cardiac waves in a chamber dissipate by colliding into either refractory cardiac tissue, or other nonexcitable regions of the heart, before another heart beat is initiated.

2.1.4 Excitation Contraction Coupling

Excitation contraction coupling is the mechanism by which electrical energy, in the form of ions, is transformed to mechanical energy, in the form of contraction of a single myocyte. This process is primarily mediated by Ca^{2+}. When a cell is at rest, it has nanomolar concentrations of intracellular Ca^{2+} [47]. During Phase 2 of an action potential, L-type Ca^{2+} channels open, which causes Ca^{2+} to enter the cell. The L-type Ca^{2+} channels are in proximity to an intracellular organelle known as the sarcoplasmic reticulum. This proximity allows Ca^{2+} to quickly diffuse and bind to ryanodine receptors on the sarcoplasmic reticulum. When L-type Ca^{2+} binds to the ryanodine receptors, it causes the sarcoplasmic

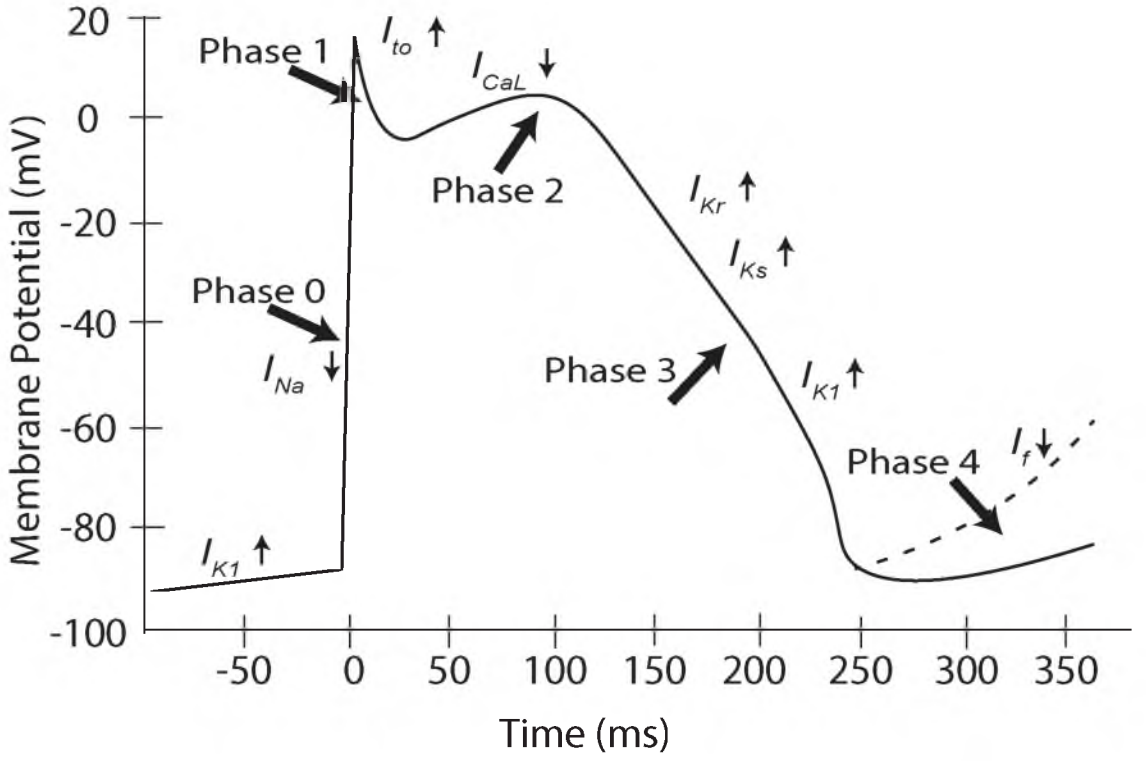

Fig. 2.2: **Representative action potential produced by a ventricular cardiac myocyte.** Membrane currents that contribute to the traditional shape and duration of an action potential. Arrows next to the currents indicate the direction of current flow (up arrow: outward current and down arrow: inward current).

reticulum to release Ca^{2+} into the intracellular space. The newly released Ca^{2+} can then stimulate nearby ryanodine receptors to release even more Ca^{2+}, and this process starts a positive feedback loop known as Ca^{2+}-induced Ca^{2+} release, and this process results in millimolar intracellular Ca^{2+} concentration. The intracellular Ca^{2+} then diffuses to actin and myosin filaments to start the process of muscle contraction. Intracellular Ca^{2+} is then reduced again to nanomolar concentration due to several mechanisms, including uptake of Ca^{2+} back into the sarcoplasmic reticulum by the SERCA pump, ATP Ca^{2+} pump, and the $Na^{+}Ca^{2+}$ (NCX) exchanger [47].

2.2 Cell-to-Cell Coupling

Individual cardiac cells can generate an action potential in response to an electric field. Cardiac cells are coupled by proteins in the plasma membrane known as gap junctions. These gap junctions are connections between the intracellular space of neighboring cardiac cells. Therefore, when Na^{+} enters a cell, it will cause the potential to increase, which then sets up a electrostatic gradient to the coupled cells. Positive ions from the depolarized cell can then conduct through the gap junctions to depolarize neighboring cells. This coupling means if a cardiac cell generates an action potential, this action potential may spread and cause the generation of action potentials in its coupled cells. This coupling results in a cardiac cell being able to excite other nearby cells. This process can continue as long as cells are coupled to excitable cells that are not in refractory. This process is why cardiac conduction is often described as propagation of electrical waves.

The coupling of cardiac cells results in electrical wave propagation. Like any other wave, the electrical wave has a conduction velocity, which can be approximated from physiological properties of the cardiac cells as follows:

$$ConductionVelocity = \sqrt{\frac{K \times D \times \frac{dV}{dt}}{R_i C}} \tag{2.3}$$

where K is a constant, D is the diameter of the cell, $\frac{dV}{dt}$ is the rate of depolarization, Ri is the intracellular resistance of the gap junctions, and C is the capacitance of the cell. Cardiac electrical waves have anisotropic conduction properties, which is caused by a preferential expression on the short axis of cardiac cells, thus coupling longitudinally. Cells are also coupled in the transverse direction; however, this coupling is less than the longitudinal coupling. Using Eqn. 2.3 the difference in conduction can be explained by an increase in intracellular resistance in the transverse direction. Conduction velocity of cardiac waves is also affected by the curvature of the wave. For the same cardiac tissue, the concave waves

propagate faster than planar waves, which propagate faster than convex waves [48]. The mechanism behind the differences in conduction velocity is due to the electrical load of other coupled cells to an excited cell. For a planar wave, each excited cell in the propagating wave has to depolarize only a single downstream cell. For a convex wave to propagate, the leading cell in the wave is now coupled not to only a single cell upstream, but also transversely to nearby cells. This increased coupling causes depolarizing currents in the propagating wave to be split between multiple cells, which will result in a reduced rate of depolarization, thus a reduced conduction velocity. Finally, a concave wave can propagate the fastest, because each cell in the propagating wave has fewer nearby cells to act as sinks as compared to a planar or a convex wave. The property of a cell being able to depolarize downstream cells relates to sources and sinks. If the source and sink are said to match, then propagation can occur because there are enough ions to depolarize downstream cells; however, if there is a source-sink mismatch, propagation will be slowed or even cease all together due to insufficient current to depolarize the cell and open voltage gated Na^+ channels [5, 48].

The safety factor is a quantitative measure to examine the source-sink relationship of cells and defines the success of cardiac propagation [49]. The safety factor is computed as the ratio of charge generated to charge consumed during the excitation cycle of a single cell in tissue and is computed as follow:

$$Safety\ Factor = \frac{\int_A I_c dt + \int_A I_{out} dt}{\int_A I_{in} dt}\ A|Q_m{>}0 \tag{2.4}$$

where I_c is the capacitive current of the cell in question and I_{in} and I_{out} are the axial currents in and out of the cell. The charge, Q, is the time integral of the current of an interval A during which the net membrane charge Q_m is positive [49]. If the safety factor is > 1, the source has enough current to depolarize the downstream cell. If the safety factor is < 1, then conduction propagation will not occur because there is not enough current to depolarize the downstream cell.

2.3 Organization of Whole-Heart Cardiac Activation

The heart is a four-chamber pump that functions to transport blood and nutrients through the body. The heart consists of the atria and the ventricles. The atria and ventricles are also subdivided into the left and right side. The right atrium (RA) and right ventricle (RV) pump deoxygenated blood to the lungs to become oxygenated, and the left atrium (LA) and left ventricle(LV) pump blood to the rest of the circulatory system. The ventricles are used as the primary driving force for circulation, whereas the atria help

to completely fill ventricles. The organization of whole-heart cardiac activation during sinus rhythm functions such that blood passively flows to the ventricles from the atria, and then the atria contract during cardiac diastole to more completely fill the ventricles. During systole, the ventricles undergo coordinate contraction, due to excitation contraction coupling and cell-to-cell coupling, to circulate blood.

A specific sequence of electrical conduction is required to coordinate the activation of the atria and ventricles such that there is sufficient blood flow. This process begins at the SA node. The SA node contains specialized cardiac cells that have high expression of the inward funny current channels, which was discussed in Section 2.1.2. These cells have lower expression of fast-activating Na^+ channels, and therefore Phase 1 is caused primarily by Ca^{2+}. The LA begins depolarization slightly after the RA through a specialized conduction system at the Bachmann bundle. After the SA node initiates the cardiac sequence, cell-to-cell coupling will cause the entire atria to conduct and contract in a process known as excitation contraction coupling. The only electrical connection between the atria and ventricle for normal hearts is through the AV node. The AV node has specialized conduction cells that have a longer refractory period than myocytes, and conduction greatly slows in this region. This slowing of conduction results in more filling time for the ventricles. The ventricular conduction system is then excited by the AV node. The ventricular conduction system electrically connects the AV node to the ventricular myocardium and consists of specialized conduction cells that conduct rapidly but do not have a contraction function. This system at the proximal end to the AV node is called the His bundle, and the distal end is known as the Purkinje system. The ventricular conduction system is located near the septum that separates the LV and RV. The ventricular conduction system is electrically coupled with the VM only at specialized sites known as the Purkinje myocardial junctions (PMJs), which are spread throughout the endocardium in humans [50]. Once multiple sites on the endocardium are activated, VM to VM electrical coupling causes the rest of the ventricles to contract. This whole process, known as sinus rhythm, then repeats itself again with the Sinus node automaticity. Table 2.2 summarizes longitudinal conduction velocities for the different types of cardiac cells during normal sinus rhythm [51].

Similar to how different cell types have different conduction velocities, they also have differences in action potential morphology. Changes in action potential morphology are due to differences in specific ion channel densities as well as differences in the kinetics of ion channels. The most obvious differences in morphology can be seen in changes between cell types, such as between conduction system, atrial, and ventricular cells. For example,

Table 2.2: Longitudinal conduction velocity of cardiac tissues.

Tissue Type	Average Conduction Velocity (m/s)
Atrial	0.8
Ventricular	0.5
SA and AV node	0.05
His-bundle	2
Purkinje	4-5

SA and AV nodal tissue does not exhibit a rapid depolarization because these cells do not have fast-activating Na^+ channels. Instead, the upstroke in these cells is primarily caused by Ca^{2+}. The slow rate of depolarization is partially responsible for the slower conduction velocities in SA and AV nodal tissue. Ventricular conduction cells have a similar action potential morphology to atrial and ventricular cells, but there are also differences. Ventricular conduction cells have a more rapid depolarization than myocytes due to a higher density of fast-activating Na^+ channels [12]. Ventricular conduction cells also have a longer action potential duration (APD) than both atrial or ventricular cells at slower cycle lengths [12]. Atrial and ventricular cells also have differences in action potential morphology. Generally, atrial cells have shorter APDs than ventricular cells. The shorter APD of atrial cells is primarily due to increased activity of K^+ channels, which more quickly repolarize the cell [52]. Finally, there even exist regional differences in action potential morphology between the same cell type. Endocardial myocytes have a prolonged APD compared with epicardial ventricular myocytes. This difference is thought to be due to an increase in density of K^+ channels near the epicardium, which quickens repolarization [53]. During normal physiological conditions, these differences in action potential morphology offer some protection against arrhythmias occurring. However, during arrhythmias, action potential morphologies quickly change, which can make arrhythmias more likely to be sustained [18, 53]. Similar to how different cell types have different conduction velocities, they also have differences in action potential morphology. Changes in action potential morphology are due to differences in specific ion channel densities as well as differences in the kinetics of ion channels. The most obvious differences in morphology can be seen in changes between cell types, such as between conduction system, atrial, and ventricular cells. For example, SA and AV nodal tissue does not exhibit a rapid depolarization because these cells do not have fast-activating Na^+ channels. Instead, the upstroke in these cells is primarily caused by Ca^{2+}. The slow rate of depolarization is partially responsible for

the slower conduction velocities in SA and AV nodal tissue. Ventricular conduction cells have a similar action potential morphology to atrial and ventricular cells, but there are also differences. Ventricular conduction cells have a more rapid depolarization than myocytes due to a higher density of fast-activating Na^+ channels [12]. Ventricular conduction cells also have a longer action potential duration (APD) than both atrial or ventricular cells at slower cycle lengths [12]. Atrial and ventricular cells also have differences in action potential morphology. Generally, atrial cells have shorter APDs than ventricular cells. The shorter APD of atrial cells is primarily due to increased activity of K^+ channels, which more quickly repolarize the cell [52]. Finally, there even exist regional differences in action potential morphology between the same cell type. Endocardial myocytes have a prolonged APD compared with epicardial ventricular myocytes. This difference is thought to be due to an increase in density of K^+ channels near the epicardium, which quickens repolarization [53]. During normal physiological conditions, these differences in action potential morphology offer some protection against arrhythmias occurring. However, during arrhythmias, action potential morphologies quickly change, which can make arrhythmias more likely to be sustained [18, 53].

A clinical method to characterize both sinus rhythm and arrhythmias noninvasively is through electrocardiography (ECG). The ECG measures the heart's electrical conduction on the body surface. In a typical three-lead ECG, there are three recording electrodes. The difference of potential at two of the body surface electrodes can be used to create a lead. Several characteristics of the ECG waveforms have been used clinically to understand cardiac excitation. For sinus rhythm, the ECG has numerous complexes that correspond to various phases in the cardiac cycle. The first peak is known as the P wave, and it corresponds to the atrial depolarization. After the P wave, there is an isopotential line that corresponds to the delayed conduction through the AV node, which is known as the PR interval. Next is the QRS complex, which corresponds to the ventricular depolarization. Then there is another isopotential line, known as the S-T interval, that corresponds to the plateau phase of ventricular cells. During the plateau phase of the ventricular cells, all the ventricular cells are depolarized, and therefore there is no dipole. Finally, the T wave is the final peak and corresponds to ventricular repolarization. Arrhythmia can be determined based on alteration in the ECG. For example, ventricular fibrillation is characterized by rapid nonregular QRS-like complexes due to the chaotic activation of the ventricles. Although there are atrial activations during VF, these atrial activations are masked by the larger ventricular activations. An ECG of AF is characterized as having no P waves, and therefore

no coordinated atrial activation, and an irregular R-R interval. The signal inbetween the R-R interval appears like noise but it is uncoordinated atrial activation. Examples of ECGs for sinus and fibrillation arrhythmias are shown in Fig. 2.3. Although the ECG is an invaluable tool for diagnosing arrhythmias, it alone is insufficient to understand the base mechanisms of fibrillation. The studies in this dissertation utilize ECG recordings as well as measurements from electrodes placed directly on the heart surface, which is a more local measure of heart activity, to understand arrhythmogenesis and what sustains fibrillation.

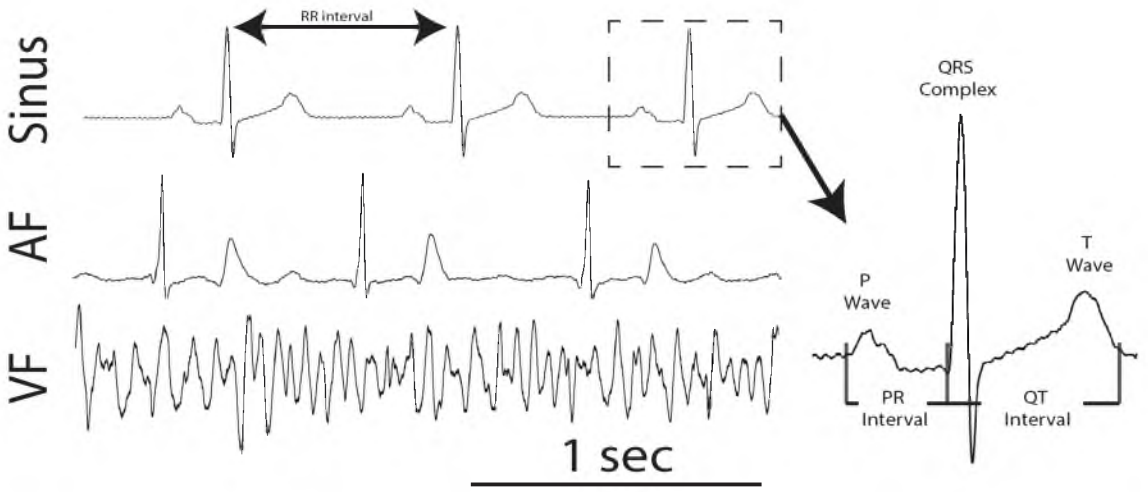

Fig. 2.3: **ECG of sinus rhythm and of fibrillatory arrhythmias.** Sinus rhythm is indicated by a clear P wave, QRS complex, and T wave. The RR interval indicates the time between ventricular activation and therefore is a measure of heart rate. The PR interval indicates the time for conduction to occur from the SA node to ventricular tissue. The QT interval indicates the time for ventricular depolarization and then repolarization. AF is indicated by irregular RR intervals as well as nondistinct P waves. VF is characterized by rapid irregular activity, in which no clear P waves or QRS waves can be detected.

CHAPTER 3

ARRHYTHMIAS OVERVIEW

Arrhythmias are broadly referred to as disorders in cardiac impulse formation and/or impulse propagation [2]. Depending on the specific type of arrhythmia, the health concerns may be relatively benign, such as bradycardia; whereas others are more serious but can be effectively treated with pharmaceutical and/or surgical intervention, such as flutter/fibrillation-type arrhythmias. This section focuses on fibrillation, the most severe arrhythmia, which is defined as turbulent cardiac electrical activity whereby propagation of electrical waves through the heart is disrupted, with consequent production of wavelets, high-frequency rotating waves, and inability of the myocardium to contract [5]. This section will first broadly cover the major theories of how fibrillation is initiated and why it sometimes spontaneously terminates, and other times it is sustained indefinitely. Next this chapter will separate out specific mechanisms for fibrillation in the ventricles and the atria. Fibrillation in the ventricles and atria have many similarities, but a primary difference between them is that VF is an acute arrhythmia and AF is often a chronic arrhythmia. VF only lasts from seconds to minutes before it is either treated or becomes fatal. However, during this time, cardiac output approaches zero, which results in ischemic conditions that can greatly affect the electrophysiology. Fibrillation in the atria is not immediately fatal and therefore this arrhythmia can persist for years, causing many electrical and structural changes to the cardiac substrate, which affect the electrophysiology.

3.1 Canonical Mechanism of Fibrillation Initiation

There are many different theories regarding the mechanisms of fibrillation; however, most researchers agree on the importance of unidirectional conduction block and reentry [5, 39, 48, 54–57]. Unidirectional conduction block is a mechanism for fibrillation in which an electrical wavefront propagates in one direction but blocks in another [39, 57, 58]. This block may be structural, in the case of a conducting wavefront colliding into regions of

unexcitable scar, but it can also be functional, where cardiac tissue in one direction is refractory and thus unexcitable [39, 59]. Under normal physiological conditions, once an electrical wavefront interacts with an unexcitable obstacle, either anatomical or functional, it breaks into two wavefronts [60]. These two wavefronts propagate on the boundary of the obstacle and then recombine again once the obstacle is bypassed. However, in cardiac tissue with slowed conduction, the two wavefronts may not recombine again and instead may propagate in a circuitous pathway. Reentry is when the circuitous pathway loops back upon itself, and under certain situations this pathway may self-sustain. A simple schematic is shown in Fig. 3.1.

Whether or not reentry occurs is dependent upon the conduction velocity of the electrical wave as well as the action potential duration (APD) of the cardiac cells in the potential reentrant path [61]. This relationship has been formalized as follows:

$$Wavelength = CV \times APD \tag{3.1}$$

where CV is conduction velocity. Eqn. 3.1 describes a cardiac wavelength. Reentry can occur if the wavelength is equal to, or shorter than, the path length. Therefore, reentry is more likely to occur in cardiac tissue with slowed conduction and shorter APDs. These factors can cause rogue wavefronts to not collide into refractory tissue to dissipate before causing reentry [61–63].

3.1.1 Cardiac Restitution

Unidirectional conduction block is related to the property of restitution. Broadly, restitution is the dependence of a cardiac property on the previous diastolic interval [63–65]. Two characteristics of cardiac tissue that show restitution are action potential duration (APD) and conduction velocity, which are both critical to develop reentry [59, 66]. Both the APD and conduction velocity restitution are dependent on the kinetics of ion channels. When heart rate increases, the APD shortens and conduction velocity decreases, which allows for a longer diastolic interval to preserve sufficient cardiac output even during varying RR intervals [39]. However, when the diastolic interval becomes very short, or there is a rapid change in the diastolic interval, the restitution properties can make fibrillation more likely to initiate [67, 68].

The mechanism behind APD restitution is incompletely understood, but is thought to be due to the repolarization currents [64]. During an action potential, Ca^{2+} flows into the cell through L-type Ca^{2+} channels. The Ca^{2+} from the L-type channels stimulates ryanodine receptors to release of Ca^{2+} from the sarcoplasmic reticulum (SR), which is known as Ca^{2+}-

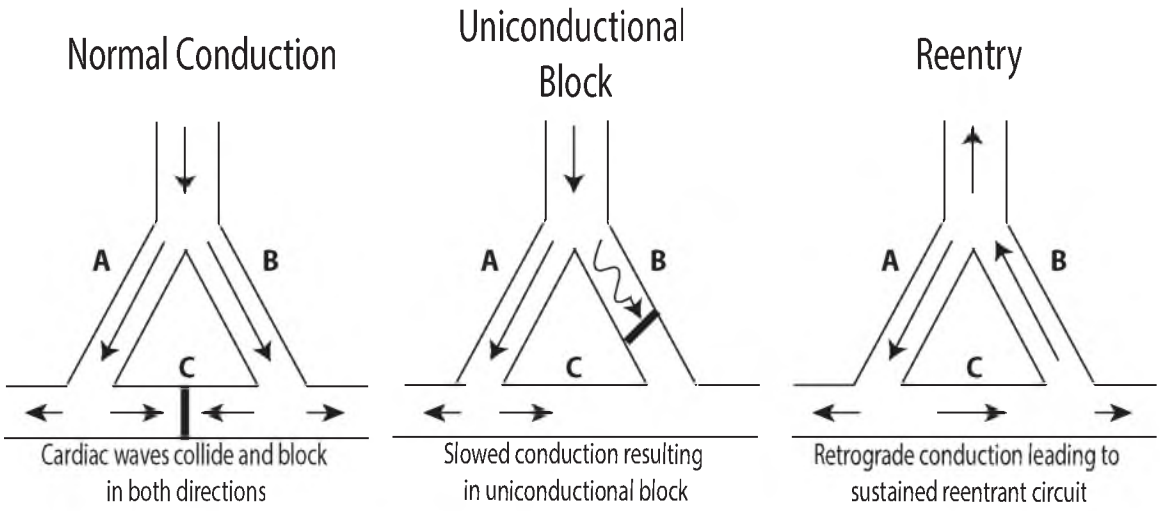

Fig. 3.1: **Schematic of reentry in cardiac tissue.** Normal conduction where cardiac waves propagate in an antegrade direction in both the A and B pathways. Conduction waves in paths A and B collide and annihilate each other in pathway C. Under certain conditions such as ectopy, pathway A may conduct in the normal antegrade direction, but pathway B may not be fully recovered from refractory, which will result in slowed conduction and block in pathway B. The cardiac wave that propagated in pathway A will now not block pathway C and may conduct retrograde in pathway B if it is now out of refractory. If now pathway A is out of refractory as well, reentry has occurred and this process may continue indefinitely.

induced Ca^{2+} release [47]. During a shorter diastolic interval, the L-Type Ca^{2+} channels have not fully recovered and therefore do not conduct as much Ca^{2+}. This reduction in Ca^{2+} causes less activation of the ryanodine receptors and therefore less Ca^{2+}-induced Ca^{2+} release from the SR [69, 70]. The reduction in intracellular Ca^{2+} causes a shortening of phase 2 of an action potential and relates to a shorter APD. Prolonged conductance of K^+ currents, specifically, I_{kr}, may also cause a shortening in APD as a result of a shorter diastolic interval. Due to the kinetics of I_{kr}, this channel may not have time to close during Phase 3 of an action potential. If I_{kr} does not close during Phase 3, it will result in increased K^+ conductance into the cardiac cell, which will decrease repolarization time. More recently, there has been evidence of Ca^{2+}-activated K^+ channel, known as apamin-sensitive small conductance Ca^{2+}-activated K^+ current, I_{KAS}, which may be responsible for causing a short APD at a short diastolic interval that may contribute to recurrent arrhythmia [71,72]. Nolasco and Dhalen were the first to formalize the relationship between diastolic interval and APD by plotting the previous diastolic interval (x-axis) versus APD (y-axis), which became known as a restitution curve [73]. A representative restitution curve is shown in Fig. 3.2.

Conduction velocity restitution describes the process in which changes in diastolic interval are followed by changes in conduction velocity. Conduction velocity restitution is primarily due to the depolarizing currents, fast-acting Na^+ channels, during Phase 0 of an action potential [74]. During a short diastolic interval, fast-acting Na^+ channels may not have enough time to recover from an inactivated state, and therefore the ion channels cannot conduct because the ion channels are in refractory. If a premature stimulus excites the tissue, some of these ion channels will not be able to open; therefore the slope of the action potential will be reduced. In section 2.1.3, Eqn. 3.1 illustrates that the slope of the action potential activation is positively associated with conduction velocity in the tissue. Therefore if some of these channels cannot conduct, the result is a lower conduction velocity.

There are two types of restitution protocols, dynamic and standard. Both measure the diastolic interval prior to action potential's APD. The main difference between dynamic and standard restitution protocols is that dynamic restitution takes into account cardiac memory, a mechanism in which delays in ionic currents, such as Ca^{2+} and K^+, with slow recovery kinetics can accumulate over several cycles [64, 75]. Dynamic restitution is measured after a series of beats (typically about 10-30 beats to allow for steady state), which are known as the S1 phase. The cycle length of the S1 beats are then shortened until the diastolic interval is shorter than the effective refractory period of the tissue, and

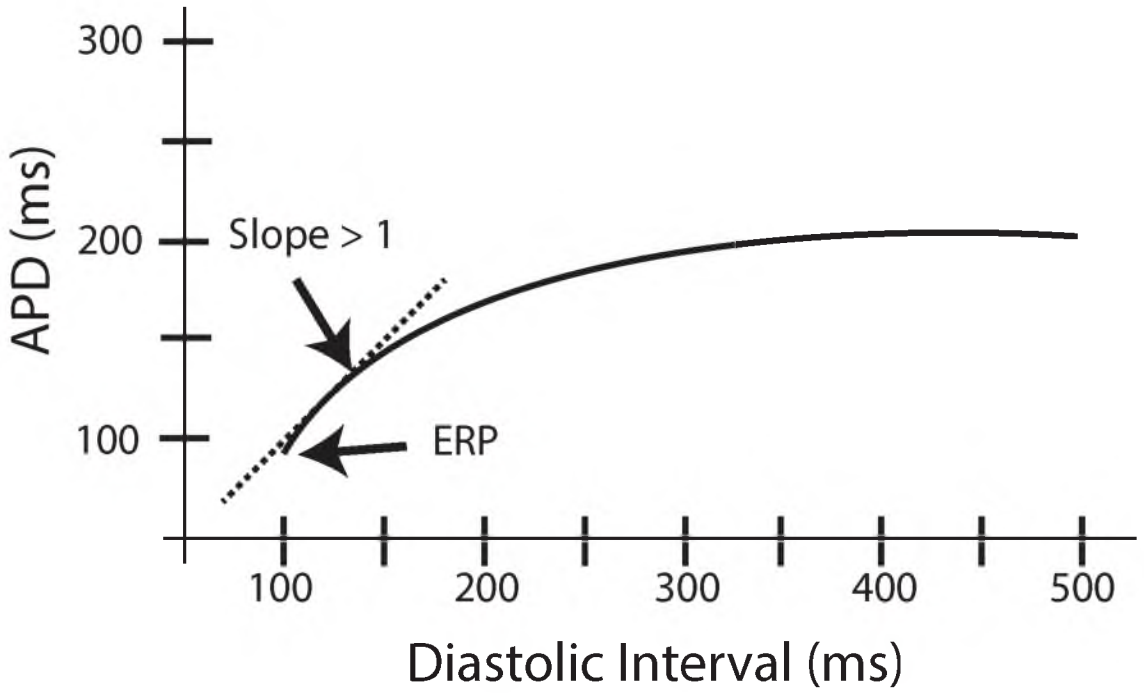

Fig. 3.2: **Representative restitution curve**. The restitution curves show little rate change at longer cycle lengths (D >300ms), however at shorter cycle lengths (D <150ms) the restitution curve begins to steepen (slope >1), which results in large changes in APD for small changes in diastolic interval. The restitution curve stops at 60ms, which is the effective refractory period (ERP).

the stimulation cannot excite the tissue. Standard restitution is measured by applying a single S2 paced beat after a series of S1 beats. The S1 beat remains at a constant cycle length throughout the protocol, but the S1-S2 interval is reduced until the diastolic interval is shorter than the effective refractory period, and therefore the S2 does not cause cardiac tissue excitation. Although both measure restitution, they produce different results [76]. There would be no difference in the two measurement types if there was no cardiac memory (i.e., no transition time into steady state) [64]. A schematic of the protocol for dynamic and standard restitution is shown in Fig. 3.3.

The slope of the restitution curve relates to the stability of electrical properties within cardiac tissue [39,68,77]. When the electrical properties are stable, slight changes in diastolic interval are accompanied by slight changes in APD and conduction velocity. However, when the electrical properties are unstable (restitution slope >1), small changes in diastolic interval greatly change APD and conduction velocity, which are both important in the occurrence of unidirectional conduction block and the development of reentry pathways to initiate fibrillation.

3.1.2 Triggered Activity

Triggered activity describes focal impulse initiation in cardiac tissues that is dependent on oscillations in membrane potential after the upstroke of an action potential, in what are known as afterdepolarizations [78]. There are two types of afterdepolarizations. The first type of afterdepolarization is an early afterdepolarization (EAD), which occurs during the repolarization phase, Phase 2 or 3, of an action potential. The other type of afterdepolarization is the delayed afterdepolarization (DAD). DADs occur when repolarization is complete. When an EAD or DAD depolarizes the membrane enough to initiate an action potential, that action potential is said to be triggered [79]. An example of an EAD and DAD is shown in Fig. 3.4.

EADs occur during Phase 2 or 3 of an action potential. The ionic mechanism responsible for EADs is incompletely understood but is thought to be due to the kinetics of primarily Ca^{2+} but also Na^{+} channels. EADs that occur during Phase 2 or early Phase 3 are thought to be due to L-type Ca^{2+} channels coming out of inactivation, which causes more Ca^{2+}-induced Ca^{2+} release from the SR to initiate another action potential. The occurrence of the EAD during late Phase 3 may be due to Na^{+} channels coming out of inactivation [80]. Also, B-adrenergic stimulation may cause an increase in the Na^{+}/Ca^{2+} exchange from NCX to raise the membrane potential to initiate another action potential [51]. A final mechanism of EADs can occur during ischemia. During ischemia, the Na^{+}/H^{+} exchange

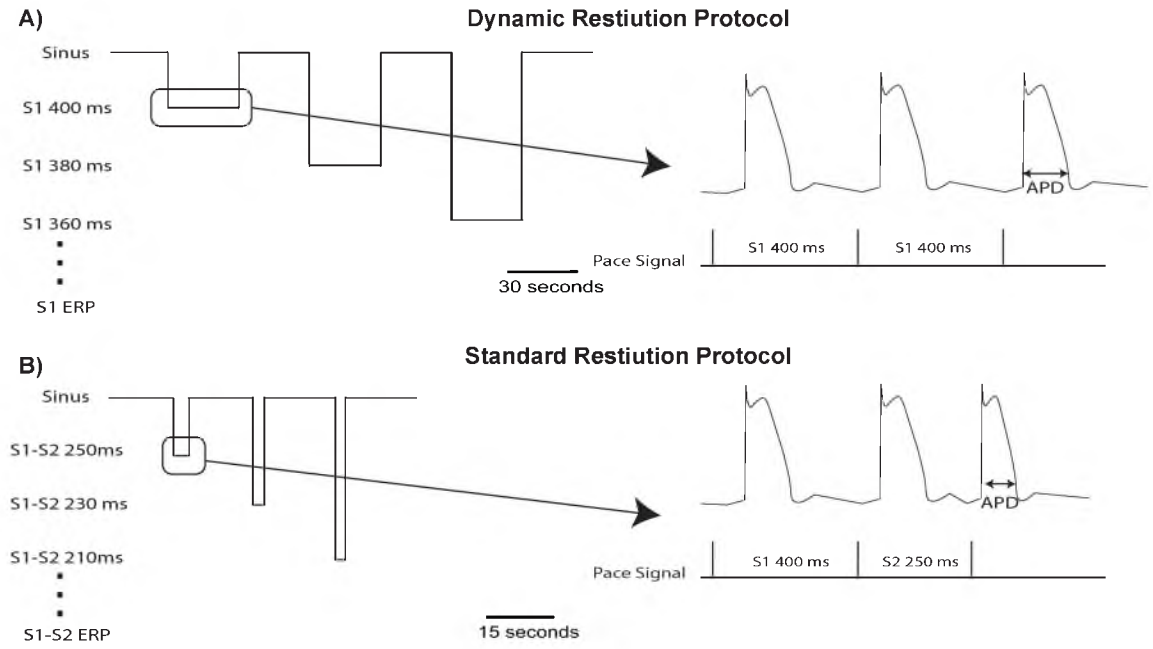

Fig. 3.3: **Schematic of dynamic and standard restitution protocol**. **A)** Dynamic restitution protocol. A series of paced beats are done until the tissue is in steady state. Then the APD restitution can be calculated as the S1 diastolic interval vs. the APD. **B)** Standard restitution protocol. A series of S1 beats, typically 7-10, are done followed by a single premature S2 beat. Then the APD restitution can be calculated as the S1 diastolic interval vs. the APD of the S2 paced beat.

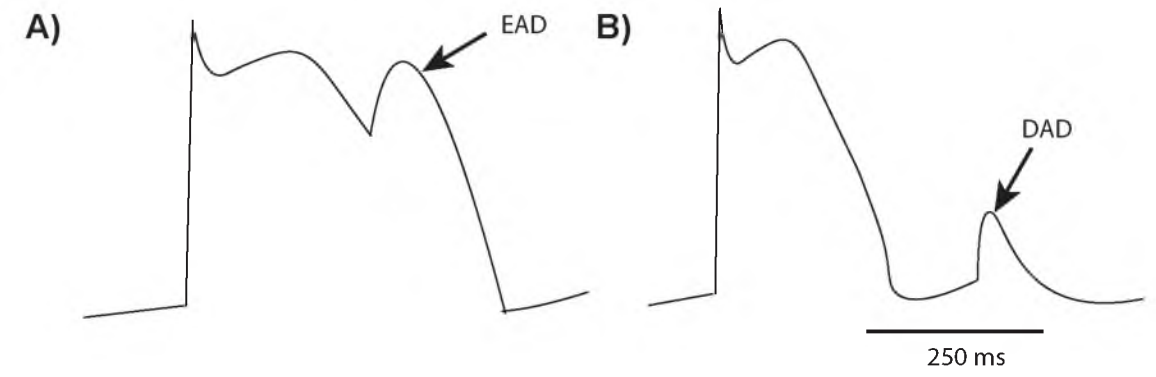

Fig. 3.4: Differences between early and delayed afterdepolarizations. A) Representative example of an early afterdepolarization (EAD). EADs are more likely to occur during bradycardia due to the longer APDs and slower heart rate. If the EADs can prolong the APD enough, it may initiate another action potential. EADs can occur during Phase 2 or Phase 3 of an action potential. If the EAD occurs during Phase 2, as in this example, it is thought that L-type Ca^{2+} channels come out of inactivation to release more intracellular Ca^{2+}. If the EAD occurs during phase 3, it is thought to be due to Na^{+} channels coming out of inactivation. **B)** Representative example of a delayed afterdepolarization (DAD). DADs are more likely to occur during tachycardia, and the ionic mechanism behind DADs is thought to be Ca^{2+} overload of the cell.

removes intracellular H^+ with an inward Na^+ to try to regulate pH. The increase in Na^+ makes EADs more likely [18]. EADs are more likely to occur during bradycardia because during a slow heart rate, there is a prolonged action potential duration and there is more time for Na^+ and Ca^{2+} channels to come out of inactivation [81].

DADs occur after complete repolarization of the cardiac cell. The ionic mechanism responsible for DADs is thought to be due to Ca^{2+} overload or ryanodine receptor dysfunction [39]. Abnormal release of Ca^{2+} from the SR has been shown to activate a composite inward current I_{ti} [82]. I_{ti} is composed of Ca^{2+}/Na^{2+} exchange, a Ca^{2+} activated Cl^+ channel and NSC Ca^{2+} channels [82–84]. DADs are more likely to occur during tachycardia because an increase in heart rate increases the frequency and amplitudes of the DADs [78].

3.2 Canonical Mechanisms of Fibrillation Maintenance

One theory of fibrillation is that it is sustained by spatially stable reentrant pathways. These spatially stable pathways are known as the mother rotors, and electrical wavefronts propagating from these mother rotors, known as daughter wavelets, cause the unorganized activity observed during fibrillation [85]. Evidence of this type of fibrillation has been shown in humans and animals as highly regular activation patterns on the endocardium and/or epicardium [86,87]. Due to the regularity of activations patterns of the heart, the fibrillation may have some organization and not be completely stochastic. Additional evidence from this type of fibrillation comes from examining the frequency content of the electrograms, which are recorded from many locations of the heart simultaneously. The frequency with the maximum peak in the power spectrum is related to the activation rate of the underlying cardiac tissue, and is called the dominant frequency [88]. If the fibrillation is stochastic, and there is not a specific region that is driving the arrhythmia, the power spectrum may look like white noise. However, if certain regions of the cardiac tissue are driving the arrhythmia, this method will show regions of the heart that have a high dominant frequency. Some studies have shown that during fibrillation, regions of high dominant frequency emerge, suggesting the presence of a driving site, which may be a mother rotor [89]. The mother rotor theory states that there are specific regions within the heart which are highly organized and that these regions sustain the fibrillation. This theory also suggest that the nondriving sites are just being passively activated by the driving site.

A competing theory to mother rotor is that fibrillation is maintained by many nonstable wavefronts known as wavelets [5, 54]. These wavelets are nonstable because they are short lasting: the wavelets collide and block with other wavelets and do not propagate along a

consistent reentrant pathway. There are still, however, some conduction properties, such as highly nonregular activation patterns on the endocardium and/or epicardium that make this fibrillation identifiable. Both computational and experimental data suggest that this type of fibrillation can occur [13,90,91]. The most traditional version of multiple wavelets theory is that fibrillation is highly unorganized, i.e., that certain regions of the heart are not any more likely to sustain fibrillation than any other region. However, this theory has recently been expanded to also state that there might be certain regions of the cardiac tissue that can maintain more reentrant pathways than other regions of the tissue. If certain regions of the heart can have more reentrant pathways, this implies that specific regions of the heart may have faster activation rates because they contain more possible pathways for reentry; however, the wavefront pathways are constantly changing and therefore inconsistent with the mother rotor [92].

Although both the wandering wavelet and mother rotor theories of fibrillation provide some insight into fibrillation mechanisms, a major limitation to these theories is that they neglect the cardiac structure and substrate in their formulation. Much evidence, however, supports the notion that cardiac substrate is critical to the formation of sustained cardiac fibrillation, specifically, when moving from generalized cardiac fibrillation to more specific examples of atrial or ventricular fibrillation. Simulation data have shown without specific regions of reduced conductivity that stable reentrant pathways could not be sustained [37]. Additional evidence has shown that without the ventricular conduction system, ventricular fibrillation is not sustained as long, and the arrhythmia has a slower activation rate [14]. These examples show why when transitioning from generalized theories of fibrillation to specific instances of fibrillation, the cardiac structure should not be ignored.

3.3 Ventricular Fibrillation

VF is the uncoordinated electrical impulse propagation and contraction of the ventricles. The uncoordinated contraction causes the cardiac output to go to zero rapidly, and if this arrhythmia is not corrected within 2-3 minutes it is fatal. The differences from generalized theories of fibrillation and VF are a result of ischemia and the ventricular conduction system.

3.3.1 Ischemia in Ventricular Fibrillation

During prolonged VF, many cellular changes occur in myocytes as a result of ischemia and high-frequency activation. These cellular changes cause an increase in fibrillation cycle length and diastolic duration and a shortening of APD [19]. The cellular changes are

a result of changes in normal biochemical and ion concentrations due to acute ischemia. These changes include an increase in extracellular K^+, acidosis, an increase in intracellular Na^+, and an increase in intracellular Ca^{2+}.

An increase in extracellular K^+ causes the cell to have a higher resting membrane potential and a decreased action potential duration. The increase in membrane potential may transiently result in increased excitability due to the resting membrane potential being closer to the Na^+ activation threshold, but if prolonged, this reduced membrane potential causes more inactivation of Na^+ channels [18]. The inactivation of Na^+ channels results in a less steep up-slope in membrane depolarization and thus a reduction in conduction velocity. There are three primary mechanisms for the increase in extracellular K^+: a decrease in the extracellular space, a decrease in active K^+ influx, and an increase in passive K^+ efflux. A decrease in the extracellular space is caused by an accumulation of lactate and phosphate in the cell [93]. The increase in particles causes a diffusion gradient that in turn causes water to shift from the extracellular space into the intracellular space. Due to the decreased volume of the extracellular space, the relative concentration of K^+ increases in the extracellular space. The second mechanism of increased K^+ is due to the inhibition of the ATP NA^+/K^+pump. Under aerobic conduction, NADH and $FADH_2$ are formed during glycosis, and in the citric acid cycle, transfer their electrons to O_2 through the electron transport chain to produce ATP [18]. However, when oxygen falls below a critical level, the electron transport stops, which slows ATP production. A combination of less ATP, an increase in ADP, and an increase in oxygen free radicals has been shown to decrease ATP NA^+/K^+pump activity [94]. The decrease in pump activity causes less influx of K^+ and thus it accumulates in the extracellular space. The final primary mechanism of increased extracellular K^+ is due to increased passive efflux of K^+. Passive efflux of K^+ is thought to occur due to increased activity of KCL cotransport caused by intracellular swelling [18].

Under normal physiological conditions, the intracellular pH is more acidic than the extracellular pH. During ischemia, there is more CO_2 retention and proton production, which further reduces pH in both the extracellular and intracellular space [95]. The reduced pH causes the inhibition of most of the primary ion channels, including Na^+, Ca^{2+}, and most K^+ channels [18]. The inhibition of these ion channels has the overall effect of reducing action potential duration, slowing conduction velocity, and increasing the resting membrane potential. Furthermore, these changes make the occurrence of EADs more likely [80]. The increase in acidic conditions is a result of several key ion channels that regulate H^+ being inhibited during ischemia. Under aerobic conditions, the Na^+/H^+

exchange and the Na^+-$HCO_3{}^+$cotransport actively remove protons from the intracellular space [96]. However, under ischemic conditions these channels have reduced activity due to a decrease in extracellular pH and an increase in intracellular Na^+ [97,98].

Intracellular Na^+ increases during ischemia. An increase in intracellular Na^+ may cause reversal of the Na^+/Ca^{2+} exchanger to increase intracellular Ca^{2+}, and increases the likelihood of arrhythmia [99]. The main mechanisms of an increase in intracellular Na^+ are the Na^+/H^+ exchange moving H^+ out of the cell and Na^+ into the cell and, decreased activity of the NA^+ K^+pump [100,101].

Intracellular Ca^{2+} increases during ischemia, which causes modulation of many Ca^{2+} ion channels. L-type Ca^{2+} channels have increased inactivation under the presence of increased intracellular Ca^{2+}, but other Ca^{2+} channels are more likely to activate, such as Ca^{2+}-induced Ca^{2+} release from the sarcoplasmic reticulum [18, 102]. The primary effect of increased intracellular Ca^{2+} is an increased tendency towards EAD and DAD to either initiate or sustain arrhythmia [81]. The main mechanism of increased intracellular Ca^{2+} is the decreased removal of intracellular Ca^{2+} from the Na^+/Ca^{2+} exchange [103]. Furthermore, as ischemia sets in, less Ca^{2+} is stored in the sarcoplasmic reticulum due to Ca^{2+}-induced Ca^{2+} release and inhibition of the re-uptake of Ca^{2+} by the sarcoplasmic reticulum [104].

Although many cellular changes occur as a result of ischemia and VF, many of these changes do not occur at once and instead have a complex time course. Due to the changes in electrophysiological properties, as a result of ischemia, it is hypothesized that there may be different mechanism of VF, depending on the duration [105]. Most simply, VF can be divided into either short duration VF or long duration VF [106]. A study by Li et al. measured endocardium activation patterns from a basket catheter placed in the left ventricle during VF. They found that during early VF (VF<3 min), the arrhythmia was maintained by nonstable reentry on the endocardium [13]. However, as VF progressed, the arrhythmia organized into two stable organization patterns. One of the organizational patterns was stable reentry on the myocardium. The other pattern was characterized by simultaneous activation of the endocardium, followed by a period of electrical silence, which was called ventricular electric synchrony (VES) [13]. VES is hypothesized to be a result of activation of rapid activation of the ventricular conduction system to drive the arrhythmia [13]. Changes to electrophysiological properties, such as activation rate and APD, of ventricular myocytes have been fairly well characterized over the time-course of VF [19]. However, these changes are much less known for the ventricular conduction system.

3.3.2 Conduction System and Ventricular Fibrillation

The ventricular conduction system has a unique structure that may be a primary driving factor for long-duration VF. During normal sinus rhythm, conduction occurs in the following order: AV node, proximal conduction system, distal conduction system, Purkinje myocardial junctions (PMJs), and VM. This direction of conduction is known as antegrade. As VF progresses and ischemia sets in, several electrophysiological changes occur in both the ventricular conduction system and the VM. One change is that the VM develops a longer period of refractory than the conduction system [107]. Another change during ischemic conditions is that distal Purkinje fibers are thought to develop abnormal automaticity and/or triggered activity. The triggered activity of the Purkinje fibers during prolonged VF may conduct up through the conduction system, perhaps as far as the proximal conduction system [12, 108]. The limited number of PMJs located only in the distal regions of the ventricular conduction system, in combination with the fast conduction velocity of the conduction system, suggests that it is unlikely that activations through the ventricular conduction system will collide and block with other activations within the conduction system before activating large portions of the conduction system. Therefore, it is likely that triggered activity in Purkinje fibers can conduct through the ventricular conduction system and drive rapid activation at distant sites, even opening the possibility of biventricular communication through the bundle branches. Evidence for this theory that the ventricular conduction system can drive fibrillation comes from experimental studies in which the Purkinje system was chemically ablated. In these studies, animals in which the ventricular conduction system was intact developed an activation rate gradient between the endocardium and epicardium, with the endocardium having a higher activation rate as VF progressed. However in the experimental group, where the Purkinje system was chemically ablated, no activation gradient developed, and VF spontaneously terminated earlier [14]. Another study by Huang et al. confirmed that canines have a more rapid endocardium rate than the epicardium during prolonged VF, but that this activation gradient did not develop in pigs [15]. The presence of an activation rate gradient is due to species-specific structural differences in the Purkinje system. In pigs, the Purkinje fibers are nearly transmural throughout the ventricular wall, and are not located only on the endocardium as in dogs or humans [109]. Therefore, if the Purkinje system has rapid activation rates, it would affect both the endocardium and epicardium. These studies indicate that the ventricular conduction system has a more rapid rate than the VM, and may be driving prolonged fibrillation [13–15, 105, 110, 111].

Although the evidence that the conduction system may have a primary role in maintaining VF is compelling, our understanding is limited due to technical aspects of studying the conduction system. One primary limitation in studying the conduction system during VF is that the signals are low amplitude compared to the VM, and there exist no reliable methods to measure these signals. For this reason, most of what is known about the conduction system's role in VF maintenance is not based on direct measurements from the conduction system, but instead its role is inferred from activation patterns present on the VM [13,112]. The studies that examine the conduction system directly measure only the Purkinje fibers at the distal end of the conduction system, but it is unknown what is occurring in other more proximal regions [14]. Aim 1 has two parts to address the limitations. The first part, which is technical in nature, is to develop novel signal processing techniques to distinguish the conduction system activation from AM and VM activity during VF. The second part is to answer a mechanistic question of whether the proximal conduction system, like the distal conduction system, is a driving force during the time course of VF, or whether it is passively being driven by the VM.

3.4 Atrial Fibrillation

AF is the uncoordinated electrical impulse propagation and contraction of the atria. The uncoordinated contraction causes blood to pool in the atria, which makes it more likely to clot and cause stroke [9]. AF is the most common cardiac arrhythmia, affecting over two million people in the United States, and its prevalence is expected to grow in the coming years [113, 114]. AF is a serious health concern associated with cardiomyopathy and increased morbidity and mortality [115]. Furthermore, even though there are multiple treatment strategies for AF, even the most successful have AF-free survival of less than 60% after only one year of treatment [116,117].

3.4.1 Progression From Paroxysmal to Persistent AF

AF has been characterized to gradually progress from short-lasting paroxysmal episodes to eventually longstanding persistent AF. To study this progression, AF has been investigated extensively with animal models, in which the animals undergo rapid atrial pacing (RAP) with a pacemaker. In these studies, it was found that the irregular rapid activations of the atria induce electrical, structural, and contractile changes to make this arrhythmia more persistent, in what was termed "AF begets AF" [118,119]. Due to the progression of AF, it is thought that the arrhythmia may be a manifestation of a diseased atria [120,121].

As AF progresses and cardiac substrate changes occur, the mechanism of the arrhythmia's initiation and maintenance may change. During paroxysmal AF, it has been shown that the pulmonary veins can initiate ectopic beats, due to either abnormal automaticity or triggered activity, to initiate AF [122]. However, as AF progresses, it is thought that atrial structural remodeling outside the pulmonary veins may be the main mechanism for initiating or sustaining AF [28, 91, 123, 124].

Electrical remodeling as a result of RAP has been shown to reduce the AERP in as little as 6 hours and can continue for weeks [125]. The lower AERP results in less excitability of Na^+ channels at low cycles due to conduction velocity restitution [126, 127]. Additionally, it was found that AF causes a shortening of the action potential duration. The decrease in action potential duration is primarily due to a decrease in L-type Ca^{2+} current [126, 128]. This electrical remodeling can result in sustained AF. The higher susceptibility of AF is a result of decreased cardiac wavelengths. As shown in Eqn. 3.1, a decrease in conduction velocity results in a decrease in the cardiac wavelength. When the cardiac wavelength is short, small regions of atrial conduction block may serve as a site for initiation of reentry [129]. A decrease in cardiac wavelength would also result in an increase in AF stability, e.g., longer episodes of AF, because more reentrant wavelengths can exist in a smaller region of the atrium. If more wavelengths are within a region of tissue, sustained reentry is more likely to occur [90, 130]. However, the electrical remodeling that occurs during AF is reversible following cardioversion and maintenance of sinus rhythm [131]. This finding has led to further research into examining structural and contractile remodeling that occurs during AF.

Three primary structural changes associated with AF are an increase in atrial cell size, an increase in intermyocyte distance, and an increase in fibrosis [129]. Atrial size increase is associated with the myolysis and pernuclear accumulation of glycogen. The increase in cell size is heterogeneous, with some cells being much more affected [132]. An increase in the intermyocyte distance is thought to be caused by an increase in extracellular matrix [40]. Fibrosis, which is a scarring process characterized by fibroblast accumulation and excess deposition of extracellular matrix proteins, has been shown to increase during AF [133]. Fibrosis has been shown to cause a disruption of side-to-side connections between muscle bundles, which results in a dissociation of conduction, and a zig-zag longitudinal conduction [134]. The zig-zag longitudinal conduction can allow for reentry to occur in a much smaller region of tissue than would be possible when the cardiac tissue is tightly electrically coupled [135]. Additionally, this electrical dissociation caused by fibrosis has been hypothesized

to decouple the synchronization of the endocardium and epicardium layers [30, 40, 136]. When the endocardium and epicardium layers are coupled, they activate simultaneously, therefore, propagation can be thought to occur in a two-dimensional medium. Once the layers desynchronize, the conduction medium is now three-dimensional and more circuitous pathways for reentry can occur. In line with these findings, patients with more fibrosis respond worse outcomes after treatment [137,138]. However, the mechanism is still unknown and debated.

AF results in uncoordinated contraction of the atrium. However, even after cardioversion to sinus rhythm, it can take up to a month before the contractile function of the atria is completely restored, with longer recovery times associated with longer durations of AF [139, 140]. The mechanism behind the loss of contractile function even after conversion to sinus rhythm is thought to be caused by a reduction in L-type Ca^{2+} conductance [141].

The main electrophysiology properties that are associated with and promote AF are a decrease in AERP and a slowing of conduction [142, 143]. However, it is unknown whether the relationship between a decrease in AERP and a slowing of conduction is cause or effect with patients who have AF. The classic "AF begets AF" shows that electrical remodeling caused by RAP can cause a decrease in AERP and conduction slowing to promote AF. However, most of this work has been done with animal models of AF. The RAP animal models, when extended to patients, then implies that patients who are prone to go into AF will have atrial remodeling to further promote the arrhythmia. Furthermore, these patients may not have much arrhythmogenic substrate before they first have AF. However, Sitles et al. found that patients who have had lone paroxysmal AF have an arrhythmogenic substrate, which included regions of slowed conduction during sinus rhythm [120]. Stiles et al. suggested that these patients, prior to going into AF, have an arrhythmogenic substrate and therefore are more likely to go into AF. Experimental research has shown that AF may either be a result of tachycardia-induced cardiac substrate, as suggested by AF begets AF, or that patients with a less healthy cardiac substrate are more likely to go into AF.

Regardless of whether AF progression is a result of tachycardia-induced remodeling, or atria that are already diseased are more likely to go into AF, the implication is that these changes make AF episodes last longer and are more likely to initiate. However, the mechanism behind what drives persistent AF is highly controversial and debated. The two main theories are based on the two mechanisms discussed in the canonical mechanisms of fibrillation maintenance. The first is that the substrate changes make more possible pathways for multiple wavelets type of AF to occur, and that there are not specific regions driving the arrhythmia. Multiple wavelets may be more likely to occur

in a remodeled atrium due to extracellular remodeling, which includes the development of fibrosis. Specifically, fibrosis may cause more disorganized conduction, and even result in endocardium to epicardium desynchronization [17,134]. Furthermore, desynchronization of the endocardium and epicardium allows for epicardium or endocardial breakthrough, which may help sustain the arrhythmia [91]. In the multiple wavelets theory, many regions are contributing to sustaining fibrillation. In the mother rotor theory, there are specific regions within the atrium driving the fibrillation, and it is argued that extracellular remodeling may be the reason. Regions of fibrosis may cause regions of abrupt conduction slowing [31] and have heterogeneity of repolarization kinetics [129], which may predispose these regions to maintain rapid reentrant/focal activity [144]. A stable reentrant pathway, or a rotor, may occur due to vortex shedding of a cardiac wave as it bypasses an inexcitable object [145]. The proposed mechanism of vortex shedding setting up stable rotors is explained in Fig. 3.5. Although controversial, there is some evidence to support the notion that the presence of stable rotors is the main driver and mechanism of persistent AF in patients [87,124,146].

3.5 Treatment Strategies

Treatment strategies for fibrillation are numerous and diverse, and include the use of pharmaceuticals, devices, and permanently altering the cardiac substrate.

3.5.1 Antiarrhythmic Drugs

Antiarrhythmic drugs are used to alter the ion channel kinetics of cardiac cells to make arrhythmias less likely to initiate and to be sustained [41,147]. This pharmaceutical approach is generally the first-line approach to control arrhythmias [148]. These drugs are divided into five classes based on their main mode of action on the cardiac cells [51]. Class I antiarrhythmics inhibit abnormal depolarizations by preferentially interfering with Na^+ channels. There are three types of Class I antiarrhythmics that are classified based on their effect on the action potential morphology. The first is a class Ia that lengthens the action potential. Examples of these drugs are disopyramide and quinidine. Class Ib antiarrhythmics shorten the action potential; examples of this class of drugs are Lidocaine, Mexiletine, and Tocainide. Class Ic does not significantly affect action potential morphology. Class II antiarrhythmics are beta-adrenergic blockers that suppress sympathetic activity on the heart. This class of antiarrhythmic primarily slows conduction through the AV node. Examples of these drugs are Metoprolol and Atenolol. Class III antiarrhythmics predominantly block K^+ channels, thereby prolonging repolarization time. The longer

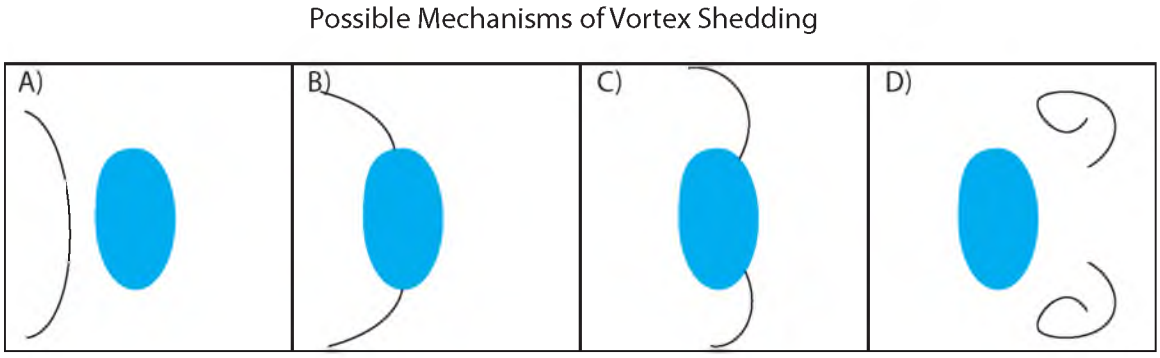

Fig. 3.5: **Schematic of initiation of a rotor due to vortex shedding**. **A)** Cardiac wave shown in black is approaching an inexcitable cardiac tissue shown in blue. **B)** Cardiac wave interacts with inexcitable cardiac tissue and begins to bypass the tissue. **C)** When cardiac wave bypasses tissue, a source sink mismatch forms at the boundary of the object. This source sink mismatch causes a convex wave shape at the boundary of the inexcitable object where conduction slows. **D)** If the curvature of the wave is large enough, the wave can start to rotate around an inexcitable center known as a singularity point. This rotational conduction around an inexcitable core is known as a rotor.

action potential durations in combination with the unaltered conduction velocities results in fewer pathways available to initiate or sustain reentry. These drugs also lessen formation of ectopic formation and EADs. Examples of these drugs are Sotalol and Ibutilide. Class IV antiarrhythmics are Ca^{2+} channel blockers. These drugs reduce conduction through the AV node, and therefore have an effect similar to Class II antiarrhythmics, but still allow the body to retain adrenergic control of heart rate and contractility. An example of this drug is Verapamil. The final class of antiarrhythmic drugs are Class V drugs, which work by other mechanisms than those discussed for the other classes. An example of a class V antiarrhythmic is Digoxin, which decreases conduction through the AV node by increasing vagal activity via central action on the central nervous system.

3.5.2 Device Therapy

Electrical shocks have been shown to terminate fibrillation. The mechanism relates to how cells respond to an external electric field. In response to an electric field, little current enters a cell due to the relatively high membrane impedance in comparison to the impedance of the extracellular space [149]. The internal voltage of the cell, therefore, does not drastically change during exposure to an external electrical field, but the extracellular voltage does change. As a result, the membrane potential, which is the difference between the internal and external voltage across the membrane, can rise above the activation threshold for the cell. If enough cells are activated with an electric field, then all propagating fibrillatory waves will collide with refractory tissue and the arrhythmia will terminate. Fibrillation can be treated with these electric shocks being applied externally, as by an external cardiac defibrillator, or internally, as by an internal cardiac device (ICD).

External cardiac defibrillation functions by placing two paddles on either side of the chest cavity, and then delivering energy to the chest. This energy then creates an electrical field that depolarizes large regions of the cardiac tissue. The depolarization causes the myocytes to become refractory, thus stopping all electrical activity. The refractory period of the entire cardiac tissue allows time for sinus rhythm to resume. This type of device is primarily used in emergency settings and can also be used to treat ventricular or atrial fibrillation.

Internal cardiac devices (ICDs) are commonly used for patients who are at high risk for ventricular fibrillation. Although ICDs can stop AF, the current injections are often too painful without sedation to be used for nonfatal arrhythmias [150]. ICDs function much like a local external cardiac defibrillator, but instead of creating an electrical field to depolarize the entire heart, ICDs inject current densities through an implanted lead to a specific site

on the ventricles. The current densities can be large enough to depolarize large regions of the ventricles which then makes the tissue refractory, thus causing cessation of the cardiac waves. A risk factor of this therapy is that large current densities can cause irreversible cardiac damage, which can make the tissue more arrhythmic in the future [151–153]. For this reason, there is active research in developing low-energy defibrillation techniques to limit the risk of injury, and also to make defibrillation less painful so that it can be used for patients with AF [154–158].

3.5.3 Ablation

Cardiac ablation is a procedure to apply energy to the cardiac tissue, through either radiofreqeuncy or cyrothearpy, to create a permanent scar that does not conduct. Cardiac ablation is an invasive procedure in which a catheter is inserted into a patient's blood vessel to provide access to the heart. Ablation is routinely used to treat patients who are at high risk for arrhythmias and do not respond to antiarrhythmic drugs [148]. Catheter ablation has the most success in treating tachycardia, where the goal is to ablate the origin of the arrhythmia [159]. The arrhythmia origin can either be an ectopic focus, caused by abnormal automaticity or triggered activity, or a region of stable reentry as shown earlier in Fig. 3.1. Ablation can be effective treatment in both cases but for different reasons. Ablation of an ectopic focus will kill the cluster of myocytes that have the abnormal automaticity or triggered activity; thus the arrhythmias will cease. Ablating the site of stable reentry will create inexcitable scar in the pathway of the reentrant circuit. For reentry to continue, a different path must be taken, and if there are no alternating pathways that satisfy Eqn. 3.1, discussed earlier, the arrhythmia will cease.

Although ablation has vastly improved over the past decades and has had success in treating tachycardia, determining the correct locations for ablating fibrillatory arrhythmias remains a challenge. Ablation is not used to treat patients susceptible to VF, since it is unknown where to target. However, ablation is standard for treating patients susceptible to AF if other methods have failed. Paroxysmal AF is thought to be driven by ectopic triggers from the pulmonary veins [160]. To treat tachycardia, triggers are directly ablated to terminate the arrhythmias. A similar method can be applied to paroxysmal AF, where the triggers are in the pulmonary veins, but instead of directly ablating the pulmonary veins, they are completely encircled with scar tissue. The scar tissue causes ectopic triggers from the pulmonary veins to collide and block with scar tissue around the pulmonary veins before interacting with propagating cardiac waves in the rest of the atria. Pulmonary vein

isolation for paroxysmal AF has been successful in treating the arrhythmia, but there has been less success in treating persistent AF [161]. Though the exact mechanism is unknown, it is believed that pulmonary vein isolation has poor outcomes in persistent AF because persistent AF causes atrial remodeling, creating regions outside the pulmonary veins that can initiate and drive the arrhythmia [26, 124, 162].

Many ablation strategies for treating persistent AF have been attempted but so far none have been proven to be more effective than pulmonary vein isolation in a randomized multiclinic study [148]. The treatment strategies in general try to find regions of the atrium that are sustaining the arrhythmia, although there is still no consensus on whether such regions exist. One targeted ablation strategy is to find regions of tissue that have complex fractionated atrial electrograms (CFAEs) [163]. Sites that contain highly fractionated electrograms are thought to be regions of conduction block, conduction slowing, or wavebreak, which all have arrhythmogenic properties [164]. However, these sites have not been found to be spatially stable, and ablation of these sites has not proved to be more effective than pulmonary vein isolation [165]. The nonstability of these sites suggests more of a multiple wavelets theory of fibrillation, since the driving sites are throughout the heart and are not spatially-temporally stable. Another proposed ablation targeting strategy is to ablate regions with high-frequency activations in the heart. A study by Kalifa et al. found that high-frequency sources drive some types of AF [166]. However, other studies have found that sites of high-frequency activation are not spatially-temporally stable throughout AF, making them not viable ablation targets [167, 168].

Targeting sites of CFAEs and high dominant frequency for ablation has not been successful in treating persistent AF, but there is promising research in the area of finding other ablation targets [169]. One such target are rotors, which are localized sources that are thought to drive AF [35]. Furthermore, some evidence suggests that ablation of these sources has better outcomes than randomized ablation [36]. These rotors have been found clinically by examining activation movies to identify sites of rotational activity around a core [87]. However, the reproducibility of identifying rotors still remains suspect, and other groups have not been able to treat AF by ablating rotors, and therefore this research needs to be further validated [170].

CHAPTER 4

CARDIAC STRUCTURE AND FUNCTION COMPARISON

This chapter provides an overview of techniques to bridge the domains of cardiac structure and electrical function. The generalized framework for each of these aims follows four stages. The first stage is to discriminate the cardiac substrate into different categories. The second stage is to acquire functional electrical measurements from these different substrates. The third stage is to register the structural and functional measurements to determine whether different cardiac substrates have different functional properties. The fourth stage is to determine how these differences in electrical properties relate to fibrillation.

4.1 Overview of Methods for Determining Cardiac Substrate

The aims in this dissertation use a combination of three techniques to determine the cardiac substrate. These techniques include differentiation of substrate-based on electrogram timing and morphology, differences in histology, and MRI-based interrogation. Each technique has several advantages and disadvantages, which is why multiple and overlapping techniques are used for each aim. Electrogram-based approaches are the least specific, and therefore can be used only if there is a drastic difference between cell types. Histology-based methods can have micrometer resolution, but these methods are typically used to examine only smaller regions of tissue. MRI-based methods are the most global, i.e., these methods can examine the entire heart; however, this method is also the most controversial and has only millimeter sensitivity.

4.1.1 Electrogram-based Interrogation

Electrogram-based interrogation of cardiac substrate examines features of electrograms to discriminate cardiac substrate. The physiological basis to this approach is that there are differences in action potential shape and timing based on the cell type. A simple form of

this approach, which is used throughout the aims, is to distinguish ventricular from atrial electrograms. This distinction is done by comparing electrogram timing to the complexes in the ECG. The different complexes in the ECG correspond to the atrial and ventricular activity. If an electrogram shows activation during the P wave, it is an atrial signal, and if the electrogram shows activation during the QRS complex, it is a ventricular signal. This approach does, however, become more complicated during fibrillation because there is less coupling between the two chambers, and atrial activations may be overshadowed if they are simultaneous with the QRS.

Electrogram-based interrogation of the substrate is a primary tool used in aim 1 to discern the ventricular conduction system from atrial and ventricular tissue. This approach is used because there is no visible difference, without magnification, among His bundle, atrial, and ventricular tissue. However, there are differences in the timing of local activations with respect to the ECG, which can be observed during sinus rhythm. In an ECG, the P wave corresponds to atrial activation. Therefore, if an electrode is placed anywhere on the atrium, the local activation will occur sometime during the P wave. Likewise, local ventricular activation will occur sometime during the QRS complex. During sinus rhythm, conduction occurs from the atrium to the ventricles through the AV node and ventricular conduction system. Therefore, the ventricular conduction system, including the His bundle, will have local activation sometime in between the P wave and QRS complex. The His bundle is a very thin structure in proximity to VM and AM. An electrode on the His bundle can often detect both VM and AM activity along with the His bundle, which results in an electrogram showing three distinct activations during sinus rhythm, with the first corresponding to the P wave, the second in the PR interval, and the third corresponding to the QRS. Using this technique the His bundle can be identified. Fig. 4.1 shows an example of an electrode plaque measuring atrial, His bundle, and ventricular activity and the corresponding ECG. A limitation to this approach is the unknown relationship between AM, His, and VM activation during VF. Therefore, examining the ECG and the electrograms during VF is of little use. His, VM, and AM activations can be differentiated by calculating the gradient of the divergence of the unipolar electrograms, which is known as the Laplacian. The gradient of electrograms within a region of tissues is proportional to the current flow between the regions of tissue. By evaluating the divergence of the gradient, current sources and sinks can be evaluated. Any Laplacian signal above the isopotential line is a current source, and negative Laplacian values are current sinks. Evaluating the Laplacian of electrograms has been shown to better quantify local tissue activation during

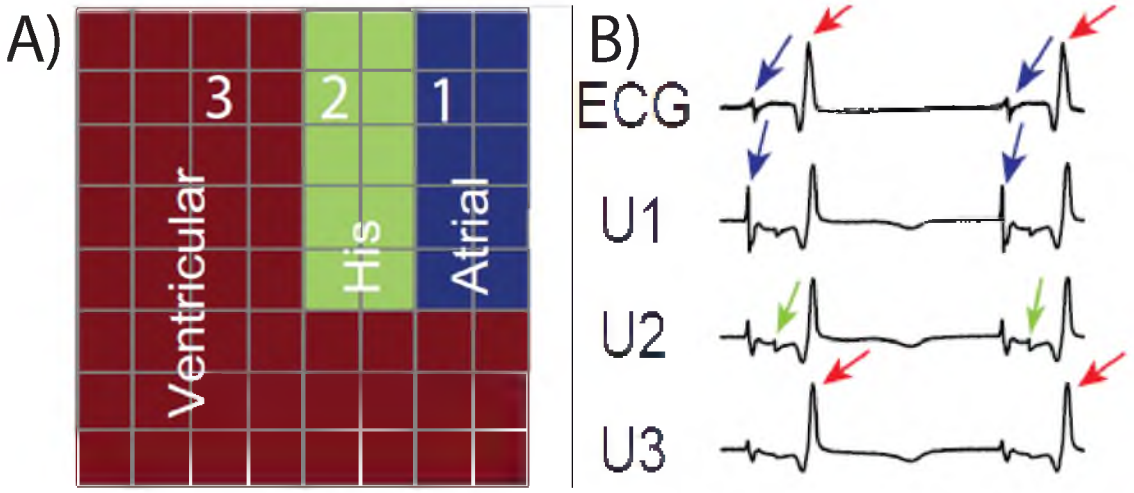

Fig. 4.1: **Recordings from an array placed over the His bundle. A)** Strong ventricular, His, and atrial signals were recorded during sinus rhythm from the three regions of the 8x8 electrode array, 300 um spaced electrodes, shown in red, green, and blue, respectively. Electrograms at sites 1, 2, and 3 are shown in B). **B)** A pseudo ECG, unipolar electrogram (from sites 1, 2, and 3 in A), during sinus rhythm. Each recording was 500 ms in duration. The unipole at site 2 shows ventricular (red arrows), His (green arrows), and atrial (blue arrows) deflection.

fibrillation [171, 172]. The Laplacian signals can be calculated using a standard central difference approach according to Punske et al. [172]:

$$V_C - \frac{V_W + V_E + V_N + V_S}{4}, \tag{4.1}$$

where V is the voltage, subscript C refers to the central electrode, and the other subscripts, W, E, N, and S, refer to the relative positions of the other electrodes in the compass directions. Activation of the underlying cardiac tissue is the zero crossing of the Laplacian, when the tissue is turning from a sink to a source. Fig. 4.2 compares a unipolar electrogram, the derivative of the unipolar electrogram, and the Laplacian of the unipolar electrogram. The advantage of utilizing the Laplacian is that stage three of the generalized approach is trivial because the registration of the cardiac substrate with the functional measurements is completed in the process of determining the substrate.

A limitation to electrogram-based interrogation is that it requires there to be drastic differences in the electrograms, and for these differences to be known. Aims 2 and 3 examine healthy and more fibrotic atrial tissue; however, there is not strong evidence of differences in electrogram characteristics between fibrotic and atrial tissue. Some studies have examined sites of fibrotic tissue, as determined by MRI, and have shown that these sites may be more fractionated or have lower voltage [173]. However, others studies disagree by showing that fibrotic tissue may have normal electrophysiological characteristics during sinus rhythm, and regions of low voltage may be present due to reasons other than fibrotic tissue [165]. Many studies have examined the impact of fibrotic tissue on cardiac conduction; however, most of these studies determine the location of fibrotic tissue as sites of low voltage and CFAEs [165]. These results are somewhat controversial because they have limited histological data to compare with their electrogram-based approaches. Therefore, there are more robust methods than electrogram-based approaches to characterize the fibrotic tissue, including histology and MRI.

4.1.2 Histology-based Interrogation

Histology is the gold standard for evaluating cardiac substrate. However, acquiring cardiac histology in human patients is often not possible. For this reason, cardiac substrate is often evaluated using animal models [29, 136]. Masson's trichrome staining, shown in Fig. 4.3, is a technique used to separate tissues into three color groups: red for myocytes, blue for collagen/fibrotic tissue, and white for nonfibrotic extracellular content. From these stains, fibrosis densities can be quantified.

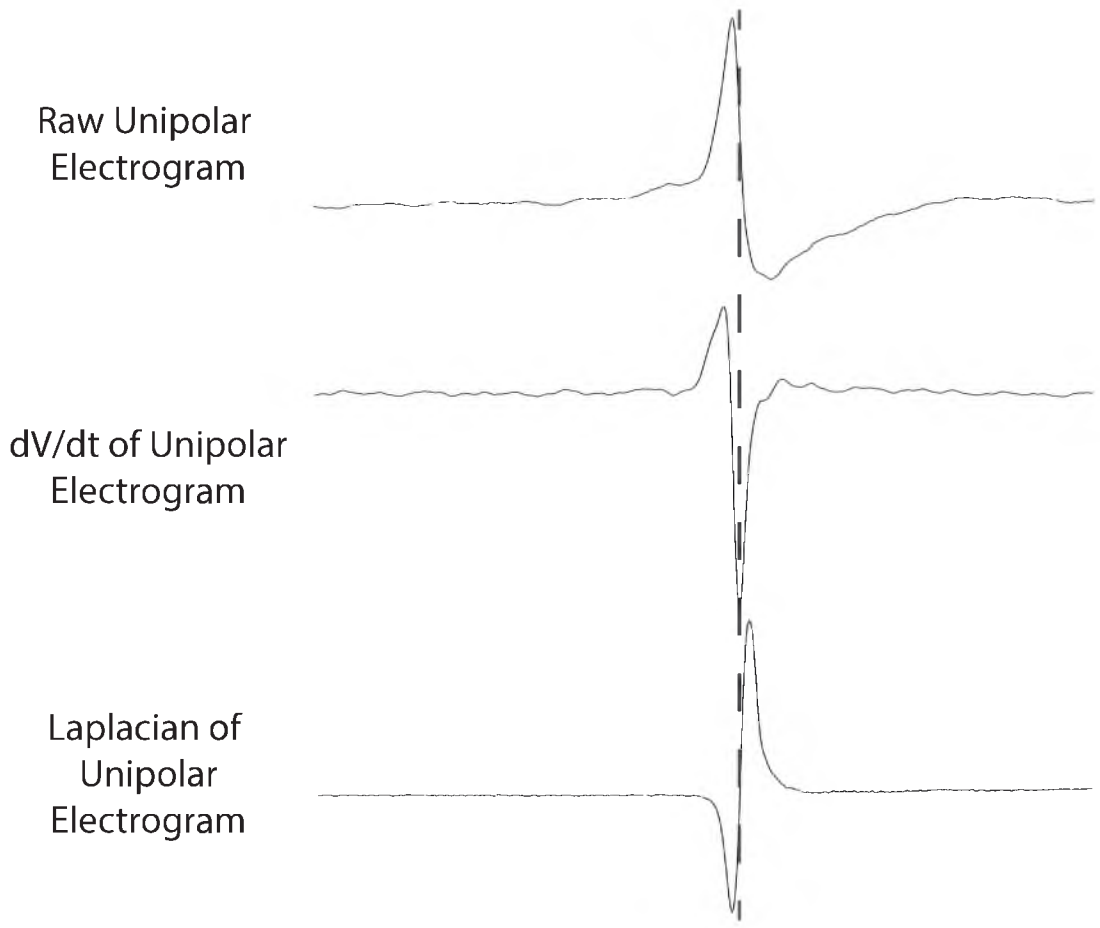

Fig. 4.2: **Comparison between unipolar and Laplacian electrograms.** A temporal derivative and Laplacian are computed from a unipolar electrogram. Activation from the unipolar electrogram is the steepest downslope, which is the local minimum of the temporal derivative. Activation in the Laplacian occurs when the tissue transitions between a current sink to a current source, which is the zero crossing. The dashed line shows the activation times for the signals. The recording is 60 ms in duration.

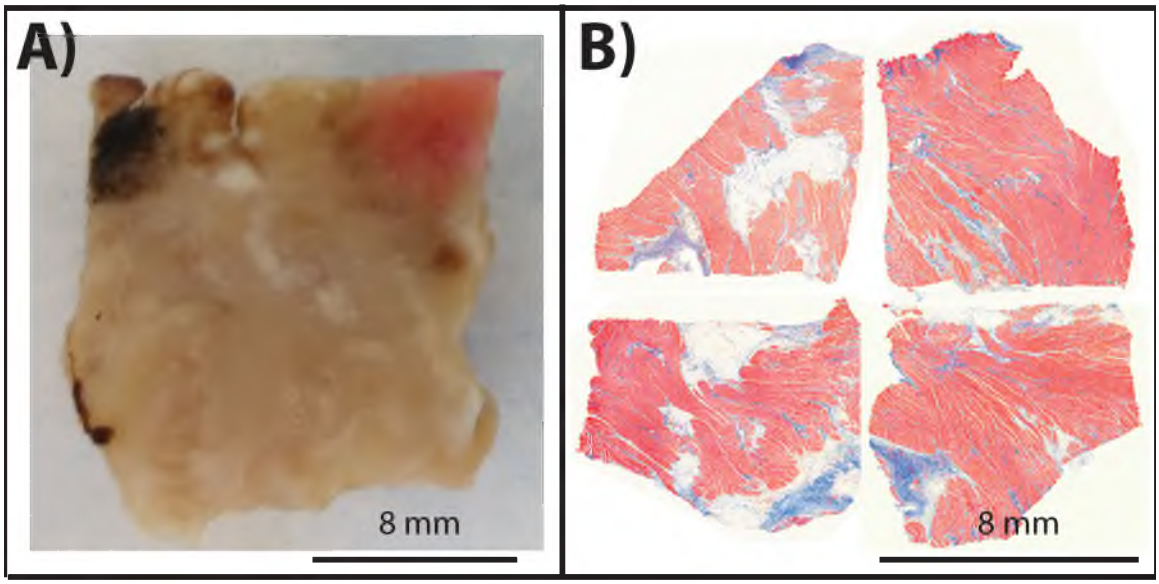

Fig. 4.3: **Masson's trichrome stain of cardiac tissue. A)** Left atrial tissue acquired from an explanted heart. The black and red spots in the corner of the histology in A) are tissue dyes which were used to mark the orientation of the electrode plaque on the histology. **B)** Example of a Masson's trichrome stain of left atrial tissue. Red indicates myocytes, blue is collagen/fibrosis, and white is extracellular content. Each square is one quarter of the mapped region that was reconstructed to the full sample.

4.1.3 MRI-based Interrogation

Cardiac MRI is one of the few nonivasive methods used to validate cardiac scar and fibrosis [174, 175]. The difference between scarred and healthy tissue can be detected with MRI because the magnetic resonance characteristics of protons vary between tissues. These tissue-level differences can be detected by measuring the T1 relaxation time (longitudinal relaxation time), which is how fast protons reequilibrate their spin following MRI pulses [175]. T1 varies by water content, fibrosis, and extracellular volume [176]. This finding makes possible noninvasive detection of fibrosis. This technique is traditionally used to determine the mean T1 time of a heart, where lower T1 times correspond to a more fibrotic heart after contrast injection. However, the technique can be expanded to determine regional differences in T1 by means of T1-mapping MRI. This measurement requires acquisition of both a T1-weighted image, I_{T1w}, and a proton-density-image, I_{PD}, after gadolinium contrast injection [177]. From these images, a pixel by pixel T1 map can be computed by solving the Bloch equation governing T1 relaxation:

$$\frac{I_{T1w}}{I_{PD}} = M_0 \frac{1 - e^{-T_D/T_1}}{M_0}, T_1 = -\frac{T_D}{\ln(1 - e^{-T_D/T_1})} \tag{4.2}$$

where M_0 is the unknown equilibrium magnetization and T_D is the saturation recovery time delay (a set parameter). With this technique, normal tissue can be distinguished from more fibrotic tissue. The only limitation is the resolution of the acquired MRI. Fig. 4.4 shows a segmentation of a T1-mapping MRI of a LA. The regions of low T1, shown in blue, correspond to an increase in fibrosis as determined by histology.

4.2 Overview of Methods to Measure Cardiac Electrical Behavior

Electrical potentials are measured to determine conduction properties of an arrhythmia. There are many methods to measure and analyze electrical potential. Each measurement and analysis tool has inherent limitations, and therefore the goal is to choose the measurement and analysis system that minimizes the effect the limitations will have on the overall results. This section will detail different methods for measuring electrical potential, including intracellular versus extracellular measurements, and then will focus on different approaches to analyzing fibrillation.

4.2.1 Measuring Electrical Potential

Traditionally, electrical potential from cardiac tissues has been measured from electrodes, which act as the interface between cardiac tissue and measurement equipment.

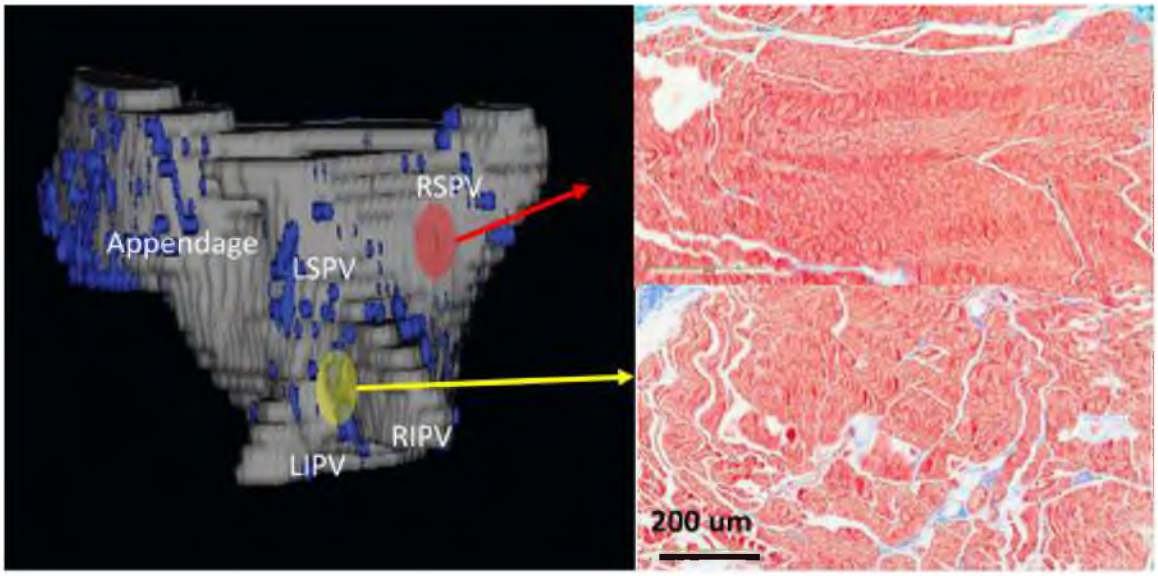

Fig. 4.4: **T1 mapping can determine regional differences in fibrotic tissue.** Left panel shows a segmented LA shell with blue regions showing the regions with the lowest 10% of T1 values, indicating fibrotic areas. On the right panel is Mason's Trichrome stained tissue from a region with low T1 (panel B) and high T1 (panel C).

Measurement equipment, usually in the form of a data acquisition system (DAQ), can measure potential, but the mode of transmission is in electrons. In the body, however, electric potential interacts with ions. Therefore, the electrode is a transducer that converts ionic current into electrical current so that it can be measured. Two major types of potential measurements can be made, depending on where the recoding and reference electrodes are placed. Intracellular electrograms are made when the recoding electrode is placed inside the plasma membrane and the reference electrode is placed in the extracellular space. For the second type of measurement, both the recording electrode and the reference electrode measure extracellular potentials.

Intracellular electrograms measure the sum of all currents that are moving in the intracellular space with reference to the extracellular space. Intracellular electrograms are primarily recorded with either glass pipette electrodes or utilizing voltage-sensitive dyes. Glass pipette needle electrodes puncture the individual cells, which allows the measurement of the intracellular space. These measurements can be technically difficult to acquire because the glass needle tip can easily break. Drugs, which stop the heart's mechanical motion while leaving the electrical properties intact, are often used to limit the likelihood of the glass needle breaking. These types of drugs are known as electrical mechanical uncouplers. A limitation to this technique is that it is difficult to have many simultaneous glass pipette recordings, and therefore these measurements are not suitable for understanding whole-heart or even regional-based conduction properties. Glass pipette measurements are ideal, however, for measuring properties within the intracellular space, such as Ca^{2+} currents, or action potential morphology under different conditions. Voltage-sensitive dyes are another method to measure intracellular electrograms, and this method can be applied over a large region of tissue. Voltage-sensitive dyes function by binding to the membrane of cardiac cells. The voltage-sensitive dye can then be excited by a specific wavelength of light. Once excited, the dye then emits fluorescent light, which is a function of the membrane potential [178]. The fluorescent light can then be recorded with an array of photodiode arrays or from charge-coupled device cameras. The major limitation of optical mapping is that heart motion can create artifacts. Each pixel in the camera recording space is assumed to record the same region of cardiac tissue throughout an optical mapping study. However, if the heart is moving, each recorded frame could be measuring fluorescence from a different location. For this reason, electrical mechanical uncouples are often used [179].

Extracellular electrograms measure changes in currents propagating in the extracellular space. The two primary extracellular electrograms are unipolar and bipolar. A unipolar

electrogram is when the recording electrode is placed on the tissue of interest, and the reference electrode is placed far away (ideally, infinitely far away). An action potential measured from extracellular electrodes looks different from an intracellular electrode, although they do contain similar information. The first complex in an intracellular electrogram corresponds with the depolarizing of the cell, where the maximum negative value of the first temporal derivative corresponds to activation. This first complex occurs as Na^+ enters the cell through gap junctions, but the extracellular electrogram is measuring the flux in extracellular current in response to Na^+ flow. As a depolarizing wave is approaching the electrode, it measures a more positive value. As the wavefront leaves, it measures a negative value. After the activation phase, the measurement will read an isopotential zero; this occurs while the cell is depolarized. During this time, intracellular Ca^{2+} release is prolonging the action potential, but there is little extracellular current. During repolarization, K^+ begins to repolarize the cell. The repolarization causes the T wave of the unipolar signal. The maximum upstroke of the T wave is the repolarization time. The T wave can have many different morphologies, depending on the repolarization of the cardiac tissue compared to the reference [180]. If the measured site depolarizes relatively early compared to the reference, the T wave is always positive. If it has relatively late repolarization, the T wave will be always negative. If a region of tissue repolarizes inbetween global early and late repolarization, the result will be a biphasic T wave (Fig. 4.5). From unipolar signals, the action potential duration can be estimated using the definitions of activation as the steepest downslope of the activation complex and repolarization as the steepest upstroke of the T wave. Another feature of interest in unipolar signals is the amplitude. Scar tissue, whether caused by infarct or ablation, has a lower unipolar amplitude. Even though a single action potential for a given cell type has approximately the same amplitude, due to the all or nothing response of an action potential, the unipolar electrogram records many nearby cells. If some of the myocytes within the electrode's recording field are scarred and no longer excitable, fewer of the myocytes will activate. When fewer myocytes activate there is less extracellular current flux, which is directly related to the unipolar electrogram's amplitude.

The other type of extracellular electrogram is a bipole. This measurement consists of subtracting two nearby electrodes from each other. The resulting signal measures less far-field signal; however, it loses many of the characteristics of unipolar electrograms that make it comparable to an intracellular electrogram. The main reason for the differences is that traditional bipolar electrograms can detect the magnitude of current only in the direction of the electrodes. For example, consider a propagating wave. If the electrodes are

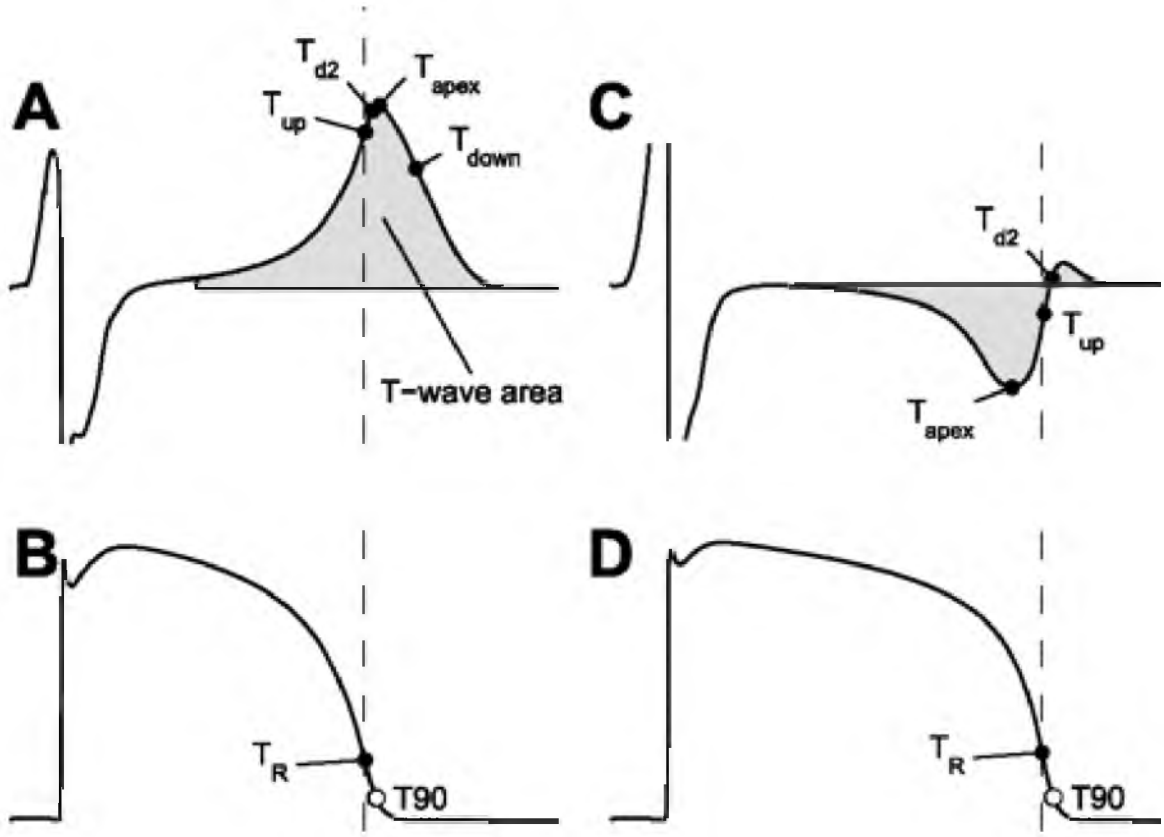

Fig. 4.5: **Extracellular versus intracellular electrograms. A) and C):** simulated unipolar electrogram (UEG). **B) and D):** simulated action potential (AP) at the same locations as A and C, illustrating the reference markers. The dashed line in each panel marks the local repolarization time (TR). T90, instant of 90% Tup, instant of steepest upstroke of the T wave; Tdown, instant of steepest downstroke of the T wave; Td2, instant of minimum second derivative of the UEG. Reproduced with permission from Potse et al. [179]

orthogonal to the wave, the bipolar electrogram will detect a large signal because as the wave passes the recording site, there is a period where one electrode may detect depolarization while another electrode in the set still is not detecting current flux, since the wave has not yet reached it. However, for this same wave, if the electrodes are parallel to the wavefront, both electrodes will detect the depolarization simultaneously, and thus no signal will be measured. For this reason, a bipolar is considered a directional measurement. However, coaxial bipolar electrograms do not have this directionality issue [181]. An example of differences in bipolar electrogram morphology and cardiac wavefront direction is shown in Fig. 4.6. One similarity to unipolar signals is that bipolar electrograms are considered to detect activation at the point of steepest downslope. However, due to the dependence of direction, these measurements have less meaning in amplitude, and have no indication of repolarization. During fibrillation, these measurements become harder to interpret due to constantly changing and unknown wavefront directions. Bipolar electrograms are often used clinically due to the removal of far field noise, which makes detecting activations simpler.

4.2.2 Cardiac Electrical Mapping

Knowing only the activation of a single electrogram is insufficient to determine whole-heart conduction. For this reason, many electrograms are often measured simultaneously, and from these measurements different maps can be made to understand cardiac conduction. There are three primary methods used for analysis of fibrillation organization from recorded electrograms, which include: examining the electrogram's amplitude, frequency, or phase characteristics, although new promising research is examining how to combine some of these metrics [182]. Every signal, including a cardiac electrogram, contains amplitude, frequency, and phase information. By analyzing these features of electrograms, conduction and the organization of fibrillation can be quantified.

The first class of mapping focuses on the time domain of electrograms and examines both voltage and relative activation times. The simplest form of this map is a voltage map. The voltage map shows the measured potential at each recording site for a given instant. In these maps, polarized tissue (approximately -80 mV) corresponds to tissue at rest, whereas more positive potentials indicate tissues in different stages of an action potential. These maps are most commonly used for optical mapping because they require high spatial resolution intracellular recordings. Clinical voltage maps are made from extracellular recordings and measure the amplitude of a detected activation. These maps can be made from both unipolar and bipolar maps; however, bipolar lead placement with the wavefront must be

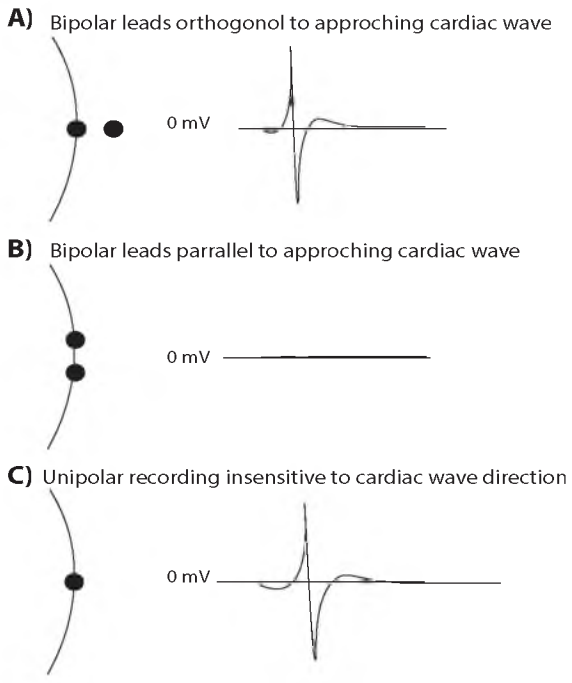

Fig. 4.6: **Bipolar electrogram morphology versus electrode position. A** Bipolar lead orthogonal to approaching wavefront. A bipolar electrogram is measured because one electrode measures extracellular current flux before the other electrode in the bipole. **B** Bipolar lead parallel to approaching wavefront, which results in a low-amplitude electrogram because both electrodes measure the extracellular current flux simultaneously, and therefore the activation is seen as common mode noise and subtracted. **C** Unipolar electrogram is invariant to wavefront direction.

considered for the bipolar voltage maps. Features of interest are regions of low voltage that are thought to be scar tissue, caused by either ablation or diseased tissue. These maps are used after ablation to detect whether the ablation resulted in scar. Another type of time domain mapping examines the relative timing between tissue activation. Activation is usually considered the local minimum of the temporal derivative of the electrogram. Activation detection can be done for each electrode and the time of activation can be plotted from each electrode that constructs an activation map. If the electrodes are close enough, an electrical wavefronts pathway can be determined. A metric that can be defined from activation mapping is how much fractionation is present in an electrogram during fibrillation. A highly fractionated electrogram will have many activations within a time window often smaller than the refractory period of a single myocyte. If an electrogram contains several activations within a single cell's refractory period, it is known as a complex fractionated atrial electrogram (CFAE). Detecting activations can be subjective due to the need to define a threshold for what local minimum of the derivative should be considered an activation. One impartial way to examine the presence of CFAEs is by computing Shannon's entropy. The significance of CFAEs remains controversial. Some reports have found that regions of complex fractionation are due to fibrosis, whereas others have shown that regions of CFAEs could also be functional, and not related to fibrosis [183]. Another common time domain analysis technique that utilizes activation detection is how regular the cycle length is during fibrillation. One metric that can examine this regularity is reg-idx. Reg-idx is computed as the standard deviation of the cycle length of an eletrogram's activations divided by the mean cycle length. As reg-idx approaches zero, the electrogram has a more regular cycle length, and as reg-idx approaches 1, it becomes less regular. Fig. 4.7 shows some examples of time domain analysis of cardiac signals.

Another class of analysis examines the frequency content of electrograms. The frequency content can be analyzed by computing a Fast Fourier transform (FFT) over at least several seconds of fibrillation. The FFT converts a signal from one domain, such as the time domain, into the frequency domain. Specifically, the FFT decomposes a signal into sinusoids of different frequencies that could reconstruct the original signal, and is computed as follows:

$$X_k = \sum_{n=0}^{N-1} x_n e^{-i2\pi k \frac{n}{N}}. \tag{4.3}$$

From the FFT, a power spectrum can be computed. The peak of this spectrum is related to the activation rate of the tissue if certain conditions are met [88]. The dominant frequency finds the local maximum of the power spectrum within a certain range of physiologically

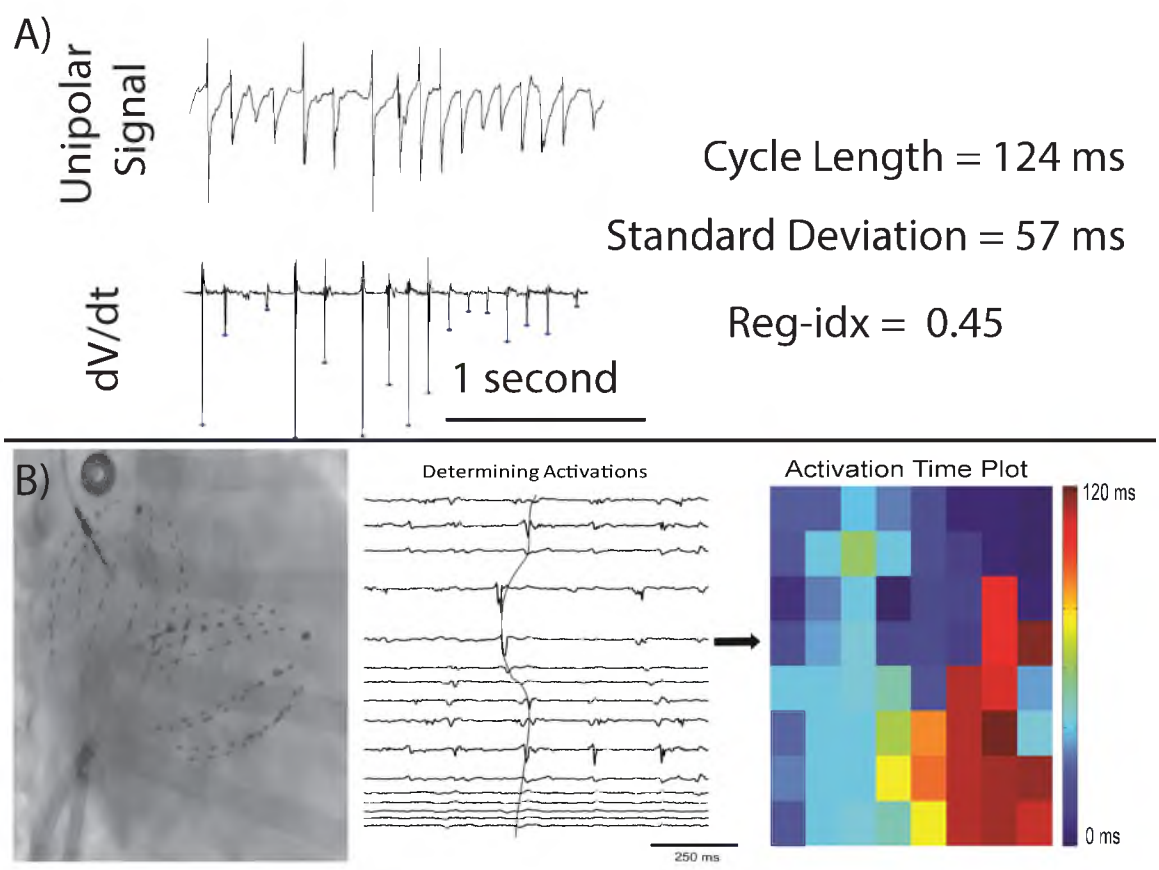

Fig. 4.7: **Time domain activation detection and signal processing. A)** Example of determining activations for a unipolar signal. Local minimums of the first derivative are selected as activation times. From these activation times, several parameters can be computed, such as cycle length, standard deviation, and reg-idx. The relatively high reg-idx value indicates that this region of tissue does not have a regular cycle length. **B)** Example of examining relative activation times from multiple electrodes. Unipolar electrograms were obtained from a basket catheter, which is shown under fluoroscopy. Activation mapping shows the relatively early and late activations for a 120ms window during fibrillation.

viable activation frequencies. A problem with this method is that the dominant frequency may not always reflect activation rate, especially for highly fractionated electrograms [184]. Despite this limitation, dominant frequency analysis is still widely used to approximate activation rates [38]. Another method to quantify the power spectrum is the organizational index. This metric analyzes the frequency range of electrograms. Narrow-frequency-ranged electrograms have a higher organizational index and are thought to be sites of rotors or focal activity to drive an arrhythmia [124]. The advantage of the spectral analysis methods is that it does not require defining activation, which can often be subjective and not apparent. Furthermore, with this method each electrogram is analyzed separately and does not require information from nearby electrodes. For this reason, this method is most appropriate for examining data with sparse spatial resolution. If the fibrillation is stochastic, and not one region is driving the arrhythmia, the power spectrum may look like white noise, or may change over time. However, if certain regions of the cardiac tissue are driving the arrhythmia, this method would show regions of the atria that have consistently high dominant frequency. Fig. 4.8 shows an example of the spatial distribution of dominant frequency on the endocardium of the LA during AF.

The final common cardiac mapping method is to examine an electrogram's phase information. The phase of a signal shows the different stages of a signal that is divided into 2π radians. If a signal is not completely random, there should be some relationship between past and present samples of that signal. This relationship can be shown using phase space plots, which were developed in the field of state-space mapping of nonlinear dynamics [185]. In a phase space plot, a signal is plotted versus a time-delayed version of itself. If there is a relationship between the current sample and past samples, the phase space plot will show organization. Specifically, the plot will take some shape and rotate around a central point known as an attractor. Therefore, in cardiac systems, if there is an organization to the conduction, the phase space plots should show rotation around an attractor. Examples of phase plots for different signals are shown in Fig. 4.9. The phase from the phase space plot can then be calculated for any time instance by computing the angle from the attractor to a point on the phase space plot. When acquiring data for analyzing cardiac signals, often an array of electrodes is used so that many points on the cardiac tissue can be recorded simultaneously. A phase angle can then be computed for every electrode within the mapping region, and plotting the phase for every electrode location is known as a phase map. Points of interest on a phase map are locations where there are phases from $-\pi$ to π around a central point. This central point is known as a phase

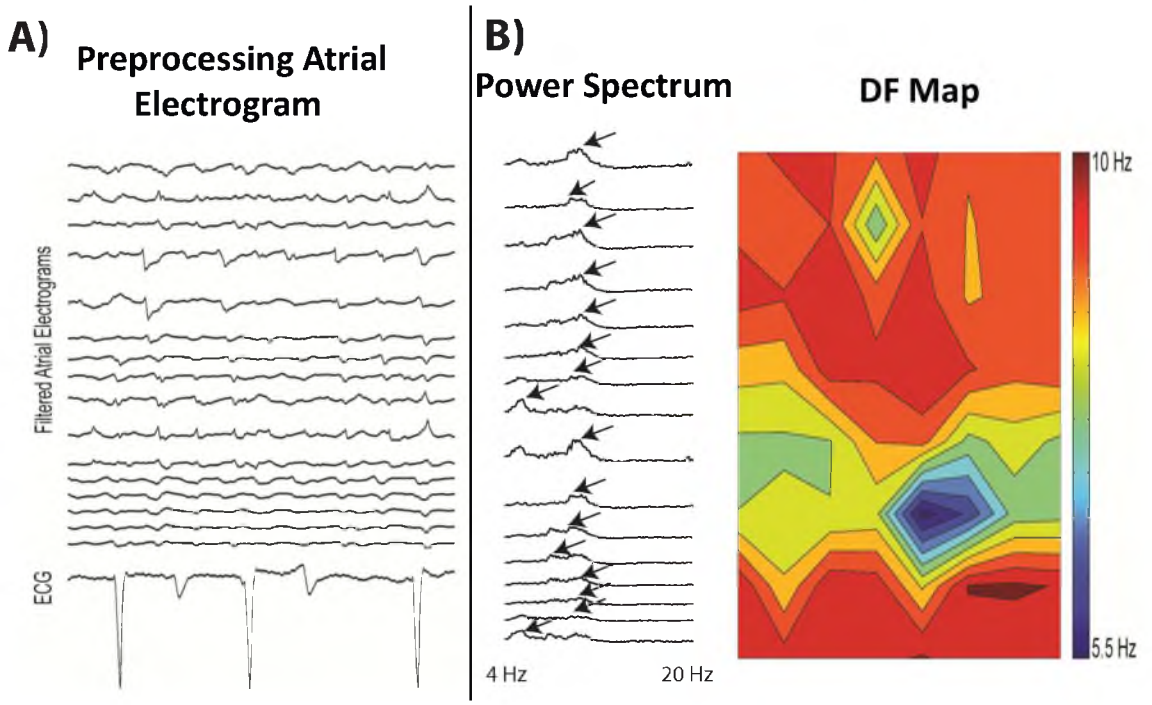

Fig. 4.8: **Spectral analysis.** **A)** Electrograms from basket catheter placed in LA of animal in chronic AF. The preprocessing phase includes QRS subtraction to remove far-field ventricular activity from the atrial electrograms. **B)** Compute power spectrum from electrogram data. The dominant frequency of each electrogram was found as the local maximum in the power spectrum from 4-12Hz. The spatial distribution of the dominant frequencies can then be shown.

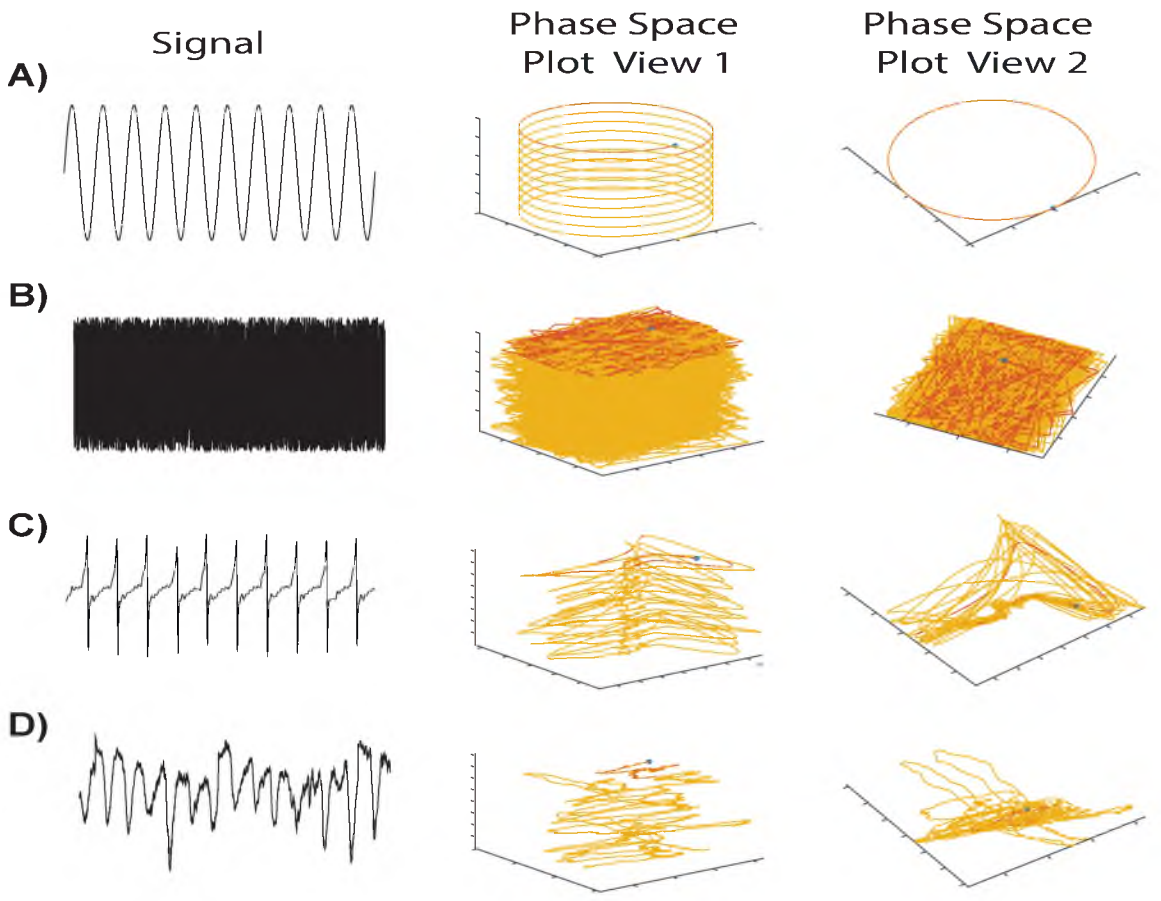

Fig. 4.9: **Phase Analysis.** Examples of signals and corresponding phase space plots are shown. In the phase space plots, the x and y axes show signal amplitude and the z axis is time. Phase space view 2 is looking down on z axis. **A)** Sinusoid signal and corresponding phase space plots. Relationship between previous input and current input is constant throughout time, which is shown by the circle with constant amplitude in the phase space. **B)** White noise and corresponding phase space plots. As expected, the phase space plots show no relationship between past and current input so there is no organization in the phase space. **C)** Atrial flutter electrogram and corresponding phase space plots. Phase space plots show a more triangular shape, which corresponds to the sharp edges in the time domain. The phase space does show organization around a point through time, which is due to the consistent, regular atrial activations. **D)** Atrial fibrillation electrogram and corresponding phase space plots. Phase space plots show much less organization than the atrial flutter phase space plot. The phase space does not show organization because fibrillation is a highly unorganized arrhythmia defined by many dynamic pathways for cardiac wavefronts.

singularity, and it is thought that these locations are pivot points for reentrant circuits and rotors [186]. An example of a phase map is shown in Fig. 4.10. Phase-mapping techniques and identifying singularity points have been applied to cardiac arrythmias to try to locate regions of stable reentry or rotors [35, 57, 185].

4.3 Methods for Determining and Registration of Cardiac Functional and Substrate Data

This next section will specify the generalized framework- stage 1: Discriminate the cardiac substrate into different categories, stage 2: Acquire the electrical measurements from these different substrates, Stage 3: Register the structural and functional measurements, Stage 4: Determine if different structures promote fibrillation- will be applied to each aim. In summary, the three aims in this dissertation are:

- Aim 1: Characterize how the activation rate and conduction velocity of the proximal conduction system change during the time course of VF.
- Aim 2: Determine how local fibrotic tissue architecture and densities in chronic AF relate to conduction changes that facilitate reentrant activity.
- Aim 3: Evaluate the relationship between fibrotic myocardium determined by magnetic resonance imaging and local drivers of persistent AF.

4.3.1 Rational for Methods in Aim 1

Aim 1 uses a high-density electrode plaque and examines sinus rhythm and fibrillation in an isolated perfused rabbit heart. The main challenge with aim 1 was to find a way to discriminate between AM, VM, and His bundle signals. To overcome this challenge, the Laplacian method was used to find clear activations for each type of cardiac tissue. In this aim, stages 1 and 3 of the generalized framework are completed simultaneously. The high-density electrode plaque is placed between the RA and RV, which is in the approximate location of the His bundle. Activations of the Laplacian electrograms can then be compared with the waves and complexes in the ECG to identify atrial, ventricular, and His bundle tissue (stages 1 and 3). Once this identification process is completed, fibrillation can be induced and functional measurements can be acquired (stage 2). Due to the unambiguous activation times that could be found with the Laplacian method, time domain analysis and creating activation maps were appropriate for this aim and were used to determine the electrophysiological properties of the VM and His Bundle, thus completing stage 4.

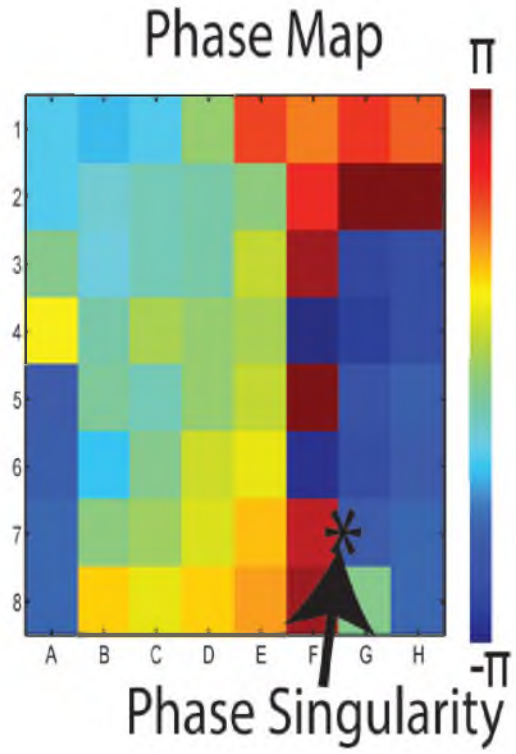

Fig. 4.10: **Phase Map**. Phase map showing a singularity point based on basket data. The x axis is the spline numbers A-H and the y axis is the electrode numbers on the corresponding spline.

4.3.2 Rational for Methods in Aim 2

Aim 2 examines the onset of AF in an open chest preparation of a chronic AF goat. Stage 1 in this aim is to separate out regions of fibrotic tissue and further subdivide fibrotic tissue based on its architecture. Masson's trichrone staining of histology from the mapped region was used to locate fibrotic tissue. The open chest preparation allows for extracting histology in the same location from which functional electrical measurements were acquired. Stage 2 of aim 2 uses both a S1 and a S1-S2 pacing protocol. Conduction velocity at the various coupling intervals is then computed. Atrial signals are small compared to ventricular signals, but since the recordings are acquired during sinus rhythm, activation mapping is again the most appropriate method for characterizing conduction velocities that require determining activations times. Stage 3 was completed by registering the orientation of the histology with the electrode plaque. This registration was done by carefully marking the extracted histology so that its orientation relative to the recording plaque was known. Stage 4 then compared the architecture of fibrotic tissue, as determined by histology, with the conduction data obtained with the pacing protocols.

4.3.3 Rational for Methods in Aim 3

Aim 3 uses basket catheters to electrically map AF in chronic AF canines in vivo. Stage 1 in this aim uses T1-MRI to determine regions of the LA that are fibrotic. Although T1-Mapping MRI is one of the few validated methods to measure fibrotic tissue noninvasivly, histology was taken from the animals a few months after the in vivo experiments. Stage 2 of aim 3 used basket catheters to electrically map large regions of the endocardium. Although much of the LA can be covered with these baskets, they have high interelectrode distances and can have poor contact with the atrial wall. Stage 3 of Aim 3 is done by creating an electroanatomical map during the in vivo study. Tthe electroanatomical map is made by placing a catheter inside the LA and recording the 3D position of the catheter. The catheter is then moved around the endocardium of the LA, which creates a geometry. This geometry was then merged with the T1-Mapping MRI geometry. The merge is accomplished by selecting known corresponding points between the two geometeries. Examples of corresponding points are the four pulmonary veins, the gaps between the pulmonary veins, the mitral valve, and the appendage. Stage 4 of this aim is challenging due to the limitations of the basket catheter, and the LA signals are often of low amplitude, which makes activation detection difficult. Furthermore, the large interelectrode distances, 4 mm, make it difficult to determine wavefronts. For example, if an activation occurs at

an electrode, then after a short delay, an activation is detected on a nearby electrode. It is not clear if these activations occurred from the same wavefront, or if during the delay, the original wavefront that caused an activation may have dissipated or turned. Thus the activation detected on the nearby electrode may be from a different wavefront. For this reason, this aim examined each electrode individually with both time and frequency domain techniques. To remove far-field ventricular activity, a QRS subtraction algorithm was used, and this technique is shown in Figure 4.11. The QRS-subtracted unipolar signals were analyzed with time and frequency domain techniques to find activation rate and regularity of activation from regions of relatively healthy myocardium and from regions of fibrosis during atrial fibrillation.

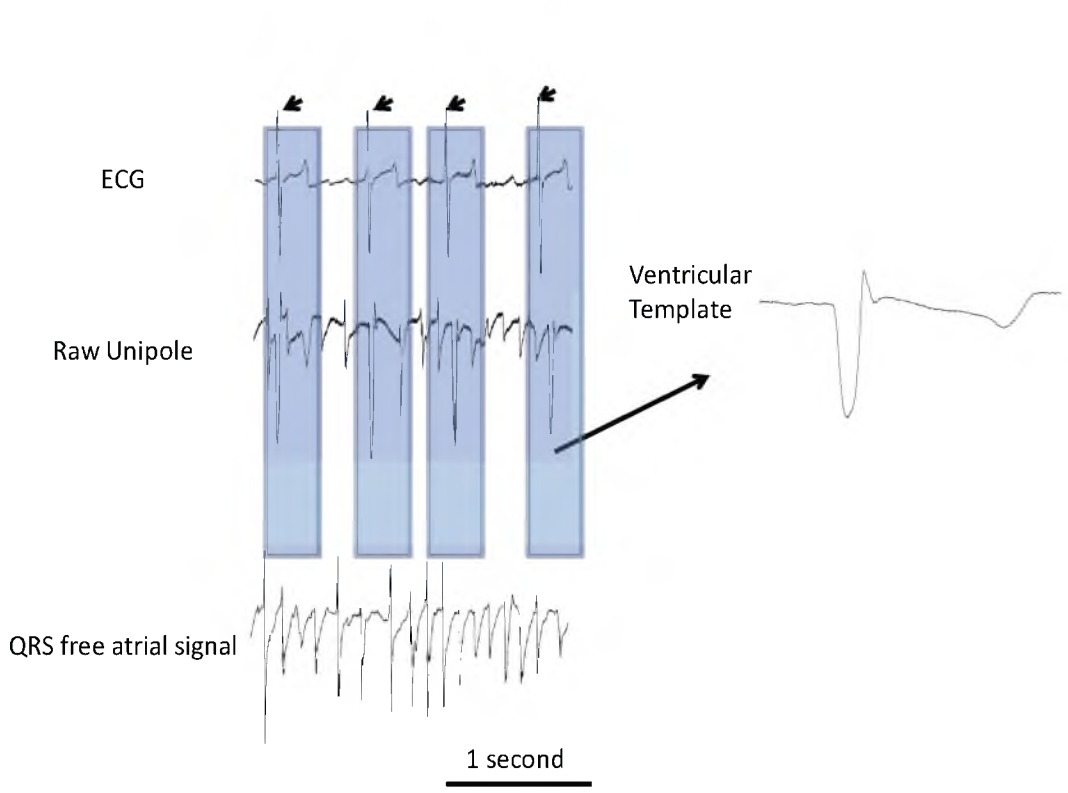

Fig. 4.11: **QRS subtraction**. The QRS of an ECG is determined, which is indicated by the arrows, using peak detection. A window encompassing the QRS and T wave is defined, which is shown in blue. This window around the ventricular activity is then projected onto each unipolar signal. The median of at least 10 of these windows was computed to create a template of the ventricular activity. A template will be created for each unipole. This template is then subtracted from each unipole for every QRS determined from the ECG. The resulting signal is an atrial unipole free from ventricular activity.

CHAPTER 5

CONDUCTION PROPERTIES OF THE HIS BUNDLE DURING PROLONGED VENTRICULAR FIBRILLATION

The distal regions of the ventricular conduction system, specifically the Purkinje fibers, have been implicated in driving long-duration VF. Most of this evidence comes from measurements from the ventricular myocardium, and from these measurements the role of the conduction system is inferred. This chapter is a published journal article, which is reprinted with permission from Plos One. The article includes a description of a method to reliably differentiate conduction system activity from ventricular activity during VF. Utilizing this method, it was found that the distal ventricular conduction system has a faster activation rate than the underlying VM during prolonged VF.

OPEN ACCESS Freely available online

PLOS | ONE

His Bundle Activates Faster than Ventricular Myocardium during Prolonged Ventricular Fibrillation

Nathan Angel[1,2], Li Li[1], Derek J. Dosdall[1,2,3]*

1 Comprehensive Arrhythmia Research & Management Center, Division of Cardiovascular Medicine, University of Utah, Salt Lake City, UT, United States of America, 2 Department of Bioengineering, University of Utah, Salt Lake City, UT, United States of America, 3 Center for Engineering Innovation, University of Utah, Salt Lake City, UT, United States of America

Abstract

Background: The Purkinje fiber system has recently been implicated as an important driver of the rapid activation rate during long duration ventricular fibrillation (VF>2 minutes). The goal of this study is to determine whether this activity propagates to or occurs in the proximal specialized conduction system during VF as well.

Methods and Results: An 8×8 array with 300 μm spaced electrodes was placed over the His bundles of isolated, perfused rabbit hearts (n = 12). Ventricular myocardial (VM) and His activations were differentiated by calculating Laplacian recordings from unipolar signals. Activation rates of the VM and His bundle were compared and the His bundle conduction velocity was measured during perfused VF followed by 8 minutes of unperfused VF. During perfused VF the average VM activation rate of 11.04 activations/sec was significantly higher than the His bundle activation rate of 6.88 activations/sec ($p<0.05$). However from 3–8 minutes of unperfused VF the His system activation rate (6.16, 5.53, 5.14, 5.22, 6.00, and 4.62 activations/sec significantly faster than the rate of the VM (4.67, 3.63, 2.94, 2.24, 3.45, and 2.31 activations/sec) ($p<0.05$). The conduction velocity of the His system immediately decreased to 94% of the sinus rate during perfused VF then gradually decreased to 67% of sinus rhythm conduction at 8 minutes of unperfused VF.

Conclusion: During prolonged VF the activation rate of the His bundle is faster than that of the VM. This suggests that the proximal conduction system, like the distal Purkinje system, may be an important driver during long duration VF and may be a target for interventional therapy.

Citation: Angel N, Li L, Dosdall DJ (2014) His Bundle Activates Faster than Ventricular Myocardium during Prolonged Ventricular Fibrillation. PLoS ONE 9(7): e101666. doi:10.1371/journal.pone.0101666

Editor: Alena Talkachova, University of Minnesota, United States of America

Received March 12, 2014; **Accepted** June 9, 2014; **Published** July 18, 2014

Data Availability: The authors confirm that all data underlying the findings are fully available without restriction. The data are publically available at USPACE (http://content.lib.utah.edu/cdm/ref/collection/uspace/id/9710).

Funding: Research reported in this publication was supported by the National Heart, Lung, and Blood Institute of the National Institutes of Health under the Award Number: R00HL091138. The content is solely the responsibility of the authors and does not necessarily represent the official views of the National Institutes of Health. The funder had no role in study design, data collection and analysis, decision to publish, or preparation of the manuscript.

Competing Interests: The authors have declared that no competing interests exist.

* Email: derek.dosdall@utah.edu

Introduction

Sudden cardiac death due to ventricular fibrillation (VF) is one of the leading causes of death in the developed world[1]. Furthermore, sudden cardiac death is often unexpected, occurring without any predetermined risk[2]. Implantable cardiac defibrillators (ICD's) have greatly reduced mortality due to VF, likely due to defibrillation shocks being applied to the myocardium soon after the onset of VF[3]. However this treatment is only available for those that have been clinically diagnosed as high risk for VF. For those without ICD's, VF often persists for 5–10 minutes before defibrillation shocks can be applied[4]. Since the probability of successful resuscitation from VF decreases 10% for every minute of VF, the survival rate for out of hospital sudden cardiac arrest is low[5]. Successful resuscitation rate is thought to decrease during prolonged VF because of electrophysiological changes to cardiac tissue under ischemic conditions[6]. These electrophysiological changes may cause permanent cardiac damage[7] and can result in failure to defibrillate successfully[8].

The Purkinje fiber system has recently been implicated as an important driver of VF activation in the maintenance of long duration VF (VF>2 min) [9–11]. Distal Purkinje fibers have been shown to develop triggered activity during VF due to the ischemic conditions which is thought to drive this rapid activation[6,12]. However it is unclear whether this rapid activation rate is limited only to the distal regions of the conduction system, or whether it is observed or conducts to the proximal regions of the conduction systems as well.

Due to the several minute delay of therapy for patients after the onset of VF, it is necessary to study the electrophysiological properties of the ventricular conduction system during prolonged VF to aid in the development of therapies to improve patient outcome. In this study, electrophysiological properties of the conduction system of interest are the activation rate of the His bundle compared to the VM and the His bundle conduction velocity during the time course of VF. The ventricular conduction system has a much higher conduction velocity than the VM and only interacts with the VM at specialized junctions known as the

Purkinje-myocardial junctions (PMJs) [13]. Due to the faster conduction velocity and limited access sites into the ventricular conduction system from the myocardium, activation in the distal Purkinje system may travel quickly throughout the conduction system. We tested the hypothesis that the proximal regions of the ventricular conduction system, like the distal conduction system, have a faster activation rate than the underlying ventricular myocardium (VM) during prolonged VF.

Methods

All animals were managed in accordance with the *Guide for the Care and Use of Laboratory Animals*[14], and the protocol was approved by the Institutional Animal Care and Use Committee of the University of Utah. All efforts were made to minimize suffering.

Animal Preparation

Twelve male New Zealand white rabbits (3.9±0.2 kg) were anesthetized with an intramuscular injection of 15 mg/kg ketamine, and 7.5 mg/kg xylazine followed by an intravenous injection of 5 mg/kg ketamine, 2.5 mg/kg xylazine, and 500 IU of heparin. The hearts were excised rapidly and Langendorff-perfused with Tyrode solution (in mmol/L 130 NaCL, 1.2 NaH_2PO_4, 1 $MgCl_2$, 4 KCl, 1.8 $CaCl_2$, $NaHCO_3$ 20.8, dextrose 11, and 0.04 g/l bovine albumin). Flow rate was adjusted to maintain a pressure at 25±3 mmHg. The hearts were also superfused with warm Tyrode solution, with temperature maintained at 37±0.5 °C. The Tyrode solution was oxygenated with O_2 and CO_2 to maintain a pH of 7.4±0.1.

Instrumentation and Experimental Protocol

An incision in the right atrium was made to expose the His bundle, which is found along the atrial-ventricular boundary high on the RV septum. Unipolar VM and His bundle activity were recorded using an 8×8-electrode plaque with electrodes spaced 0.3 mm apart with a reference electrode in the solution bath. Electrograms were low pass filtered at 1640 Hz, sampled at 8 KHz, and recorded at 24 bit resolution (Active Two System, Biosemi, Inc, Amsterdam, Netherlands). Electrodes were placed in the perfusate on either side of the heart (one near the atrium and the other near the ventricle) to calculate a bipolar pseudo-ECG. VF was induced with 15–30 seconds of 50 Hz burst pacing, with amplitude of 5 mA through bipolar leads placed in the right ventricular apex. After 30 seconds of sustained VF, perfusion was stopped and VF persisted until it spontaneously terminated. The electrode plaque was lifted off of the myocardium and His bundle using a micromanipulator every 30 seconds to avoid ischemia of the His bundle.

Measurements and Data Analysis

His, VM, and atrial myocardium (AM) activations were differentiated by calculating a 5-point Laplacian from the unipolar electrograms. The Laplacian signals were calculated according to Punske et al. [15]. In brief, a standard central difference approach was used as shown in the formula,

$$V_C - \frac{(V_W + V_E + V_N + V_S)}{4}, \qquad (1)$$

where V is the voltage, subscript C refers to the central electrode, and the other subscripts, W, E, N, and S, refer to the relative positions of the other electrodes surrounding the central electrode according to the compass regions. If the electrode site was on the corner or edge of the array, values from the two or three nearest sites were averaged and subtracted from the central electrode site.

Channels that contained strong His and VM activations were used for the analysis of activation rate and conduction velocity. An activation rate for the His and VM was determined by averaging the cycle length of the first 10 successive activations of each minute, up to 8 minutes, of VF. Activations times were determined using a thresholding approach with manual oversight via custom software developed in MATLAB (Mathworks, Inc., MA, USA). This software computed a 21-point temporal derivative of the Laplacian. During sinus rhythm, the local maximums of this filtered signal were taken as the activation times. Activation times during VF were determined by finding local maximum that had a peak that was at least 50% of the sinus rhythm local maximums. An activation map for each of the 10 His activation used to calculate the activation rate was made to determine His conduction velocity. For each of the 10 activation maps a His conduction velocity was calculated by subtracting the activation times from the most proximal and distal activation along the His bundle fiber, then dividing by the distance between those electrodes. The average of these 10 His conduction velocities were then taken as the conduction velocity for sinus, perfused, and for the 8 minutes of unperfused VF. The data are publically available at USPACE (http://content.lib.utah.edu/cdm/ref/collection/uspace/id/9710).

Statistical Analysis

Results are expressed as mean±SD. The overall difference between VM and His bundle activation rate and the effect of time on His bundle conduction velocity was tested with repeated-measure ANOVA (XLSTAT Version 2014. 1.08). Differences between the activation rate of the VM and His bundle for perfused VF and each minute of unperfused VF were tested using a post-hoc paired *t*-test with a Holm-Bonferroni correction for multiple comparisons. His sinus conduction velocity was compared with unperfused VF and 1–8 minutes of VF with an unpaired *t*-test with a Holm-Bonferroni correction for multiple comparisons. The null hypothesis of no difference for all tests was rejected if the probability value was less than 0.05.

Results

Hearts in which unperfused VF persisted less than 2 minutes were excluded from the analysis (n = 2). The average duration of sustained VF was 9.13 minutes±4.52 minutes (n = 10). For sinus rhythm, perfused VF, and for minutes 1–4 of VF, data from 10 hearts was analyzed. VF spontaneously terminated as time progressed so that at 5 minutes, n = 8, at 6 minutes n = 5, and at 7–8 minutes, n = 6. At 6 minutes of unperfused VF, a time point was excluded from the analysis because VF spontaneously converted to VT for 30 seconds then converted back into VF. In one heart, unperfused VF self-terminated during the 6th minute but was burst paced for 10 seconds, which reinitiated VF for another 13 minutes.

Figure 1A is a representative example from one experiment of the location of the three primary cardiac signals (VM, AM and His) recorded on the electrode plaque once the Laplacian had been computed. The His bundle signals were always in a thin line, (2 to 3 electrodes wide, by 3 to 5 electrodes long), in between predominate AM and VM signals. Figure 1B shows example unipolar and Laplacian recordings of the AM, VM and His signals from the array.

Figure 2 shows the processing of electrograms to determine the activations rates for the His bundle and the VM. The raw

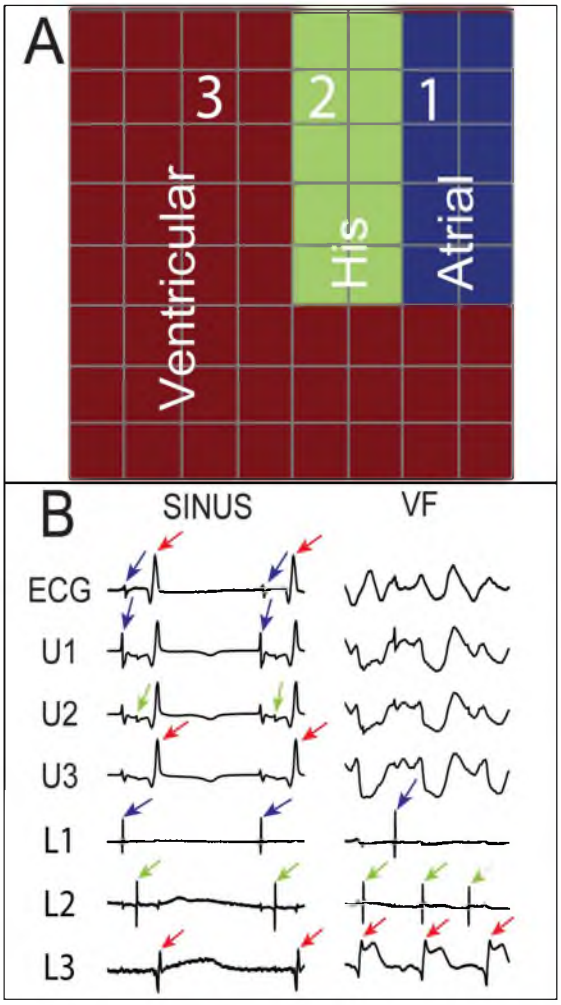

Figure 1. Recordings from an array placed over the His bundle of an isolated rabbit heart. A) Strong ventricular, His, and atrial signals were recorded during sinus rhythm from the 3 regions of the 8×8 array, 300 μm spaced electrodes, shown in red, green, and blue, respectively. Electrograms at sites 1, 2, and 3 are shown in **B)** A pseudo ECG, unipolar electrogram (from site 2 in **A**), and 3 Laplacian recordings (from sites 1, 2, and 3 in **A**) during sinus and VF. Each recording was 500 ms in duration. The unipole at site 2 shows ventricular (red arrows), His (green arrows), and atrial (blue arrows) deflection, while the Laplacians isolate the strongest local signal and eliminate far field signals. During VF, it is difficult to distinguish different activation types with the unipolar signal, but the different Laplacians facilitate waveform identification.
doi:10.1371/journal.pone.0101666.g001

electrograms contain little information about the activation times of the tissue. Using the minimums of the derivative is a standard method to detect activation times of cardiac tissue, however it is still not clear whether the activations are local or from far field signals. Furthermore the temporal derivative often produces multiple local minimums, making the choice of the activation time ambiguous. Due to these limitations, distinguishing His-bundle and VM activation during VF was difficult with the unipolar electrograms and derivatives. In theory, Laplacian signal

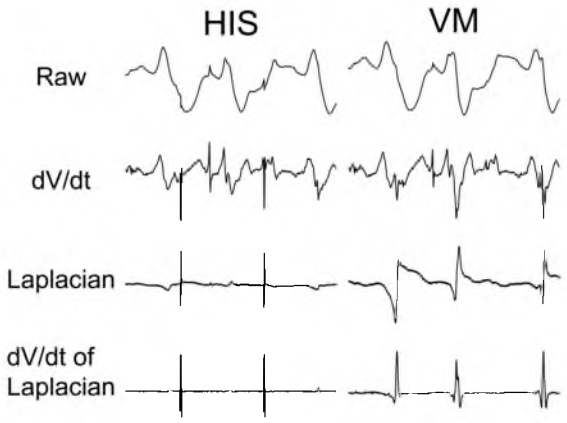

Figure 2. Signal processing to detect activation times for His and VM signals. His and VM signals were recorded at the location 2 and 3 from Figure 1A, respectively. The raw electrograms contain little information to detect activation times. The 21-point dV/dt of the electrograms shown above contains too much far field activation for robust local activation time detection. The Laplacian isolates the strongest local signal, attenuating far field signals. With baseline noise the zero crossing is not always clear therefore the 21-point derivative of the Laplacian was calculate which produced clear peaks, which allowed for activation detection with a thresholding approach to detect activation times. Each recording was 500 ms in duration.
doi:10.1371/journal.pone.0101666.g002

shows activations at the zero crossing, however with baseline noise the zero crossing was not always clear therefore further processing was required. The 21-point temporal derivative of the Laplacian produced unambiguous peaks which were used to find activation times for the His and VM.

Figure 3 shows example recordings of the filtered His bundle and VM signals for sinus, early and late VF. The local maximums in the signals shown in Figure 3 were the activation times used to calculate an activation rate for the His bundle and VM and conduction velocity for the His bundle. During sinus rhythm the His bundle and VM activations were coupled because the His system activates the VM. Conversely, the His bundle and VM activations became uncoupled during VF.

The repeated-measures ANOVA showed a statistically significant effect of cell type (His or VM) on activation rate and that time had a significantly effect on VM activation rate. However, time did not have a statistically significant effect on His bundle activation rate over the 8 minute time course of VF. This is shown by the similar activation rate of the His bundle during the eight minutes of unperfused VF. The activation rate for the His bundle and VM are shown as a function of time for both the His and VM with the error bars reporting the standard deviation of the measurement, representing the differences among animals (Figure 4). During perfused VF, at time 0, the average VM activation rate was significantly higher than the His rate. At 1–2 minutes there is no significant difference between VM and His activation rates, however at the 3–8 minutes the His bundle activates faster than the VM.

Time had a statistically significant effect on His conduction velocity. The His conduction velocity decreased from 94% at perfused VF to 67% of the sinus conduction velocity at 8 minutes of unperfused VF (Figure 5). The His conduction velocity at unperfused VF, 1 minute and 5 minutes of VF was not significant different than sinus His conduction velocity. 5 minutes of VF

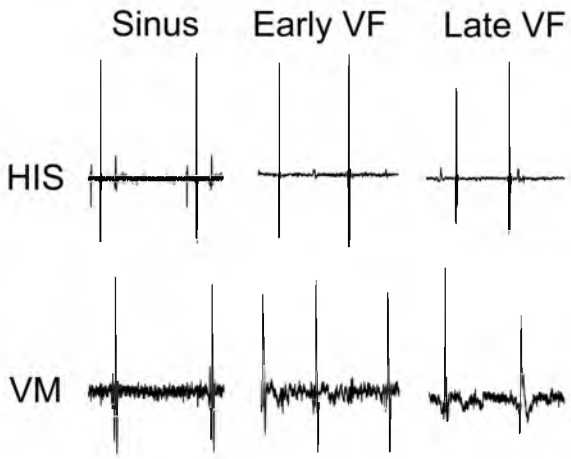

Figure 3. His and VM dV/dt of Laplacians during time course of VF. Early VF recording during perfused VF. Late VF is after 4 minutes of unperfused VF. Each recording was 500 ms in duration.
doi:10.1371/journal.pone.0101666.g003

trended towards significance, with a corrected p-value of 0.053, and likely was not significant due to the large standard deviations. The sinus rate was 0.46±0.08 m/s with n = 10. The conduction direction in the His bundle was antegrade, His bundle to VM, during sinus rhythm and nearly entirely retrograde, VM to His bundle, during VF (Figure 6) (1 out of 650 examined activations were antegrade during VF).

Discussion

The main findings of this study are as follows: 1) Calculating a Laplacian from unipolar electrograms aids in the identification of His-Purkinje signals. 2) The His bundle activation rate does not significantly change over the time course of VF. 3) During early VF, the VM has a higher activation rate than the His bundle, but from 3 minutes on, this relationship reverses, and the His bundle activates faster than the VM. 4) Conduction in the His bundle is nearly entirely retrograde during VF and conduction velocity gradually decreases during the time course of VF.

Laplacian signals have been used previously to accurately detect activation times during VF[15,16]. Unique to this study is the utilization of Laplacian signals to distinguish local His bundle activations from the underlying VM activations. The traditional method to detect activation within cardiac tissue is to take the time of the minimum temporal derivative of the signal[17]. This method can produce multiple peaks, making identifying an activation time unclear, and therefore subject to arbitrary criteria[18,19]. The Laplacian reduces far field effects, emphasizing local activity. This technique has been particularly useful when attempting to identify activations of the conduction system in VF when the relative timing of the conduction system and the underlying VM activation are unknown. During sinus rhythm, activation propagates through the conduction system to the working myocardium, therefore, the conduction system activation temporally precedes the activation of the local VM. The zero crossing of the Laplacian occurs when the local tissue is transitioning from a current source to a current sink and therefore is considered the activation. The slope of the Laplacian is also at a maximum as the activation passes immediately beneath the central electrode of the Laplacian. By calculating the temporal derivative of the Laplacian, clear peaks can be distinguished which allows for a thresholding method to calculate an activation rate. The derivative of the Laplacian simplifies the detection of local activation time and provides some immunity to noise inherent in these signals.

During perfused VF the activation rate of the VM is significantly higher than the His bundle. This is consistent with the traditional theory that VF is maintained through rapid

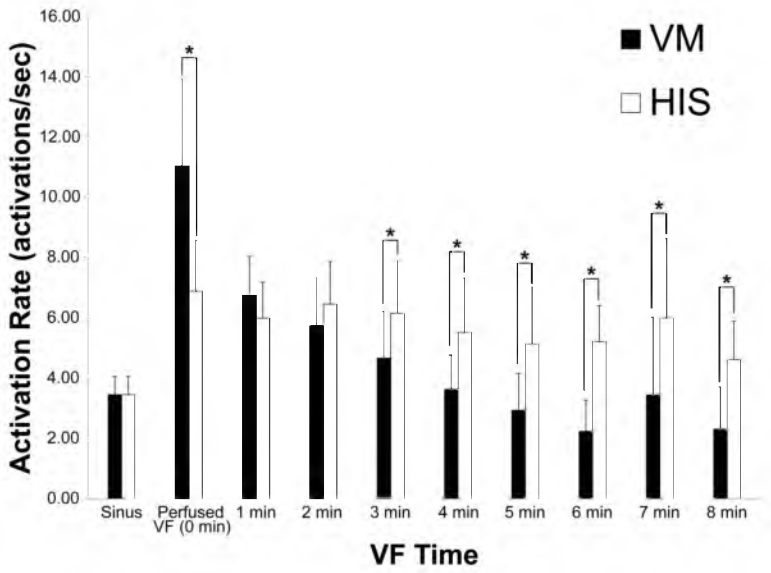

Figure 4. Mean and standard deviation of His and VM activation rate during eight minutes of unperfused VF. The average sinus rate for the rabbits was 3.46+0.61 activations/sec for both the His bundle and VM. *denotes $p<0.05$.
doi:10.1371/journal.pone.0101666.g004

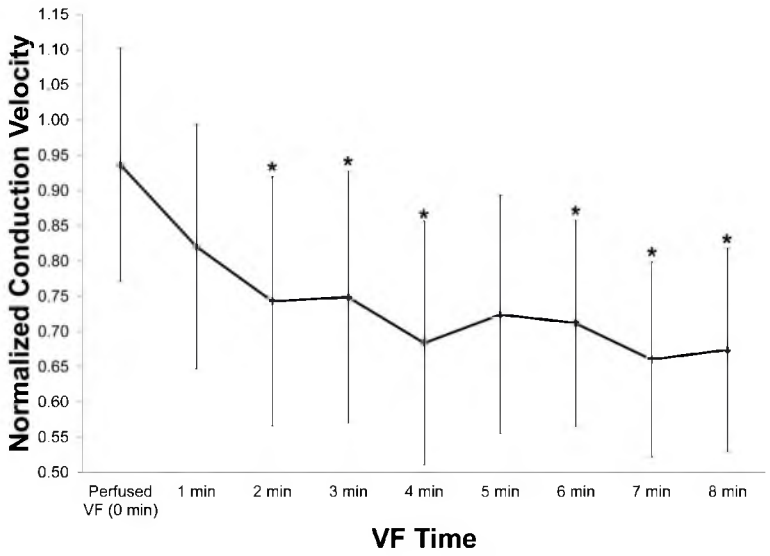

Figure 5. Mean and standard deviation of His conduction velocity as a function of VF duration. Values were normalized to mean His sinus conduction velocities. A repeated-measures ANOVA analysis showed that time has a significant effect on His Bundle conduction velocity. *denotes a significant difference ($p<0.05$) between non-normalized sinus conduction and the corresponding time point.
doi:10.1371/journal.pone.0101666.g005

reentrant wavefronts within the VM[20–22]. However after 1–2 minutes of VF a transition occurs in which the His bundle activates faster than the VM. The VM activation rate decreases quickly during VF while the His bundle activation rate does not significantly decrease. It is possible that the activity in the conduction system may be overdrive suppressed by the rapid activation rate in the VM, and that the conduction system does not drive VF activation until the VM rate has slowed below the inherent activation rate of the conduction system. This finding suggest that the proximal conduction system may be an important driver of VF>2 minutes and is consistent with a more recent theory that the ventricular conduction system may have a critical role in VF maintenance, particularly after the first couple of minutes[10,18,23 26]. Three-dimensional simulations of the ventricles that attempt to include the conduction system suggest that the ventricular conduction system may be an important source for focal activity and may have a critical role in the development and sustaining of reentry during VF[27,28]. A recent study demonstrated that ablation of the purkinje fibers slowed the activation rate during prolonged VF, and VF spontaneously terminated earlier than in control hearts[11]. This observation supports the simulation data that the ventricular conduction system may be required to maintain long duration VF.

Time may have a significant effect on the VM but not on the His bundle due to several mechanisms. First the His bundle has less metabolic load than the VM and therefore may take longer to deplete its reserved resources[29]. Second, much of His-Purkinje system is located directly on the endocardial surface and it may receive substantial nutrients from the fluid in the LV cavity. Our preliminary results suggested that if the electrode plaque was left on the His bundle for extended periods (>1 min), the His bundle developed slowed conduction or even blocked (unpublished data). Finally differences in ion channel kinetics and restitution properties of the ventricular conduction system and VM[26], may be responsible for the observed differences in the His and VM activation rate as a function of time.

The His bundle may have a slower activation rate than the VM during early VF but more rapid activation rate during prolonged VF due to several mechanisms. During sinus rhythm the VM has a shorter refractory period than the conduction system therefore electrical wavefronts on the myocardium may not be able to activate the conduction system at such a rapid rate [29]. As VF progresses and ischemic sets in, several electrophysiological changes occur in both the ventricular conduction system and the VM. One change is that the VM develops a longer refractory period than the conduction system [29] and the VM cannot maintain as high of activation rate. Another change during ischemic conditions is that distal purkinje fibers are thought to develop abnormal automaticity and/or triggered activity during ischemic conditions [6,12,26]. Triggered or abnormal automaticity in the distal purkinje fibers may conduct to the His bundle but block at the VM, due to several reasons. The first reason is due to the longer refractory period of the VM as compared to the conduction system. Second, there is a source-sink mismatch between the distal purkinje fibers and the VM[30–32]. This mismatch results in conduction occurring more readily from VM to distal purkinje fibers than from distal purkinje fibers to the VM[31]. The combination of longer refractory period of the VM as compared to the ventricular conduction system and the presence of a source sink mismatch between the distal purkinje fibers and the VM could result in a higher activation rate in the His bundle than the VM. Reentry involving both the VM and the conduction system [27] is another mechanism that could cause a more rapid activation rate in the ventricular conduction system. A single ventricular wavefront may conduct into the ventricular conduction system to the His bundle. Due to the limited access sites into the conduction system and the fast conduction velocity, a single VM wavefront, either propagating on the VM or which propagated through the conduction system, may activate the conduction system multiple times.

The His bundle conduction velocity reported for sinus rhythm in this study of 0.46 ± 0.08 m/s ($n=10$) was similar to previous

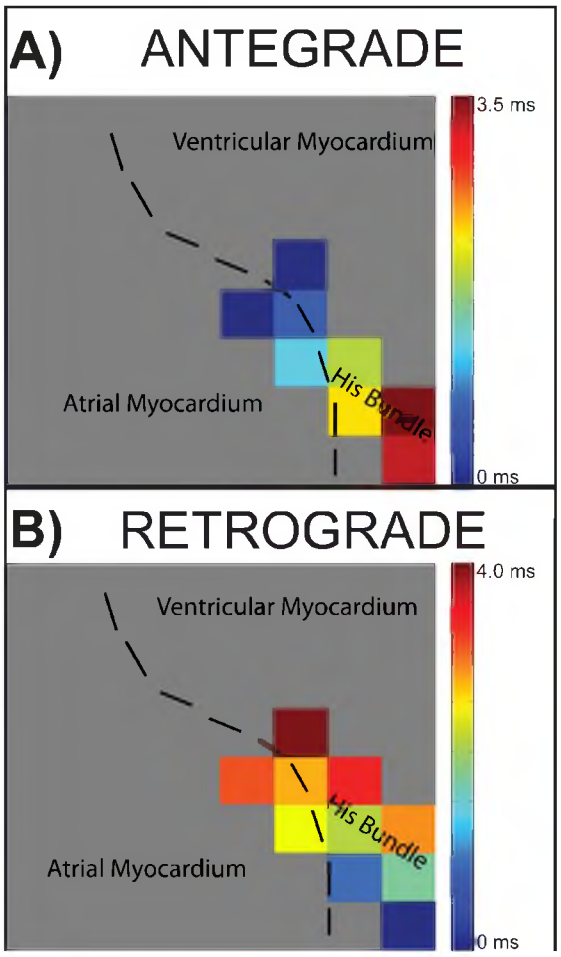

Figure 6. Example of His bundle antegrade and retrograde conduction. The plaque shown is a 8×8 array with 300 um electrode spacing, which covers a 2.1 mm x 2.1 mm region of the endocardium. Regions not containing strong His activity are shown in gray. **A)** Conduction during sinus rhythm was in the antegrade direction. **B)** Conduction in the His bundle during VF was almost always in the retrograde direction. The example shown is during perfused VF.
doi:10.1371/journal.pone.0101666.g006

reported ventricular conduction system velocities of 0.60±0.09 m/s (n = 3)[33]. The direction of conduction in the His bundle was nearly entirely retrograde during VF, consistent with activation propagating from the distal purkinje fibers through the bundle branches back to the His bundle. Antegrade conduction in the His bundle may only be observed if activation emerged from the AV node or through automaticity or triggered activity in the His bundle itself. However novel to this study was recording changes in His conduction velocity during the time-course of VF. Conduction in VF was slower for perfused VF with a normalized conduction velocity of 94% of sinus rhythm, which gradually decreased to 67% of sinus rhythm conduction at 8 minutes of VF. The initial 6% decrease in conduction velocity from sinus to perfused VF may due to the slower retrograde than antegrade conduction in the ventricular conduction system[34] or slowing associated with the higher activation rate in VF[35] due to conduction velocity restitution[34]. The decrease in conduction velocity during the time course of VF is most likely due to a combination of ischemia and a rise in resting potential and inactivation of Na+ channels during prolonged VF[35].

Recently published studies support the hypothesis that the distal conduction system is responsible for driving the rapid activation rate during long duration VF[10,18,23–26]. Studies of long duration VF have shown that activation patterns of the Purkinje system and working myocardium often propagate in patterns similar to the spread of activation through the conduction system during sinus rhythm[10,36]. This work is the first to show direct evidence that the proximal ventricular conduction system activates more rapidly than the underlying working myocardium during long duration VF. The ventricular conduction system has a much faster conduction velocity than the VM, and only interacts with the VM at limited sites known as PMJs which are located only in the distal regions of the ventricular conduction system[13]. Therefore it is likely that once a distal Purkinje fiber is activated, it will quickly activate a large region of the conduction system, and as this study suggests, even conduct to the His bundle. The limited number of PMJs located only in the distal regions of the ventricular conduction system, in combination with the fast conduction velocity of the conduction system suggest that it is unlikely that activations through the ventricular conduction system will collide and block with other activations within the conduction system before activating large portions of the conduction system. Therefore it is likely that triggered activity in Purkinje fibers can conduct through the ventricular conduction system and drive rapid activation at distant sites, even opening the possibility of biventricular communication through the bundle braches.

Limitations

A rabbit VF model was used for our study of properties of the His bundle during VF. VF is more difficult to initiate and maintain in rabbits than larger hearts such as humans. While it was difficult to initiate VF in rabbits, once it initiated, it was sustained for extended periods of time (with two exceptions). Another limitation is the use of an isolated heart preparation. In this preparation, the autonomic nervous system is severed which may influence VF. Due to these limitations the results of these findings may not directly translate to humans. In spite of these limitations, the isolated rabbit heart model is widely used and well accepted for studying VF[37–39]. A final limitation is that we mapped only a small region of the VM near the His bundle and atrial tissue therefore there may be regions of faster VM activation that were not a measured.

Conclusion

In early VF (perfused VF), the VM has a faster activation rate than the His bundle. We concluded that the VM is likely the major driver of early VF, with the conduction system being driven by the activation of the VM. After 3 minutes of VF, the activation rate of the His bundle is faster than that of the VM. This observation suggests that activations in the distal ventricular conduction system propagate through the conduction system to activate the His bundle and may drive activation at distant sites. This finding supports the conclusion that the conduction system plays a critical role in the mechanisms of prolonged VF maintenance and may be a target for interventional therapy.

Acknowledgments

The authors thank Jose Reyes for excellent technical animal support.

Author Contributions

Conceived and designed the experiments: NA LL DD. Performed the experiments: NA DD. Analyzed the data: NA. Contributed reagents/materials/analysis tools: NA LL DD. Contributed to the writing of the manuscript: NA LL DD.

References

1. Zipes DP, Wellens HJJ (1998) Sudden Cardiac Death. Circulation 98: 2334–2351.
2. Turakhia M, Tseng ZH (2007) Sudden cardiac death: epidemiology, mechanisms, and therapy. Curr Probl Cardiol 32: 501–546.
3. Zipes DP (1999) An overview of arrhythmias and antiarrhythmic approaches. J Cardiovasc Electrophysiol 10: 267–271.
4. De Vreede-Swagemakers JJ, Gorgels a P, Dubois-Arbouw WI, van Ree JW, Daemen MJ, et al. (1997) Out-of-hospital cardiac arrest in the 1990's: a population-based study in the Maastricht area on incidence, characteristics and survival. J Am Coll Cardiol 30: 1500–1505.
5. Eisenberg MS, Horwood BT, Cummins RO, Reynolds-Haertle R, Hearne TR (1990) Cardiac arrest and resuscitation: A tale of 29 cities. Ann Emerg Med 19: 179–186.
6. Carmeliet E (1999) Cardiac ionic currents and acute ischemia: from channels to arrhythmias. Physiol Rev 79: 917–1017.
7. Van Rees JB, Borleffs CJW, de Bie MK, Stijnen T, van Erven L, et al. (2011) Inappropriate implantable cardioverter-defibrillator shocks: incidence, predictors, and impact on mortality. J Am Coll Cardiol 57: 556–562.
8. Friedman PL, Stewart JR, Wit AL (1973) Spontaneous and Induced Cardiac Arrhythmias in Subendocardial Purkinje Fibers Surviving Extensive Myocardial Infarction in Dogs. Circ Res 33: 612–626.
9. Tabereaux PB, Walcott GP, Rogers JM, Kim J, Dosdall DJ, et al. (2007) Activation patterns of Purkinje fibers during long-duration ventricular fibrillation in an isolated canine heart model. Circulation 116: 1113–1119.
10. Huang J, Dosdall DJ, Cheng K, Li L, Rogers JM, et al. (2014) The Importance of Purkinje Activation in Long Duration Ventricular.
11. Dosdall DJ, Tabereaux PB, Kim JJ, Walcott GP, Rogers JM, et al. (2008) Chemical ablation of the Purkinje system causes early termination and activation rate slowing of long-duration ventricular fibrillation in dogs. Am J Physiol Heart Circ Physiol 295: H883–9.
12. Friedman PL, Stewart JR, Fenoglio JJ, Wit a L (1973) Survival of Subendocardial Purkinje Fibers after Extensive Myocardial Infarction in Dogs: IN VITRO AND IN VIVO CORRELATIONS. Circ Res 33: 597–611.
13. Myerburg RJ, Nilsson K, Gelband H (1972) Physiology of Canine Intraventricular Conduction and Endocardial Excitation. Circ Res 30: 217–243.
14. Committee for the Update of the Guide for the Care and Use of Laboratory Animals, Institute for Laboratory Animal Research, Division on Earth and Life Studies, National Research Council. (2011). Guid Care Use Lab Anim Washingt DC: Nation.
15. Punske BB, Ni Q, Lux RL, MacLeod RS, Ershler PR, et al. (2003) Spatial Methods of Epicardial Activation Time Determination in Normal Hearts. Ann Biomed Eng 31: 781–792.
16. Coronel R, Wilms-Schopman FJ, de Groot JR, Janse MJ, van Capelle FJ, et al. (2000) Laplacian electrograms and the interpretation of complex ventricular activation patterns during ventricular fibrillation. J Cardiovasc Electrophysiol 11: 1119–1128.
17. Steinhaus BM (1989) Estimating cardiac transmembrane activation and recovery times from unipolar and bipolar extracellular electrograms: a simulation study. Circ Res 64: 449–462.
18. Bogun F, Good E, Reich S, Elmouchi D, Igic P, et al. (2006) Role of Purkinje fibers in post-infarction ventricular tachycardia. J Am Coll Cardiol 48: 2500–2507.
19. Joyner RW, van Capelle FJ (1986) Propagation through electrically coupled cells. How a small SA node drives a large atrium. Biophys J 50: 1157–1164.
20. Efimov I, Ripplinger CM (2006) Virtual electrode hypothesis of defibrillation. Heart Rhythm 3: 1100–1102.
21. Decker KF, Heijman J, Silva JR, Hund TJ, Rudy Y (2009) Properties and ionic mechanisms of action potential adaptation, restitution, and accommodation in canine epicardium Properties and ionic mechanisms of action potential adaptation, restitution, and accommodation in canine epicardium. Am J Physiol Heart Circ Physiol 296: H1017–H1026.
22. Weiss JN, Garfinkel A, Karagueuzian HS, Qu Z, Chen P-S (1999) Chaos and the Transition to Ventricular Fibrillation: A New Approach to Antiarrhythmic Drug Evaluation. Circulation 99: 2819–2826.
23. Ben-Haim SA, Cable DG, Rath TE, Carmen L, Martins JB (1993) Impulse propagation in the Purkinje system and myocardium of intact dogs. Am J Physiol 265: H1588–95.
24. Scheinman MM (2009) Role of the His-Purkinje system in the genesis of cardiac arrhythmia. Hear Rhythm 6: 1050–1058.
25. Haïssaguerre M, Shah DC, Jaïs P, Shoda M, Griffith M, et al. (2002) Role of Purkinje conducting system in triggering of idiopathic ventricular fibrillation. Lancet 359: 677–678.
26. Dun W, Boyden P a (2008) The Purkinje cell; 2008 style. J Mol Cell Cardiol 45: 617–624.
27. Berenfeld O, Jalife J (1998) Purkinje-Muscle Reentry as a Mechanism of Polymorphic Ventricular Arrhythmias in a 3-Dimensional Model of the Ventricles. Circ Res 82: 1063–1077.
28. Behradfar E, Nygren A, Vigmond EJ (2014) The Role of Purkinje-Myocardial Coupling during Ventricular Arrhythmia: A Modeling Study. PLoS One 9: e88000.
29. Bagdonas AA, Stuckey JH, Piera J, Amer NS, Hoffman BF (1961) Effects of ischemia and hypoxia on the specialized conducting system of the canine heart. Am Heart J 61: 206–218.
30. Huselsing D, Pollard A (1999) Membrane and tissue level contributions to Purkinje-ventricular interactions: A model study. J Biol Syst 7: 491–512.
31. Mendez C, Mueller WJ, Urguiaga X (1970) Propagation of Impulses across the Purkinje Fiber-Muscle Junctions in the Dog Heart. Circ Res 26: 135–150.
32. Huelsing DJ, Spitzer KW, Cordeiro JM, Pollard a E (1999) Modulation of repolarization in rabbit Purkinje and ventricular myocytes coupled by a variable resistance. Am J Physiol 276: H572–81.
33. Odening KE, Kirk M, Brunner M, Ziv O, Lorvidhaya P, et al. (2010) Electrophysiological studies of transgenic long QT type 1 and type 2 rabbits reveal genotype-specific differences in ventricular refractoriness and His conduction: 643–655.
34. Akhtar M, Damato a N, Batsford WP, Ruskin JN, Ogunkelu JB (1975) A comparative analysis of antegrade and retrograde conduction patterns in man. Circulation 52: 766–778.
35. Weiss JN, Qu Z, Chen P-S, Lin S-F, Karagueuzian HS, et al. (2005) The dynamics of cardiac fibrillation. Circulation 112: 1232–1240.
36. Robichaux RP, Dosdall DJ, Osorio J, Garner NW, Li L, et al. (2010) Periods of highly synchronous, non-reentrant endocardial activation cycles occur during long-duration ventricular fibrillation. J Cardiovasc Electrophysiol 21: 1266–1273.
37. Oriente V, Koike MK, Coutinho MP, Velasco IT, Scalabrini-Neto A (2009) Induction and maintenance of in vivo ventricular fibrillation in rabbits. Resuscitation 80: 1417–1419.
38. Ferrari de França Camargo A, Carvalho Rubin de Celis A, Velasco IT, Pontieri V, Neto AS (2005) New model of ventricular fibrillation. J Electrocardiol 38: 226–229.
39. Tovar OH, Jones JL (2000) Electrophysiological Deterioration During Long-Duration Ventricular Fibrillation. Circulation 102: 2886–2891.

CHAPTER 6

EFFECT OF FIBROSIS ON ATRIAL CONDUCTION FOLLOWING CHRONIC ATRIAL FIBRILLATION

Patients with paroxysmal AF often transition between sinus rhythm and AF. However, the mechanism of how this transition occurs is not well understood. For AF to initiate, there must be both a trigger and a substrate that facilitate reentrant activity. The trigger is often caused by a premature atrial contraction or focal activations within the atria. This chapter examined the interactions between triggers for AF and the cardiac substrate. This article shows that long strands of fibrotic tissue are related to conduction slowing to make the tissue more susceptible to fibrillation. This chapter is a published journal article, which is reprinted with permission from the Journal of Cardiovascular Electrophysiology.

1352

Diverse Fibrosis Architecture and Premature Stimulation Facilitate Initiation of Reentrant Activity Following Chronic Atrial Fibrillation

NATHAN ANGEL, M.S.,*,‡ LI LI, PH.D.,* ROB S. MACLEOD, PH.D.,*,‡ NASSIR MARROUCHE, M.D.,*,† RAVI RANJAN, M.D., PH.D.,*,‡ and DEREK J. DOSDALL, PH.D.*,†,‡

From the *Comprehensive Arrhythmia Research & Management Center, Division of Cardiovascular Medicine, Salt Lake City, Utah, USA; †Center for Engineering Innovation, Salt Lake City, Utah, USA; and ‡Department of Bioengineering, University of Utah, Salt Lake City, Utah, USA

Fibrosis Architecture and Conduction in Chronic AF. ***Introduction:*** **Patients with paroxysmal atrial fibrillation (AF) often transition between sinus rhythm and AF. For AF to initiate there must be both a trigger and a substrate that facilitates reentrant activity. This trigger is often caused by a premature atrial contraction or focal activations within the atrium. We hypothesize that specific architectures of fibrosis alter local conduction to enable AF.**

Methods and Results: **Control goats (n = 13) and goats in chronic AF (for an average of 6 months, n = 6) had a high-density electrode plaque placed on the LA appendage. Conduction patterns following a premature atrial contraction, caused by an electrical stimulation, were quantified to determine regions of conduction slowing. These regions were compared to architecture, either diffuse fibrosis or regions of obstructive fibrosis, and overall fibrosis levels as determined by histology from the mapped region. The chronic AF goats had more obstructive fibrosis than the controls (17.5 ± 8.0 fibers/mm^2 vs. 8.6 ± 3.0 fibers/mm^2). Conduction velocity of the AF goats was significantly slowed compared to the control goats in the transverse direction (0.40 ± 0.04 m/s vs. 0.53 ± 0.15 m/s) but not in the longitudinal direction (0.70 ± 0.27 m/s vs. 0.76 ± 0.18 m/s).**

Conclusions: **AF-induced atrial remodeling leads to increased obstructive fibrosis and conduction velocity slowing transverse to fiber orientation following premature stimuli. The decrease in conduction velocity causes a decrease in the cardiac wavelength, and increases the likelihood of reentry and AF onset.** *(J Cardiovasc Electrophysiol, Vol. 26, pp. 1352-1360, December 2015)*

atrial fibrillation, conduction, electrophysiological mapping, fibrosis, remodeling

Introduction

Atrial fibrillation (AF) is the most common cardiac arrhythmia, affecting over 2 million people in the United States, and its prevalence is expected to grow in the coming years.[1] AF is a serious health concern and is a high risk factor for stroke[1] and cardiomyopathy.[2] In paroxysmal AF, the pulmonary veins have focal activations that can initiate and drive AF. Ablating around the ostia of pulmonary veins to isolate these focal sources from the rest of the left atrium has shown success in treating paroxysmal AF.[3] However, ablation has poor outcomes for treating more extreme forms of AF, persistent and longstanding persistent.[3] The current hypothesis for these poor outcomes in treating persistent AF is that the atrial structural remodeling, most notably the development of fibrosis, may cause conduction slowing in regions of the myocardium beyond the pulmonary veins that can initiate and maintain AF.[4,5] To improve outcomes for persistent AF, it is of utmost importance to study the structural changes associated with this disease as well as the mechanistic links between such changes and reentrant activity.

AF persistence has been shown to increase with arrhythmia duration, due to both structural and electrical remodeling of the atria.[4,6-8] In animal models electrical remodeling can occur as soon as 6 hours, with a decrease in atrial effective refractory period (AERP).[9] As AF transitions from paroxysmal to persistent, many structural changes occur that make AF episodes more common and increased in duration, a phenomenon that has come to be known as "AF begets AF."[8,10] A major component of atrial structural remodeling is the increase in fibrosis,[4,7,11] which has been linked to a decrease in endocardial and epicardium synchronization[7] and an increase in conduction anisotropy,[12] both of which facilitate AF maintenance. Furthermore, the amount of fibrosis pre-ablation has been linked to post-ablation outcomes, which indicates that atrial fibrosis is a major component of atrial structural remodeling that stabilizes AF.[13]

Although these studies suggest that AF fibrosis affects global conduction and AF maintenance, the associated mechanisms of initiation of AF are unknown. Patients who have

This work was supported by the Utah Science Technology and Research (USTAR) Initiative for the Utah Multidisciplinary Arrhythmia Consortium (UMAC). R. Ranjan is currently supported by a K23 (5K23HL115084) grant from NIH. N. Angel, L. Li, and D.J. Dosdall, were in part supported by NIH grant 5R00HL091138. D.J.Doddall is currently supported by a grant (1R01HL128752) from NIH.

Medtronic donated the neurostimulators and pacing leads used in this study.

Disclosures: None.

Address for Correspondence: Derek J. Dosdall, Ph.D., Center for Engineering Innovation, 36 S. Wasatch Dr., SMBB 3100, Salt Lake City, UT 84112, Fax: (801)585-5361; E-mail: derek.dosdall@utah.edu

Manuscript received 18 May 2015; Revised manuscript received 20 July 2015; Accepted for publication 26 July 2015.

for transition to occur there must be a trigger followed by a transition via reentrant activity into fibrillation. This trigger is often caused by a premature atrial contraction or focal activations within the atrium. We hypothesize that specific fibrosis architectures, i.e., the spatial organization, density, and extent of fibrosis, alter local conduction such that the cardiac tissue is more vulnerable to initiating AF. We have classified atrial fibrosis into 2 distinct categories and attempted to determine how local fibrosis architecture alters conduction during a triggered event and the subsequent transition between sinus rhythm and AF. We have also been able to determine whether these conduction changes facilitate reentrant activity to initiate AF. Our findings suggest that long continuous strands of fibrosis, termed obstructive fibrosis, but not of nonobstructive diffuse fibrosis alter local conduction to facilitate the initiation and development of sustained atrial fibrillation, but only during a premature simulation.

Methods

We carried out animal studies in accordance with the *Guide for the Care and Use of Laboratory Animals,*[14] under a protocol approved by the Institutional Animal Care and Use Committee of the University of Utah. All efforts were made to minimize suffering.

Experimental Preparation

Animals

Mixed breed goats (n = 6, 34 ± 5 kg) were implanted with pacemakers and chronic AF was induced with rapid atrial pacing (RAP). Control goats (n = 13, 37 ± 7 kg) were used for comparison and both groups underwent the same electrophysiological and histological study.

Pacemaker Implantation and Programming

Procedures for the pacemaker implantation and programming have been described in detail previously.[11] In brief, mixed breed goats were fasted 12–24 hours prior to surgery, anesthetized with propofol (5–8 mg/kg iv), and maintained with inhaled isoflurane dosed to effect (1.5–4%) in inspired oxygen. A subcutaneous pocket on the lateral neck was made, and a neurostimulator (Itrel 3 or InterStim, Medtronic, Minneapolis, MN, USA) was implanted to serve as a pacemaker. A pacing lead (Medtronic) with active fixation was introduced into the right atrium through a jugular vein. After at least a 1-week recovery period, pacemakers were programmed to stimulate continuously at 50 Hz with 1 second of stimulation followed by 1 second without stimulation at 2–3 times the diastolic pacing threshold. Every 1–2 weeks, the ECG was recorded, the rhythm was evaluated, and the pacemaker turned off to determine if AF was sustained for a minimum of 20 minutes. Once AF was sustained, the pacemaker was programmed to stimulate 1 second every minute to reinitiate AF if the heart spontaneously returned to sinus rhythm.

Terminal Study

An open-chest electrophysiological study was performed on control goats that were not paced and chronic AF goats (RAP 6 ± 1 months). Animals received unlimited water but no food for 12- 24 hours prior to the experiment. The goats were anesthetized with propofol (5–8 mg/kg iv), intubated, and maintained with inhaled isoflurane dosed to effect (1.5–4%) in inspired O_2 under positive pressure ventilation. An orogastric tube (S-50-HL, 1/2-in. inner diameter, 3/4-in. outer diameter, Tygon Tubing) was advanced into the rumen to evacuate gas and prevent bloat. A medial thoracotomy was preformed to expose the heart. Chronic AF goats had their pacemakers turned off; then they were defibrillated with 1–5 50 J biphasic QRS synchronized shocks delivered with paddles placed on either side of the atrium from a defibrillator. Electrophysiological measurements did not begin for at least 10 minutes after cardioversion.

Electrical Mapping Procedure and Analysis

An electrode array consisting of 256 electrodes arranged in a 16-by-16 grid with uniform interelectrode spacing of 1 mm was placed on the LA appendage. The electrograms recorded from the electrodes were referenced to a remote electrode placed in the left hind leg. In addition to recording unipolar electrograms from the electrode plaque, an ECG, a ventricular electrogram, and a pacing signal were also simultaneously recorded. The ventricular electrogram was recorded with a single, ventricular hook electrode that was referenced to the left hind leg. All signals were band passed filtered between 0.3 and 500 Hz, had a gain of 100, were digitized at 12-bit resolution, and sampled at 8 KHz with a custom-built data acquisition system.

The electrophysiological study consisted of 3 pacing protocols. Monophasic stimuli were used for pacing and were produced using a custom build current controlled stimulator. In all the pacing protocols, stimulation pulses were applied to a pair of electrodes at the center of the plaque. The first protocol was a standard restitution protocol that consisted of a series of 10-, 400-millisecond S1 pulses followed by a premature S2.[15] The S2 cycle length was decremented from 350 milliseconds by 10 milliseconds until loss of atrial capture. After loss of atrial capture at the 10-millisecond resolution, the S2 cycle length was increased by 5 milliseconds to determine the AERP within 5 milliseconds. The last S2 pulse cycle length that caused atrial capture was considered the AERP. The pulse width for this protocol was 2 milliseconds at a current of twice the diastolic threshold, which was determined as the minimum current for atrial capture at a cycle length of 400 milliseconds.

The second pacing protocol was a dynamic restitution protocol, which consisted of 30 S1 stimuli for entrapment, followed by 15 seconds of continuous S1 pacing.[15] Atrial capture was determined after the entrapment period. The S1 cycle length was decremented from 350 milliseconds by 10 milliseconds until loss of atrial capture and the last S1 pulse cycle length that caused atrial capture was considered the S1-AERP.

The third protocol was an AF inducibility test, which consisted of burst pacing the atrium at 50 Hz for 30–45 seconds at twice the diastolic pacing threshold. If AF persisted for up to 10 minutes it was considered sustained. The pulse width for this protocol was 0.5 milliseconds at a current of twice the diastolic threshold, which was determined as the minimum current for atrial capture at a cycle length of 400 milliseconds.

If any of the protocols induced AF, it was allowed to persist for at least 10 minutes to determine whether the arrhythmia would self-terminate. If AF did not self-terminate

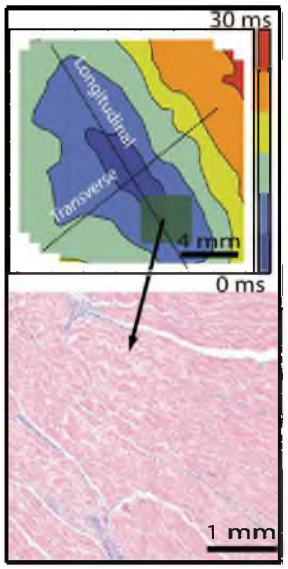

Figure 1. *Dividing mapped region into longitudinal and transverse propagation direction. Mapped region divided into 2 transverse and 2 longitudinal directions. An extra beat is considered either longitudinal or transverse if it is within ± 45° (within dashed lines). Green box shows the histology sample to confirm that the longitudinal direction as determined with the isochrone map agrees with the myocardial fiber direction as determined through histology. For a high quality, full color version of this figure, please see Journal of Cardiovascular Electrophysiology's website: www.wileyonlinelibrary.com/journal/jce*

after 10 minutes, the heart was defibrillated with one to five 50 J biphasic QRS synchronized shocks delivered with paddles placed on either side of the atrium from a defibrillator. Care was taken to ensure that the recording plaque did not move during defibrillation. Electrical recordings were then resumed after 10 minutes of sinus rhythm. Arrhythmias were classified as sustained AF, nonsustained AF, or extra beats. Sustained AF was AF lasting at least 10 minutes, nonsustained AF was AF lasting from 5 s to 10 minutes, and short cycle length excitations lasting less than 5 seconds were classified as extra beats.

Differences between AF initiations were determined by examining the direction of propagation of extra beats across the mapping surface. Only the first extra beat after an S2 was analyzed and the propagation direction spontaneously resulting from the S2 was determined as either longitudinal or transverse (within ± 45°) in relation to the generalized fiber orientation. The longitudinal direction was assessed by determining the direction of fastest conduction based on isochrone activation maps created during beats paced at 400-millisecond cycle lengths from the center of the mapped region and was verified with myocardial fiber orientation from histology (Fig. 1). The transverse fiber orientation was assumed to be 90 degrees from the longitudinal fiber orientation, this assumed fiber direction agreed well with the fiber direction as determined through histology. Each animal was then grouped into 1 of 2 groups based on whether extra beats propagated primarily in the longitude or transverse directions across the recording plaque and a Fisher's exact test was used to determine differences between the AF and control groups.

We measured conduction velocity transverse and longitudinal to the generalized fiber orientation for an S1 of 400 milliseconds, and during an S2 of 160 milliseconds. Conduction velocity was quantified with a previously validated algorithm that can distinguish between transverse and longitudinal conduction.[16] In brief, this algorithm creates an isochrone map based on the activation times from the electrograms on the plaque. Activations were taken as the local minima of the first temporal derivative of the unipolar atrial electrograms. Conduction velocity was calculated by selecting 15–25 activation times within a region of the plaque. Each activation time point contained x and y spatial information that corresponded to the relative distances between the electrodes. From the temporal (activation times) and spatial information (distance between points), a conduction velocity was determined by using a least square fitting of the time and space information to a plane. The conduction velocity and angle of propagation were determined from the fitted parameters as described previously.[16,17] By this method, 2 transverse and longitudinal conduction velocities were found for each isochrone activation map. For each animal, an averaged longitudinal and transverse conduction velocity for both S1-400 milliseconds and S2-160 milliseconds, respectively, were found by averaging the results from 2 to 3 activation maps. An anisotropy ratio was calculated from these conduction velocities, which is the ratio of longitudinal to transverse conduction velocity. A higher anisotropy ratio indicates more anisotropy and a value of 1 indicates isotropic conduction.

Histological Data Acquisition and Analysis

After the electrophysiological study the heart was excised and the LA region that contained the high-density recording plaque was removed and placed in a 10% buffered formalin solution. All 6 AF goats and a randomly selected 6 of the control goats had histological tissue samples stained with Masson's trichrome after a 1-month fixation period and evaluated for fibrosis. Histology was sectioned parallel to the epicardium at a depth of 500 μm below the epicardium with a thickness of 4 μm. Images from the samples were imported into ImageJ software (National Institutes of Health) for fibrosis quantification. The images were segmented into 3 color groups: red for myocytes, blue for collagen/fibrosis, and white for nonfibrotic extracellular content. Each color was manually sampled 7–12 times per image, after which a hidden Markov model was used to automatically segment the entire image into the 3 colors. The hidden Markov model outputs the total percentage for each color in the image and the percentage of blue served to estimate the total amount of fibrosis in the tissue sample. The percent fibrosis was then compared with both longitudinal and transverse conduction velocity.

Atrial fibrosis was further quantified and to 2 groups, nonobstructive and obstructive fibrosis. Obstructive fibrosis was considered fibrosis that was at least the length of a myocyte (100 μm), thus potentially disrupting transverse cell to cell conduction. Nonobstructive fibrosis was fibrosis that was less than 100 μm. This classification was done by examining the maximum length of fibrosis strands in the histology images using a custom MATLAB program. In brief, this program imported the segmented ImageJ images, which were segmented into blue, white, and red. These images were then converted into a binary image where the blue was a value

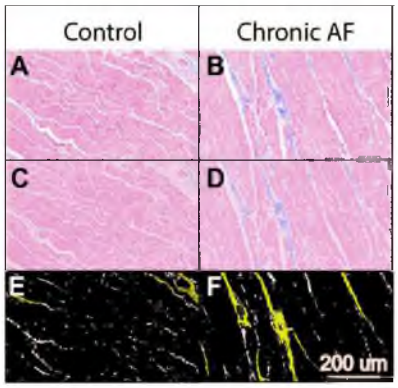

Figure 2. *Determining obstructive fibrosis. A and B: Raw histology from a control and AF animal. C and D: ImageJ 3 color segmentation. Red indicates myocytes, blue indicates fibrosis/collagen, and white indicates nonfibrotic extracellular content. E and F: Binary image with white showing fibrosis. The white fibrosis has been binary dilated by 5 pixels (2.52 um). Yellow has been overlaid onto fibrosis strands that are greater than 100 μm in length, which is considered obstructive fibrosis. E has 4 fibrotic groups and F has 8 fibrotic groups that met the 100 μm threshold to be considered obstructive fibrosis. For a high quality, full color version of this figure, please see Journal of Cardiovascular Electrophysiology's website: www.wileyonlinelibrary.com/journal/jce*

of 1 and the red/white had a value of 0. A binary dilate of 5 pixels, 2.52 μm, was then applied to the binary image. An 8 neighbor connected components analysis from the MATLAB image processing toolkit was then applied to the binary image to find regions of continuous fibrosis. The maximum distance of each fibrotic connected component for each image was then computed. Strands greater than 100 μm were considered obstructive fibrosis since they could disrupt an entire cell's transverse conduction. Figure 2 shows an example of how obstructive fibrosis was quantified. The local fibrosis densities and architecture of fibrosis in our histological samples were compared with local conduction data, as determined through the electrical mapping studies.

Statistical Analysis

Differences in AERP and S1-AERP between control and chronic AF goats were examined with unpaired *t*-tests. Differences between initiation of sustained AF, nonsustained AF, and extra beats between the control and AF groups were determined with a Fisher's exact test. Extra beat propagation direction between the control and chronic AF goats was examined with a Fisher's exact test. Differences between conduction velocity (average transverse and average longitudinal) between the AF and control groups were determined with an unpaired *t*-test at both 400-millisecond and the 160-millisecond cycle length. Differences in percent fibrosis between the AF and control groups were determined with an unpaired *t*-test. Differences in the anisotropy ratio between the AF and control groups were determined with an unpaired *t*-test. Differences in the number of obstructive fibrotic strands per square mm between the AF and control groups were determined with an unpaired *t*-test. Differences in the density of fibrosis predicting the direction of slowest conduction between the AF and control groups were determined using a 1-sided chi-square. Statistical tests in which

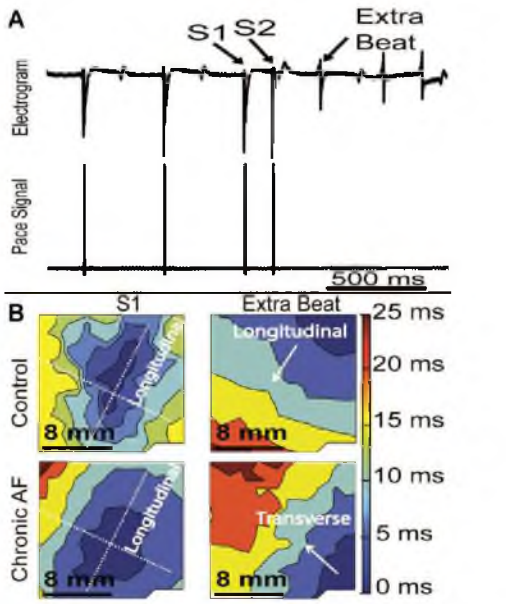

Figure 3. *Example of extra beat propagation direction of chronic AF vs. control. A: An atrial electrogram that shows the initiation of extra beats following the S2 pacing pulse. The first extra beat at the initiation of extra beats was examined to determine its propagation across the recording plaque. B: The S1 column shows isochrone activation maps after an S1 pacing pulse, which was used to determine fiber orientation. The extra beat column shows isochrone activation maps of an extra beat following an S2-induced beat. The arrow shows the direction of extra beat propagation. For a high quality, full color version of this figure, please see Journal of Cardiovascular Electrophysiology's website: www.wileyonlinelibrary.com/journal/jce*

Results

AERP and AF Inducibility

AF was persistent in all RAP goats prior to the electrophysiological procedure. In 2/6 of these chronic AF goats, AF could not be cardioverted to sinus rhythm and the protocol could not be completed. There was a significant shortening of AERP (controls: 147 ± 21 milliseconds vs. chronic AF: 118 ± 23 milliseconds, $P < 0.05$) but not the S1-AERP (controls: 180 ± 53 milliseconds vs. chronic AF: 169 ± 15 milliseconds, $P > 0.05$) in the chronic AF goats as compared to the controls. The RAP goats had sustained AF more often than those in the control group; however, there was no significant difference in frequency of nonsustained AF or extra beats. All 6 of the chronic AF goats had sustained AF whereas 2/13 of the control goats showed sustained AF during the electrophysiological study. Nonsustained AF occurred in 9/13 of the control goats. A total of 20 extra beats following the S2 pacing pulse were observed in 6/13 of the control goats. Extra beats ($n = 22$) were observed in 4/6 of the AF goats. The 2 chronic AF goats that did not have extra beats could not be defibrillated; therefore, the S1–S2 protocols could not be performed on these animals. The extra beats in the hearts of the control goats propagated longitudinally along the fiber (19/20 beats), with 6/6 of the goats having extra beats that propagated primarily in the longitude direction. In the AF goats, the extra beats propagated transversely to the fiber orientation (14/22 beats), with 3/4 of the goats having extra beats that propagated primarily in the transverse direc-

TABLE 1
Summary of AF Inducibility

Control Data				AF Data			
Goat Number	**Sustained AF**	**NonSustained AF**	**Extra Beats**	**Goat Number**	**Sustained AF**	**NonSustained AF**	**Extra Beats**
1	No	No	No	1	Yes	Yes	Yes
2	Yes	Yes	Yes	2	Yes	Yes	Yes
3	No	No	No	3	Yes	Yes	Yes
4	No	Yes	No	4	Yes	Yes	Yes
5	No	Yes	Yes	5	Yes	No*	No*
6	No	Yes	Yes	6	Yes	No*	No*
7	Yes	Yes	Yes	Totals	6/6	4/4	4/4
8	No	No	No				
9	No	Yes	Yes				
10	No	Yes	Yes				
11	No	Yes	No				
12	No	No	No				
13	No	No	No				
Totals	2/13	8/13	6/13				

AF = atrial fibrillation.
*Animals could not be defibrillated.

direction of the AF goats compared to the controls. Table 1 summarizes AF inducibility.

Conduction Velocity

Conduction velocity of the AF goats was significantly slowed compared to the control goats in the transverse direction (0.40 ± 0.04 m/s vs. 0.53 ± 0.15 m/s, $P < 0.05$) but not in the longitudinal direction (0.70 ± 0.27 m/s vs. 0.76 ± 0.18 m/s) following a premature atrial contraction, caused by an S2-160 milliseconds. There was no significance difference in either transverse (0.63 ± 0.14 vs.0.58 ± 0.19 m/s) or longitudinal conduction (0.96 ± 0.21 m/s vs. 0.87 ± 0.18 m/s) at an S1 of 400 milliseconds between the AF and control goats. Figure 4 shows examples of transverse slowing in the AF goats as compared to the controls following S2 stimulation. Figure 5 shows an example of the initiation of extra beats and AF when the conduction velocity restitution becomes steep. Figure 5C shows an increase in the anisotropy for the AF animals as the coupling interval decreases. There was no significance difference in anisotropy ratio at an S1 of 400 milliseconds (1.55 ± 0.42 vs. 1.57 ± 0.33) or an S2 of 160 milliseconds (1.72 ± 0.55 vs. 1.47 ± 0.25) between the AF and control animals.

Histology Analysis

The AF goats had a higher density of fibrosis as compared to controls ($5.2 \pm 0.7\%$ vs. $3.5 \pm 1.0\%$, $P < 0.05$) and more diverse fibrosis architecture. The AF animals had more obstructive fibrosis than the controls (17.5 ± 8.0 fibers/mm^2 vs. 8.6 ± 3.0 fibers/mm^2, $P < 0.05$). The control group had more nonobstructive, diffuse fibrosis than the AF animals (1109.3 ± 308.5 fibers/ mm^2 vs. 718.1 ± 380.0 fibers/mm^2, $P = 0.07$, N.S.) however, the result did not meet significance. The organization of this obstructive fibrosis was in strands that were located primary parallel to myocyte bundles, potentially interrupting transverse connections between cells. Figure 6 shows specific examples of the different fibrosis architectures in chronic AF and control animals.

The density of fibrosis in the chronic AF goats, but not the controls, predicted the direction of slowest conduction. Fibrosis density was analyzed in both the longitudinal and transverse directions. These densities were then compared to the conduction velocities in these regions (Fig. 7). In 3/4 of the AF animals, the direction of highest fibrosis density predicted the direction of slowest conduction. In 1/6 of the control animals the direction of highest fibrosis predicted the direction of slowest conduction ($P < 0.05$ for AF vs. control).

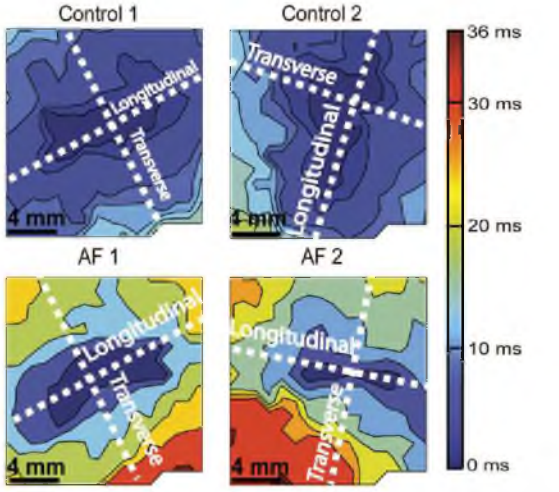

Figure 4. *Examples of transverse conduction slowing during a premature stimulus. Examples from 2 AF animals and 2 control animals are shown. Activation maps were created from an S2 stimulation at 160 milliseconds. The white dashed lines indicate the generalized fiber direction as determined from S1 pacing and confirmed with histology. The 2 activation maps from the chronic AF group show that the transverse conduction was greatly slowed compared to the controls as a result of a premature. This finding was consistent across all the AF animals. For a high quality, full color version of this figure, please see Journal of Cardiovascular Electrophysiology's website: www.wileyonlinelibrary.com/journal/jce*

Discussion

The major findings of this study are as follows: (1) AERP was significantly reduced as a result of chronic AF but S1-AERP is not. (2) Conduction velocity was significantly

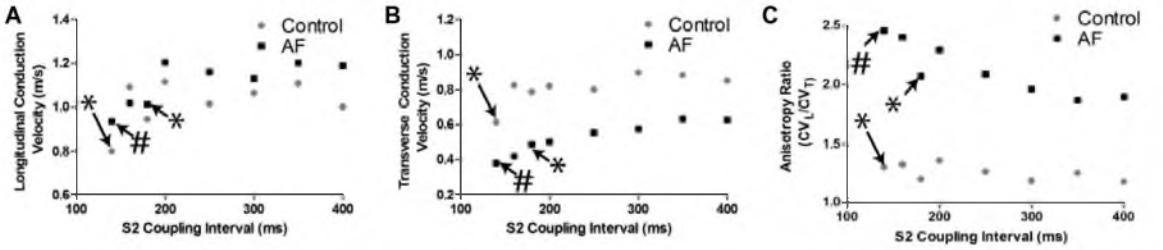

Figure 5. *Examples of conduction velocity restitution. A: Longitudinal conduction velocity restitution curve for a control and chronic AF animal. B: Transverse conduction velocity restitution curve for a control and chronic AF animal. C: Anisotropy ratio restitution curve for a control and chronic AF animals. Extra beats are indicated with a * and sustained AF is indicated with a #. The control and AF animals began initiated extra beats when restitution started to become steep at an S2 of 140 milliseconds and 160 milliseconds, respectively. When the S2 coupling interval was further reduced the chronic AF animal initiated sustained AF at an S2 of 140 milliseconds. Both chronic AF and controls had nonlinear restitution curves as the coupling interval reduced; however, in the chronic AF animals the anisotropy ratio increased, whereas in the controls it saw little change.*

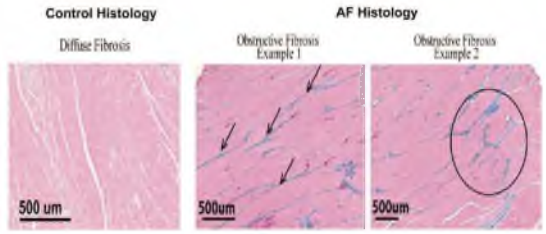

Figure 6. *Architecture of fibrosis is more diverse in chronic AF as compared to control. The control groups had low levels of diffuse fibrosis (location 1) with few strands of obstructive fibrosis. The chronic AF group had regions of myocardium with obstructive fibrosis (location 2 and location 3) that are indicated by the long, compact groups of fibrotic strands located primarily along the generalized longitudinal cell direction. Examples of obstructive fibrosis are shown with arrows in location 2 and is circled at location 3. For a high quality, full color version of this figure, please see Journal of Cardiovascular Electrophysiology's website: www.wileyonlinelibrary.com/journal/jce*

slower in chronic AF, but only in the transverse direction following a premature atrial contraction, indicating that there is functional slowing in chronic AF but only at short coupling intervals. (3) Extra beats in chronic AF propagated across the mapping region via transverse conduction; however, in the controls the extra beats propagated across the mapping region via longitudinal conduction. (4) Chronic AF goats developed diverse structures of fibrosis (i.e., obstructive fibrosis) that were less common in controls, and this difference was quantitatively defined.

The AERP values we obtained (controls: 147 ± 21 milliseconds and chronic AF: 118 ± 23 milliseconds) agree with a study by Schotten *et al.* that showed that after 5 days of RAP the LA AERP decreased from a baseline of 132 ± 19 milliseconds to 72 ± 7 milliseconds.[9] The AERP relates to fibrillation initiation and maintenance through restitution. The restitution hypothesis states that an action potential duration restitution slope of > 1 alterations between short and long APD, or alternans, can occur.[15,18,19] Alterations in action potential durations will cause heterogeneity in repolarization gradients and may result in unidirectional conduction block, which can initiate spiral wave reentry.[15,20-22] Our data also support the finding that the initiation of extra beats and AF occurs when the conduction velocity restitution curve became steep. The atrial myocardium of our chronic AF animals could capture at shorter cycle lengths as compared to the controls. This indicates that hearts experiencing chronic AF can, at least transiently, support more rapid activations, which could lead to alterations in APD, thus causing a greater chance of AF initiation. The S1-AERP, obtained from a dynamic restitution protocol, did not show any differences between the AF and control groups. The main difference between dynamic and standard restitution protocols is that dynamic restitution takes into account cardiac memory,[19,23] a mechanism in which delays in ionic currents, such as calcium and potassium, with slow enough recovery kinetics can accumulate over several cycles. Another possible mechanism is that rapid pacing can induce changes in gene expression.[23] During the S1-AERP protocol the myocardium was in a steady state due to the uniform pacing. Cardiac memory may have a more primary role in determining AERP during uniform activations (steady state) than any structural/functional remodeling as a result of AF. However, the S2 (nonsteady state)-AERP did show a difference, suggesting that the structural/functional remodeling as a result of AF does have a major role in determining AERP after a premature atrial contraction. This supports Kawara *et al.*,'s findings that suggested that conduction slowed as a result of a premature stimulus but not at slower pacing cycle lengths.[24]

AF is also known to alter cardiac conduction anisotropy, which under normal conditions arises because conduction velocity is faster along the direction longitudinal to the myocytes compared to transverse. This anisotropic condition is due to both fiber orientation of the myocytes and the higher density of gap junction connecting the cells in the longitudinal direction. Verheule *et al.* also showed that atrial fibrosis causes further conduction anisotropy in the longitudinal vs. transverse directions.[7] Our results agree with the finding that conduction anisotropy increases during atrial remodeling but only after a premature stimulus. This finding agrees with those from Kawara *et al.*, who suggest that in the ventricles, fibrosis only causes transverse conduction slowing following a premature stimulation.[24] Their explanation was that the long strands found in stringy fibrosis cause slowing of conduction. Our results demonstrate that AF-induced fibrosis shares similar effects to what has been shown previously only in ventricular preparations with extensive fibrosis.

Extra beats in chronic AF propagated across the mapping region via transverse conduction; however, in the controls the extra beats propagated across the mapping region via longitudinal conduction. This finding was observed by Kawara *et al.* in which they found that large patches of what they called patchy fibrosis could block longitudinal conduction,

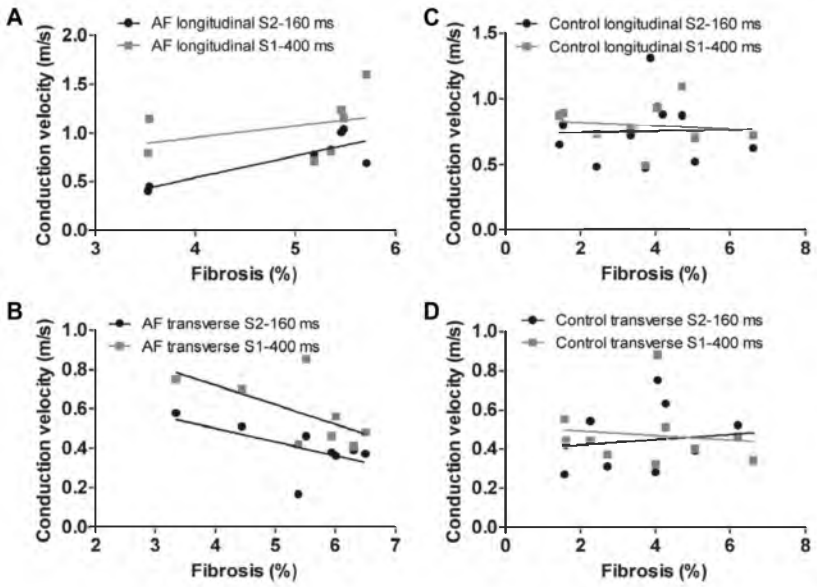

Figure 7. *Fibrosis densities and conduction slowing. (A) The chronic AF animals had increased longitudinal conduction velocity with increased fibrosis at an S2 of 160 milliseconds (correlation P = 0.02) but not at S1 of 400 milliseconds (P = 0.43). (B) The chronic AF animals had no correlation with fibrosis densities and transverse conduction velocity at an S2 of 160 milliseconds or S1 of 400 milliseconds, but was trending towards significance (P = 0.12 and 0.10). (C) Control animals had no correlation with longitudinal conduction velocity at an S2 of 160 milliseconds or S1 of 400 milliseconds (P = 0.93 and 0.75). (D) Control animals had no correlation with transverse conduction velocity at an S2 of 160 milliseconds or S1 of 400 milliseconds (P = 0.67 and 0.72).*

thus causing conduction transverse to fiber orientation. There may be large patches of fibrosis outside the mapped region in the AF animals that cause this shift in longitudinal to transverse conduction.

There was more fibrosis in the chronic AF animals than in the control goats but, more importantly, the fibrosis architecture was different. The AF goats had more obstructive fibrosis and less nonobstructive fibrosis than the controls, which demonstrates a difference in the structure of the fibrosis. As AF develops, the strands of fibrosis that are nonobstructive may start to connect, forming obstructive fibrosis that may slow or even block transverse conduction. The organization of this obstructive fibrosis was in strands that were located primary along cells, potentially interrupting transverse connections between cells. This obstructive fibrosis architecture is similar to interstitial fibrosis, which has been described to appear in intermuscular spaces previously devoid of collagen.[25] Krul *et al.* classified LA appendage fibrosis and related the fibrosis to conduction properties in humans. They found that regions of thick interstitial collagen were associated with increased longitudinal conduction velocity and transverse activation delay.[26] These long strands of fibrosis located parallel to the myocytes may expand the distance between neighboring cells, reduce the electric conductance, and explain why the transverse conduction velocity was slowed while longitudinal was not.[7,27,28] Our results are similar to the findings of Krul *et al.* in humans for transverse conduction slowing. Although we did not observe a significant increase in longitudinal conduction velocity as was found by Krul *et al.*, we did observe the correlation between increased longitudinal conduction velocities with increased levels of fibrosis, which is similar to what they showed in left atrial appendage samples with thick collagen strands. The increase in longitudinal conduction velocity with increased fibrosis may also be explained due to the structure of the fibrosis. The fibrosis appears to be deposited parallel to myocytes, thus obstructing the transverse conduction, and potentially causing a source–sink mismatch. This source–sink mismatch may not only slow transverse conduction, but may also shunt conduction along the longitudinal direction, thus increasing longitudinal conduction velocity. This may explain why many studies show an increase in conduction anisotropy following development of fibrosis in animal models of AF[7] as well as in human ventricular tissue[24] and human atrial tissue.[28]

The chronic AF goats had higher incidence of sustained AF than the control goats, which may be the result of slowed conduction in the AF animals. Conduction in the AF animals slowed because of 2 mechanisms. First, conduction slowed transverse to fiber orientation only during short cycle lengths, which could result from a premature atrial contraction or due to the rapid activation rate that is present during AF. The second mechanism of conduction slowing that we observed was that extra beats propagated transversely to fiber orientation, instead of longitudinally, during AF. Under normal physiological conditions this directional variance alone would slow conduction due to conduction anisotropy. However, in the chronic AF animals this slowing was even further exaggerated, which would result in more AF susceptibility due to 2 mechanisms. The first, more classical method is that slowed conduction would result in more possible pathways for reentry due to the decreased wave length (wavelength = conduction velocity x APD). For reentry to occur the wavelength must be shorter than the reentrant path. Therefore a smaller wavelength will allow for more possible reentrant pathways and make AF more likely to be initiated and sustained.[29,30] The second mechanism of slowed conduction velocity increasing AF susceptibility is due to an increase in rotor stability. Rotors circulate around an unexcitable center known as a singularity point.[23] For the singularity to remain unexcitable, and for the rotor to be sustained, the cardiac tissue must have a so-called source–sink mismatch, which results in slowed conduction velocity and a steep curvature around the singularity point.[21-23] Debate continues as to whether or not calculating wavelengths has relevance to explaining reentry and fibrillation due to antiarrhythmic drugs that decrease conduction velocity yet still terminate AF.[31] Slowed conduction has been shown in patients with paroxysmal AF, suggesting that it may be critical to sustaining AF,[32,33] and

this may occur either by the classical view of decreasing wavelengths, or the more modern view of setting up steep curvature for rotors.[21,22,30]

There was no statistical difference in conduction velocity at slow cycle lengths and in S1-AERP between the AF and control goats, indicating that during normal physiological conditions, such as sinus rhythm, the AF affected myocardium and the control myocardium exhibit similar conduction. However, once a premature atrial contraction occurs, the AF cardiac substrate affects the local conduction differently than the non-AF substrate. Such a response suggests that the AF fibrosis may produce a substrate that has little effect during sinus rhythm, but following a premature atrial contraction may display the conduction slowing that could lead to reentry and AF.

Clinical Implications

The clinical relevance of these findings is that reentrant activity observed in patients with chronic AF may be a result from 2 separate but necessary components. First, reentry is more likely to occur due to slowed conduction that occurs only due to premature contractions. This has been shown in human data, which found that AF could initiate via spiral wave reentry at sites of dynamic conduction slowing.[34] Therefore, patients who have more premature atrial contractions or increased activity of focal sources will be more likely to cause this functional slowing as a result of the short coupling interval to initiate and sustain AF. The second component is the architecture of fibrosis. We observed obstructive fibrosis that significantly slowed transverse conduction. Markides *et al.* reported that patients with paroxysmal AF have an abnormal atrial substrate with regions of slowed conduction, specifically where there is an abrupt change in subendocardial fiber orientation, and under certain pacing parameters these regions of conduction slowing could cause block.[33] If patients have substantial obstructive fibrosis, it will make these regions of abrupt changes in fiber orientation more susceptible to conduction block, thus increasing the likelihood of AF. These findings suggest that both a tendency of frequent premature contractions and specific fibrosis architecture are required for development of sustained AF.

Limitations

This study was limited to AF developed through rapid atrial pacing without the presence of any existing heart disease. Although such a scenario may apply to some of the human patient population, more often AF is accompanied by some form of heart disease that may induce substrate changes in the atrium. In addition, this study was performed in goats and, although goat and human hearts are of roughly similar size, there may be meaningful differences in electrophysiology. Hence, the results of these findings may not directly translate to humans. In spite of these limitations, the chronic rapid atrial paced AF goat model is widely used and well accepted for studying AF.[6-8,11] Another limitation is we took only a 4 um thick sample of histology 500 μm from the epicaridal surface to determine a generalized fiber direction. A remodeled atrium has very complicated atrial structure including a dissociation of epicardium and endocardium.[6,7] Therefore, we used a generalized fiber direction in our classifications and electrophysiological measurements. Our histology measurements included determination of fibrosis but no measure of alternation within the gap junctions. Several studies have shown that gap junctional remodeling during AF may lead to conduction slowing.[4,35] A final limitation is that only a region of the left atrial appendage was mapped and our findings may not translate to the rest of the atrium. We made electrophysiological measurements on the left atrial appendage because our mapping protocol required a large continuous surface to calculate accurate conduction velocities.

Conclusion

Structural and electrophysiological remodeling in chronic AF leads to extra beat propagation and conduction velocity slowing transverse to fiber orientation. These 2 mechanisms combine to decrease global conduction velocity, to decrease the cardiac wavelength, and to increase the likelihood of reentry. This sequence may lead to more extra beats and the establishment of stable reentry in tissue with structural and electrical remodeling. The major histological difference between chronic AF and control hearts is the amount and architecture of the fibrosis. Histology from goats with a history of chronic AF had much more obstructive fibrosis, which may lead to the conduction slowing and alteration in conduction pathways to make the tissue more susceptible to AF.

Acknowledgments: The authors thank Layne Norlund, Orvelin Roman, and Jose Reyes for excellent technical animal support. The authors would also like to thank Anders-Peter Larsen for assisting with the conduction velocity program. The authors would also like to thank the faculty and staff of the Nora Eccles Harrison Cardiovascular Research and Training Institute (CVRTI) at the University of Utah for allowing us to use their facilities and recording equipment to conduct these studies. The authors would also like to thank Medtronic for donating the neurostimulators and pacing leads used in this study.

References

1. Deshpande S, Catanzaro J, Wann S: Atrial fibrillation: Prevalence and scope of the problem. Card Electrophysiol Clin 2014;6:1-4.
2. Di Donna P, Olivotto I, Delcrè SDL, Caponi D, Scaglione M, Nault I, Montefusco A, Girolami F, Cecchi F, Haissaguerre M, Gaita F: Efficacy of catheter ablation for atrial fibrillation in hypertrophic cardiomyopathy: Impact of age, atrial remodelling, and disease progression. Europace 2010;12:347-355.
3. January CT, Wann LS, Alpert JS, Calkins H, Cleveland JC, Cigarroa JE, Conti JB, Ellinor PT, Ezekowitz MD, Field ME, Murray KT, Sacco RL, Stevenson WG, Tchou PJ, Tracy CM, Yancy CW; ACC/AHA Task Force Members: 2014 AHA/ACC/HRS Guideline for the Management of Patients with Atrial Fibrillation: A Report of the American College of cardiology/American Heart Association Task Force on Practice Guidelines and the Heart Rhythm Society. Circulation 2014;130:2071-2104.
4. Allessie M, Ausma J, Schotten U: Electrical, contractile and structural remodeling during atrial fibrillation. Cardiovasc Res 2002;54:230-246.
5. deGroot N, Houben R, Smeets J: Electropathological substrate of longstanding persistent atrial fibrillation in patients with structural heart disease epicardial breakthrough. Circulation 2010;1674-1682.
6. Eckstein J, Maesen B, Linz D, Zeemering S, vanHunnik A, Verheule S, Allessie M, Schotten U: Time course and mechanisms of endo-epicardial electrical dissociation during atrial fibrillation in the goat. Cardiovasc Res 2011;89:816-824.
7. Verheule S, Tuyls E, Gharaviri A, Hulsmans S, vanHunnik A, Kuiper M, Serroyen J, Zeemering S, Kuijpers NHL, Schotten U: Loss of continuity in the thin epicardial layer because of endomysial fibrosis increases the complexity of atrial fibrillatory conduction. Circ Arrhythm Electrophysiol 2013;6:202-211.

8. Wijffels MC, Kirchhof CJ, Dorland R, Allessie MA: Atrial fibrillation begets atrial fibrillation. A study in awake chronically instrumented goats. Circulation 1995;92:1954-1968.
9. Schotten U: Electrical and contractile remodeling during the first days of atrial fibrillation go hand in hand. Circulation 2003;107:1433-1439.
10. Rostock T, Steven D, Lutomsky B, Servatius H, Drewitz I, Klemm H, Müllerleile K, Ventura R, Meinertz T, Willems S: Atrial fibrillation begets atrial fibrillation in the pulmonary veins on the impact of atrial fibrillation on the electrophysiological properties of the pulmonary veins in humans. J Am Coll Cardiol 2008;51:2153-2160.
11. Dosdall DJ, Ranjan R, Higuchi K, Kholmovski E, Angel N, Li L, Macleod R, Norlund L, Olsen A, Davies CJ, Marrouche NF: Chronic atrial fibrillation causes left ventricular dysfunction in dogs but not goats: Experience with dogs, goats, and pigs. Am J Physiol Heart Circ Physiol 2013;305:H725-H731.
12. Allessie M, Ausma J, Schotten U: Electrical, contractile and structural remodeling during atrial fibrillation. Cardiovasc Res 2002;54:230-246.
13. Marrouche NF, Wilber D, Hindricks G, Jais P, Akoum N, Marchlinski F, Kholmovski E, Burgon N, Hu N, Mont L, Deneke T, Duytschaever M, Neumann T, Mansour M, Mahnkopf C, Herweg B, Daoud E, Wissner E, Bansmann P, Brachmann J: Association of atrial tissue fibrosis identified by delayed enhancement mri and atrial fibrillation catheter ablation. JAMA 2014;311:498.
14. Committee for the Update of the Guide for the Care and Use of Laboratory Animals, Institute for Laboratory Animal Research, Division on Earth and Life Studies, National Research Council Committee for the Update of the Guide for the Care and Use of Laboratory Animals. Washington, DC: 2011.
15. Koller ML, Riccio ML, Gilmour RF: Dynamic restitution of action potential duration during electrical alternans and ventricular fibrillation. Am J Physiol 1998;275:H1635-H1642.
16. Larsen AP, Sciuto KJ, Moreno AP, Poelzing S: The voltage-sensitive dye di-4-ANEPPS slows conduction velocity in isolated guinea pig hearts. Heart Rhythm 2012;9:1493-1500.
17. Bayly PV, KenKnight BH, Rogers JM, Hillsley RE, Ideker RE, Smith WM: Estimation of conduction velocity vector fields from epicardial mapping data. IEEE Trans Biomed Eng 1998;45:563-571.
18. Riccio ML, Koller ML, Gilmour RF: Electrical restitution and spatiotemporal organization during ventricular fibrillation. Circ Res 1999;84:955-963.
19. Cherry EM, Fenton FH: Suppression of alternans and conduction blocks despite steep APD restitution: Electrotonic, memory, and conduction velocity restitution effects. Am J Physiol Heart Circ Physiol 2004;286:H2332-H2341.
20. Comtois P, Kneller J, Nattel S: Of circles and spirals: Bridging the gap between the leading circle and spiral wave concepts of cardiac reentry. Europace 2005;7(Suppl 2):10-20.
21. Vaquero M, Calvo D, Jalife J: Cardiac fibrillation: From ion channels to rotors in the human heart. Hear Rhythm 2008;5:872-879.
22. Pandit SV, Jalife J: Rotors and the dynamics of cardiac fibrillation. Circ Res. 2013;112:849-862.
23. Weiss JN, Qu Z, Chen P-S, Lin S-F, Karagueuzian HS, Hayashi H, Garfinkel A, Karma A: The dynamics of cardiac fibrillation. Circulation 2005;112:1232-1240.
24. Kawara T, Derksen R, de Groot JR, Coronel R, Tasseron S, Linnenbank AC, Hauer RNW, Kirkels H, Janse MJ, deBakker JMT: Activation delay after premature stimulation in chronically diseased human myocardium relates to the architecture of interstitial fibrosis. Circulation 2001;104:3069-3075.
25. Weber KT, Brilla CG: Pathological hypertrophy and cardiac interstitium. Fibrosis and renin-angiotensin-aldosterone system. Circulation 1991;83:1849-1865.
26. Krul SPJ, Berger WR, Smit NW, vanAmersfoorth SCM, Driessen AHG, vanBoven WJ, Fiolet JWT, vanGinneken ACG, vander Wal AC, deBakker JMT, Coronel R, deGroot JR: Atrial fibrosis and conduction slowing in the left atrial appendage of patients undergoing thoracoscopic surgical pulmonary vein isolation for atrial fibrillation. Circ Arrhythmia Electrophysiol 2015;8:288-295.
27. Spach MS, Dolber PC, Heidlage JF: Influence of the passive anisotropic properties on directional differences in propagation following modification of the sodium conductance in human atrial muscle. A model of reentry based on anisotropic discontinuous propagation. Circ Res 1988;62:811-832.
28. Spach MS, Boineau JP: Microfibrosis produces electrical load variations due to loss of side-to-side cell connections: A major mechanism of structural heart disease arrhythmias. Pacing Clin Electrophysiol 1997;20:397-413.
29. Rensma PL, Allessie MA, Lammers WJ, Bonke FI, Schalij MJ: Length of excitation wave and susceptibility to reentrant atrial arrhythmias in normal conscious dogs. Circ Res 1988;62:395-410.
30. Allessie MA, Bonke FI, Schopman FJ: Circus movement in rabbit atrial muscle as a mechanism of tachycardia. III. The "leading circle" concept: A new model of circus movement in cardiac tissue without the involvement of an anatomical obstacle. Circ Res 1977;41:9-18.
31. Nattel S, Harada M: Atrial remodeling and atrial fibrillation: Recent advances and translational perspectives. J Am Coll Cardiol 2014;63:2335-2345.
32. Stiles MK, John B, Wong CX, Kuklik P, Brooks AG, Lau DH, Dimitri H, Roberts-Thomson KC, Wilson L, DeSciscio P, Young GD, Sanders P: Paroxysmal lone atrial fibrillation is associated with an abnormal atrial substrate. Characterizing the "second factor." J Am Coll Cardiol 2009;53:1182-1191.
33. Markides V, Schilling RJ, Ho SY, Chow AWC, Davies DW, Peters NS: Characterization of left atrial activation in the intact human heart. Circulation 2003;107:733-739.
34. Schricker AA, Lalani GG, Krummen DE, Rappel W-J, Narayan SM: Human atrial fibrillation initiates via organized rather than disorganized mechanisms. Circ Arrhythmia Electrophysiol 2014;7:816-824.
35. Polontchouk L, Haefliger JA, Ebelt B, Schaefer T, Stuhlmann D, Mehlhorn U, Kuhn-Regnier F, DeVivie ER, Dhein S: Effects of chronic atrial fibrillation on gap junction distribution in human and rat atria. J Am Coll Cardiol 2001;38:883-891.

CHAPTER 7

RELATIONSHIP BETWEEN REGIONS OF HIGH-FREQUENCY ACTIVATION AND FIBROSIS FOLLOWING CHRONIC ATRIAL FIBRILLATION

This study determined the relationship between fibrosis and AF maintenance. As AF persists, single episodes of AF last longer before the patient transitions into sinus rhythm. In some cases, AF can become permanent. The second study examined how patients who are prone to AF transition into this arrhythmia from sinus rhythm, and the third project examines why some patients may never transition from AF to sinus rhythm. Specifically, this project examines the relationship between fibrosis and the drivers of AF. Fibrosis was found to anchor rapid activations within the LA, and removing these driving sites may improve treatment outcomes.

7.1 Introduction

Atrial Fibrillation (AF) is the most common cardiac arrhythmia. AF patients experience significant increases in morbidity and mortality and are at increased risk for strokes [187]. Radiofrequency ablation is routinely used to treat AF and even though it is the most successful treatment strategy the recurrence rate continues to be very high at 40-60% [188].

Typically, AF starts as brief, self-terminating episodes (paroxysmal AF) with gradual increase in AF burden, ultimately lasting long periods of time and becoming persistent [189]. The pulmonary veins are known triggers for paroxysmal AF, and isolation of these triggers from the rest of the atrium through ablation can successfully treat paroxysmal AF [190]. However, pulmonary vein isolation often results in poor long-term success for patients with persistent AF [161]. Structural remodeling that occurs due to AF may lead to regions in the atria, outside the pulmonary veins, that can drive AF [57]. Focal impulse and rotor modification (FIRM)-guided ablation has shown some success in treating persistent AF by

locating and ablating these driving sites [36]. However, the stability of these sites over prolonged recording periods remains controversial, and it is not clear if there is a structural component to the cardiac substrate that may, at least transiently, stabilize rapid foci or reentrant activity to a location.

Myocardial fibrosis is a well-established marker of adverse structural remodeling in a variety of heart diseases, including AF [24]. Higher levels of fibrosis, as determined by late gadolinium enhancement magnetic resonance imaging (LGE-MRI) prior to an ablation has been linked to poorer ablation outcomes [137]. MRI, specifically postcontrast T1-Mapping MRI, is one of the few validated noninvasive methods for determining cardiac fibrosis [191]. We tested the hypothesis that regions of the atria with significant fibrotic structural remodeling anchor rapid focal or reentrant activity which drive AF and that cardiac T1-mapping MRI can noninvasively locate these sites.

7.2 Methods

All animals were managed in accordance with the Guide for the Care and Use of Laboratory Animals, and the protocol was approved by the Institutional Animal Care and Use Committee of the University of Utah.

7.2.1 Experimental Preparation

Animal Model: Mongrel dogs (n=12) weighing 25-35 kg were used for this study. Neurostimulators were implanted in 6 of the dogs and chronic AF was induced with rapid atrial pacing (RAP). The other 6 dogs were used as controls for the electrophysiological study and were not evaluated with MRI.

7.2.2 MRI Study

In 5/6 of the chronic AF dogs, the cardiac substrate was evaluated with high-resolution, whole-heart T1-Mapping MRI at baseline, before the RAP began. In one animal, pacing was started before a baseline MRI was acquired. All of the chronic AF dogs were again evaluated with whole-heart T1-Mapping MRI after 183 months of AF and 1-3 weeks prior to a detailed electrophysiological study.

7.2.3 Electrophysiological Study

A detailed electrophysiological (EP) study was done in both the controls and in the chronic AF animals. For the chronic AF animals the EP study was done 1-3 weeks after whole-heart T1-mapping.

For the chronic AF animals, an electrical anatomical map (EAM) of the left atrium (LA) was made and was merged with the Corview segmentations of T1-Mapping MRI using the EnSite mapping systems fusion application. The Corview segmentation contained the LA wall and the regions of fibrosis as determined by T1-Mapping MRI. A 64-pole basket catheter (Constellation, Boston Scientific Corp, Natick, MA, USA) was then placed into the LA. The size of the basket catheter was 38 mm for the controls and 48 mm for chronic AF. The MRI segmentation and basket placement within the fused geometry is shown in Fig. 7.1. An ECG and endocardial unipolar electrograms from the 64 electrodes of the basket catheter were recorded for up to 30 minutes of AF. AF was induced in the controls with 30 seconds of 50 Hz burst pacing at 5 mA from a quad catheter placed in the right atrium. If AF was not induced or sustained less than 30 minutes in the controls, burst pacing was reapplied with a maximum of five attempts.

The ECG and unipolar electrograms were evaluated in the time and frequency domain to determine whether specific regions of the LA had stable regions of high dominant frequency (DF). The ECG and unipolar electrograms were sampled at 4096 Hz with 24-bit resolution with an Active Two mapping system (Active Two System, Biosemi, Inc, Amsterdam, Netherlands). Far-field ventricular activity was reduced using a well-documented QRS subtraction algorithm [88]. The QRS-subtracted unipolar signals were then analyzed with DF spectral analysis. High-DF sites were determined as the highest 10% DF sites for each minute of AF, and had to be at least 1 Hz higher than the average of the DF from the rest of the LA. The high-DF sites for each minute of AF were placed in a spatial map of probability to determine stability of the sites during the 30 min AF episode. Stable sites of high-DF were determined as an electrode site with 75% or higher stability over the time course of the AF episode.

The sites of stable high-DF activation organization were quantified using a regularity index (reg-idx). The reg-idx was computed for each channel and then averaged among the stable high-DF sites and among the other electrodes within the LA for each animal.

The sites of stable high-DF were directly compared with the sites of T1-Mapping MRI determined fibrosis by exporting the electrode location's position with reference to the T1-Mapping MRI segmentation in the chronic AF animals. Each electrode was projected onto the closest location on the LA wall segmentation using a linear least squares approach. Each position on the LA wall was assigned a binary value of whether it is a region of healthy or fibrotic tissue, where fibrotic tissue corresponded to the lowest 10% T1 values within the entire LA wall. Every stable high-DF site for each animal was then classified as either on border zones of fibrosis or in regions of healthy tissue. Border zones were

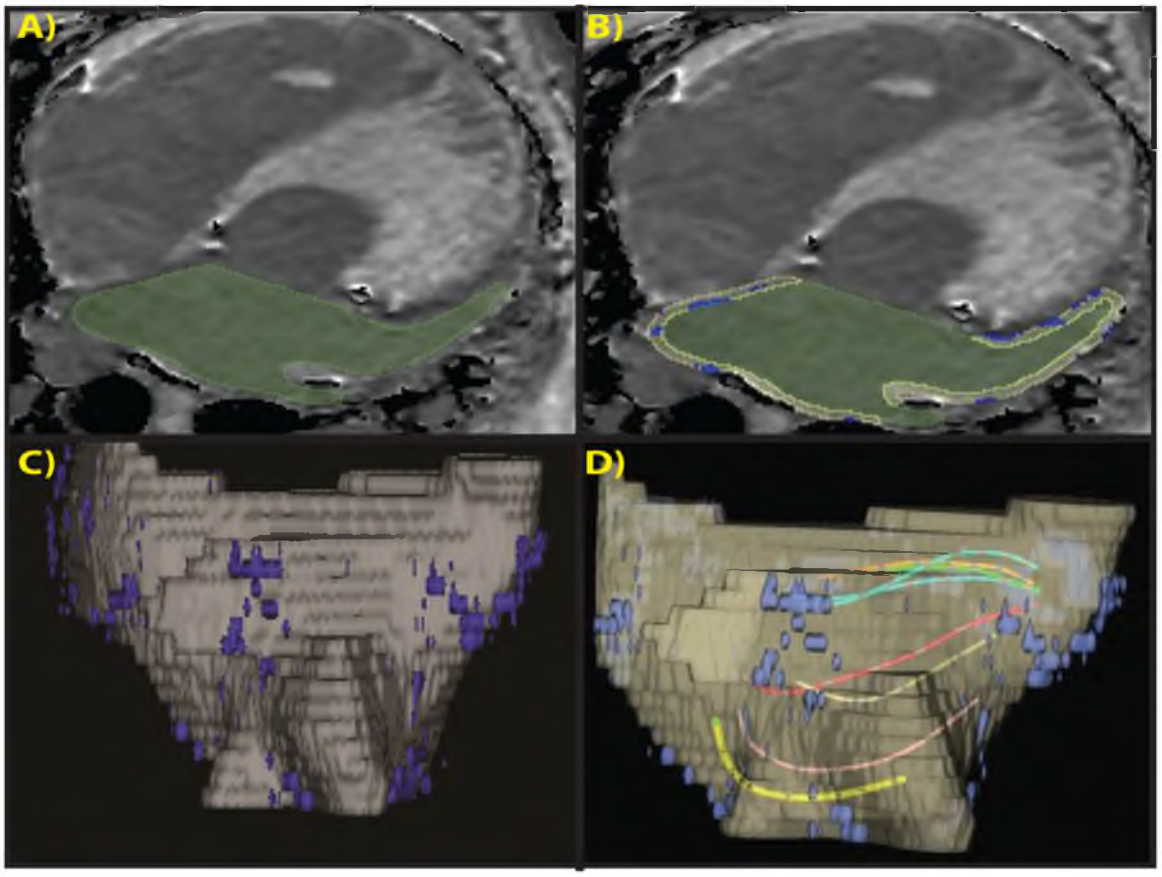

Fig. 7.1: **Determining regions of fibrosis using T1-Mapping MRI. A)** One axial slice from a series of 52 slices of the T1 Map. LA blood pool segmentation is in green. **B)** LA wall segmentation, shown in grey, and the lowest 10% T1 values in blue from the T1 map slice in A). **C)** 3D segmentation of LA wall and lowest 10% T1 values. This segmentation is imported into the EnSite mapping system for merge with the geometric shell created from a mapping catheter. **D)** Basket catheter shown in segmentation merged with EnSite created EAM of the LA. Grey is the LA wall and the blue are the regions of lowest 10% of T1 value.

determined as electrode locations on or within 2 mm of fibrosis. For each chronic AF animal a percent of the number of stable high-DF sites on the border zones was then computed. The average distance between the stable high-DF sites and closed region of dense fibrosis was also computed.

7.2.4 Histology

Histological tissue samples stained with Massons trichrome were collected from 4/6 of the chronic AF animals after the animals were sacrificed. Multiple tissue samples were collected from regions of T1-Mapping MRI-determined fibrosis and from nonfibrotic areas of the LA. Images from the samples were imported into ImageJ software (National Institutes of Health) for fibrosis quantification. For each animal the percent fibrosis was averaged among tissue samples obtained from fibrotic regions as well as nonfibrotic areas of the LA.

7.2.5 Statistical Analysis

Paired t-test was used to analyzed continuous variables (T1 relaxation time, amount of fibrosis from histology, DF, and reg-idx) A chi-square test was used to determine whether regions of stable high-DF were observed in the fibrotic border zones more often than in nonfibrotic zones. The expected value was the percent of the electrodes that were within 2 mm of fibrosis. Results were considered significant at $p<0.05$.

7.3 Results

As AF progresses, it resulted in significantly lower T1 relaxation time (Baseline: 593±41 ms vs. Chronic AF: 463±79 ms, $p<0.05$). In the chronic AF animals, the regions of lowest 10% T1 values had an average T1 time of 283±32 ms, and these regions were in patches and not diffuse throughout the LA wall for all of the chronic AF animals. Histology confirmed that regions of T1-Mapping MRI-detected fibrosis had higher fibrosis densities (Fig. 7.2) as compared to other LA regions. (20.0±1.1% vs. 11.5±2.3%, $p<0.05$) (Fig. 7.3).

All of the chronic AF animals could sustain AF for the full 30 minutes, whereas none of the controls could. One of the controls sustained AF for 14 minutes and another two had AF sustain less than 1 minute. In the other 3/6 of the controls no AF was induced. In the one control that sustained AF for the 14 minutes, there were no stable high-DF sites (Fig. 7.4). The chronic AF animals had at least one site of stable, high-DF for at least 22.5 (75%) of 30 minutes of AF. The mean DF was 8.5±1.2 Hz and the stable high-DF sites had a mean DF of 10.3±1.1 Hz ($p<0.05$). The DF value for the stable sites sometimes varied by as much as 1 Hz throughout the 30 minute AF episode, however, these sites still remained

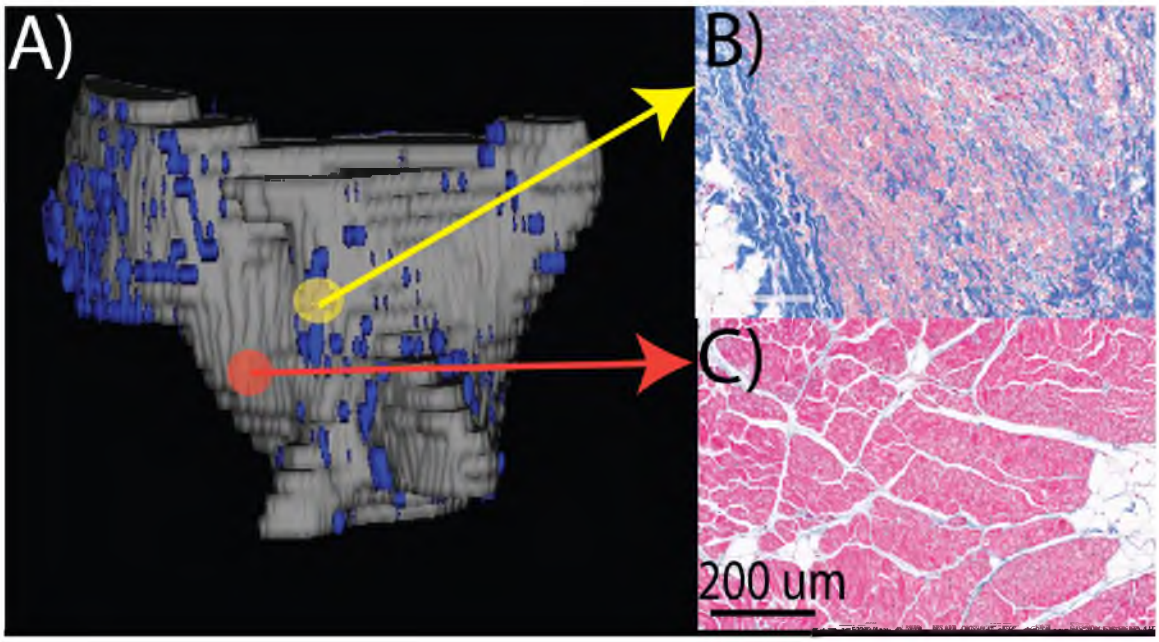

Fig. 7.2: **T1-Mapping magnetic resonance imaging and histological correlation.** **A)** Segmented left atrial geometric shell with gray showing healthy myocardium and blue showing the regions with the lowest 10% T1 values, indicating fibrotic areas. **B)** Massons Trichrome staining from yellow circle shown in A), indicating a fibrotic region. **C)** Massons Trichrome staining from red circle in A) indicating a nonfibrotic region.

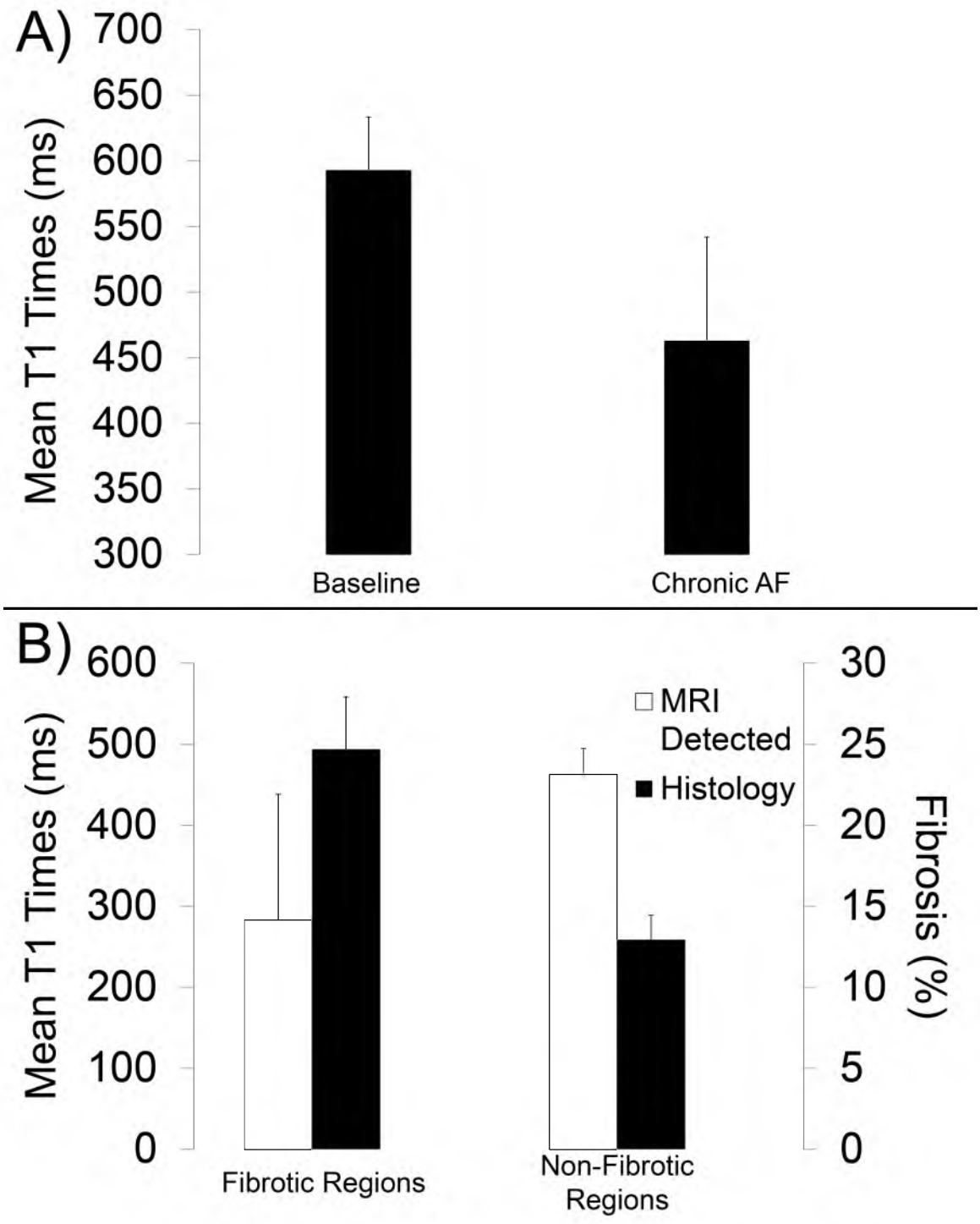

Fig. 7.3: **T1-Mapping MRI-detected Fibrosis agrees with Histology. A)** Decrease in T1 times following chronic AF. **B)** Regions of fibrosis as detected by T1-Mapping MRI have increased fibrosis as determined by histology. Lower T1 times corresponds to more fibrosis.

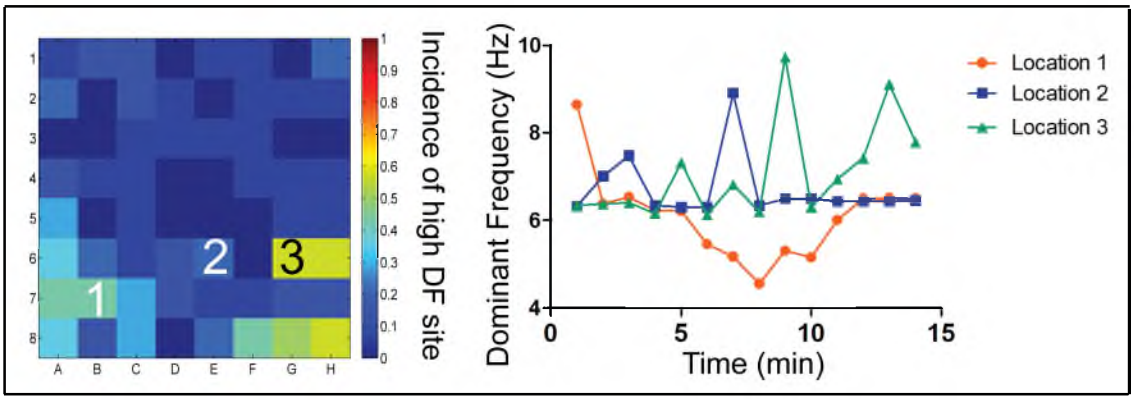

Fig. 7.4: Example of nonstable high-DF sites in left atrium without a history of AF. Example of the spatial instability of high-DF sites in a control animal that maintained AF for 14 minutes. X axis shows the spline numbers A-H and Y axis show electrode numbers on the corresponding spline. Each electrode site contains the incidence that it had a DF value within the top 10% over the AF episode. DF values for 3 locations, labeled 1-3, are shown over the time course of a 30 min AF episode.

higher than other nearby locations (Fig. 7.5). In all the animals, the DF value from the stable sites agreed well with the activation rate of the tissue (Fig. 7.6).

The reg-idx at the high-DF sites in the chronic AF animals was significantly less than the reg-idx at other locations within the LA (0.25 ± 0.06 vs. 0.31 ± 0.04, $p<0.05$). This indicates that the sites of high-DF also have a more regular cycle length, thus are more organized. An example of the regularity of activations at a high-DF site vs. another location in the LA is shown in Fig. 7.7.

In the chronic AF animals, 82% of stable high-DF bordered regions of fibrosis as determined by T1-Mapping MRI (Fig. 7.8). The average distance of the stable high-DF sites to the closest region of dense fibrosis was 1.4 ± 1.2 mm. Although the fibrotic border zones consisted of a large region of the basket-mapping field in some animals, this was primarily due to the constraint that if a basket could be placed in multiple locations, the location with the highest DF was used for the analysis. Fibrosis was defined as regions of the LA wall with the lowest 10% of T1 values, therefore at most the fibrotic regions would occupy 10% of the entire LA.

7.4 Discussion

The major findings of this study are as follows: 1) High-resolution T1-Mapping MRI can determine LA wall areas with dense fibrosis. 2) During chronic AF, but not in controls, there are specific regions within the LA that have stable sites of high-DF over a prolonged recording period. 3) These sites of stable high-DF have more regular activity than other sites in the LA. 4) The sites of stable high-DF anchor to the border of dense fibrotic regions.

Whole-heart T1-Mapping MRI can noninvasively detect regions of the LA with significant fibrotic atrial structural remodeling. Postcontrast T1 measurements have primarily been used to detect changes in ventricular tissue after myopathy or AF [192]. In addition this technique has been validated in ventricular tissue to show an increase in collagen in a wide range of cardiac diseases [193]. However, more recent reports have used postcontrast T1 measurements to predict ablation success before ablation. A study by Marrouche et al. which found that atrial tissue fibrosis estimated with LGE-MRI was associated with recurrent arrhythmia [137]. One limitation with LGE-MRI, however, is in measuring diffuse fibrosis [194]. T1 MRI can measure diffuse fibrosis by measuring absolute values of the T1 relaxation time for each voxel and hence can be used to not only localize fibrosis by means of relative enhancement but also compare fibrosis changes over time in the same subject using this quantitative measurement [177]. The finding by Marrouche et al. suggest that

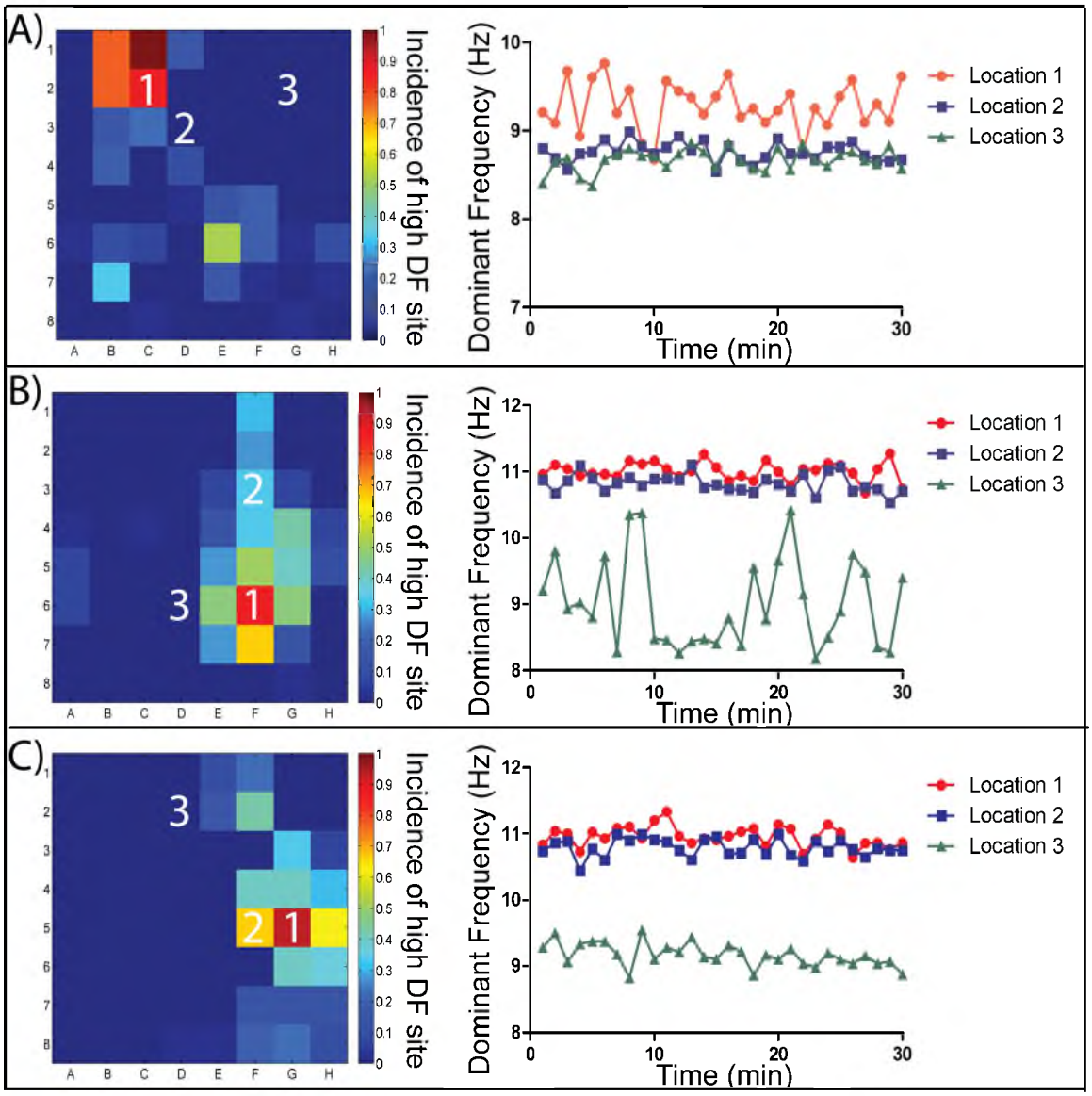

Fig. 7.5: **Stability of high-DF sites in chronic AF. A)** Examples of spatial stability of high-DF sites over 30 minute time course of AF averaged every minute for three chronic AF animals. X axis shows the spline numbers A-H, and Y axis shows electrode numbers on the corresponding spline. Each electrode site contains the incidence that it had a DF value within the top 10% over the AF episode. **B)** DF values for three locations, labeled 1-3, are shown over the time course of a 30 min AF episode.

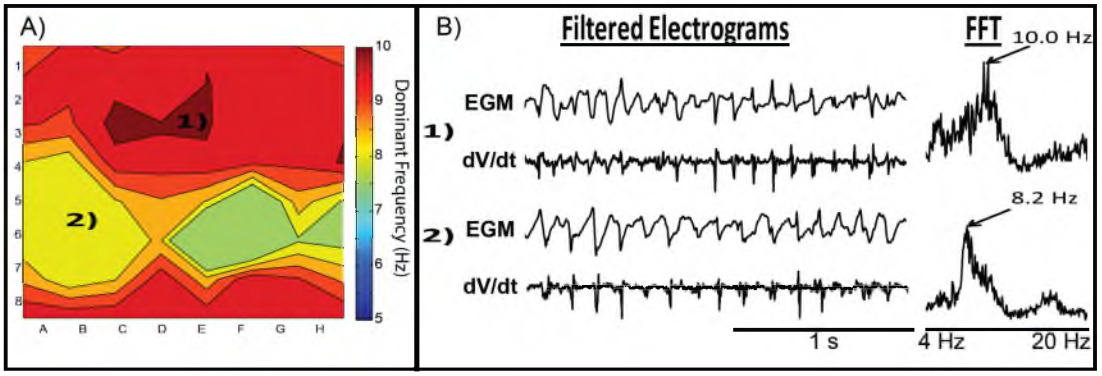

Fig. 7.6: **DF map corresponds to the activation rate. A)** DF map from 1 minute of the 30-minute time course of atrial fibrillation. Labels 1) and 2) indicate regions with a DF of 10.0 and 8.2 Hz. **B)** Electrogram and FFT from regions 1) and 2) on the DF map. Location 1) has 20 activations in 2 second (approximately 10 Hz) and location 2 has 16 activation in 2 seconds (approximately 8 Hz).

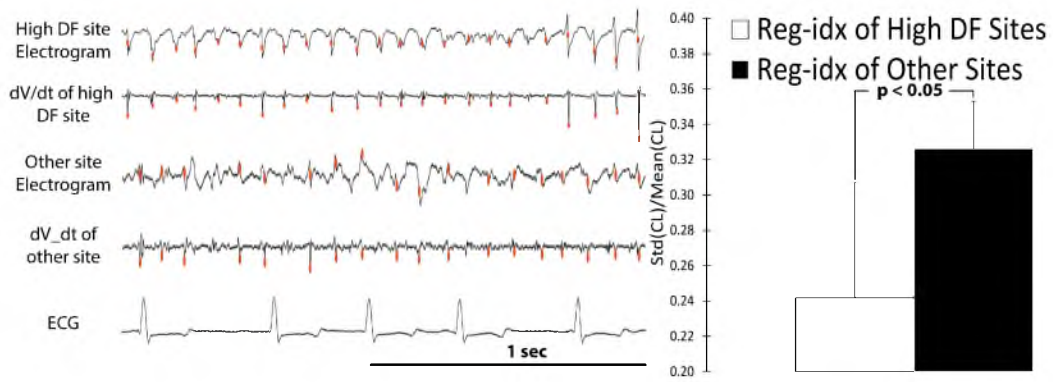

Fig. 7.7: **high-DF sites have higher reg-idx as compared with other sites in LA.** Electrogram and first derivative are shown for a high-DF site and another site in the LA. Local minimums of the first derivative are selected as activation times, shown as blue dot on dV/dt. From these activation times the reg-idx was computed for the high-DF sites and was compared with the other LA sites. The bar graph summarize the regularity data for all the subjects.

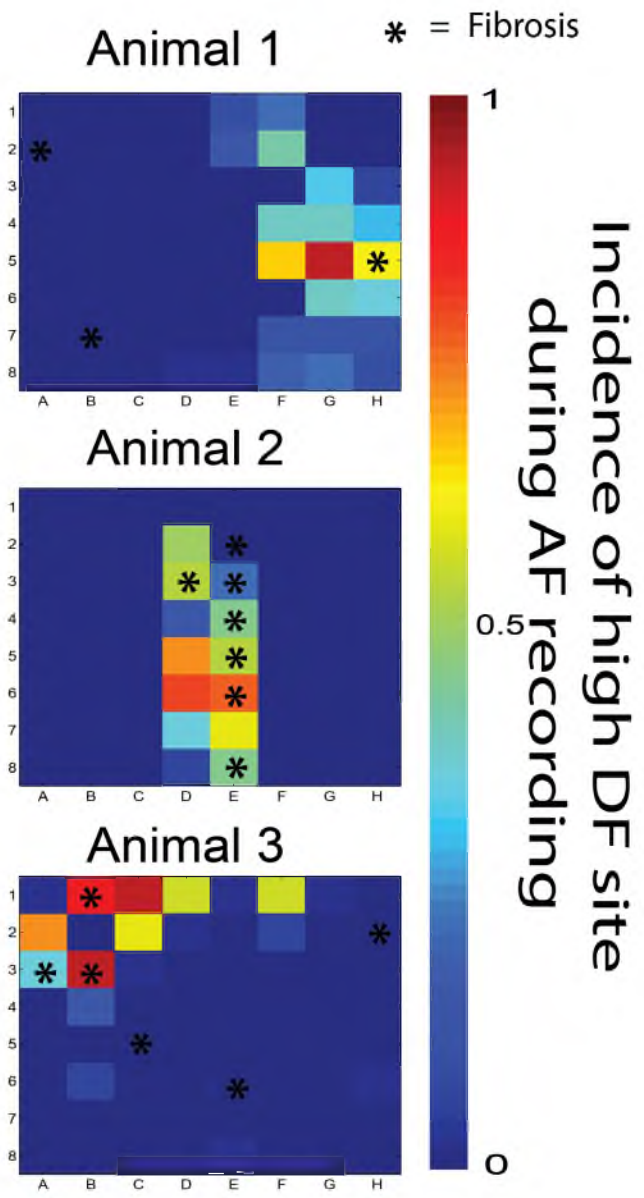

Fig. 7.8: **Relationship between regions of high-DF and fibrosis.** Four example spatial probability plots of DF and regions of fibrosis. X axis for each plot shows the spline numbers A-H and Y axis shows electrode numbers on the corresponding spline. Each electrode sites contains the incidence that it had a DF value within the top 10% over the atrial fibrillation episode. Examples 1-3 show examples of the DF on the border of fibrosis.

fibrotic atrial structural remodeling that occurs during AF may facilitate the arrhythmia's maintenance. As AF was induced with RAP in the animals, T1 times significantly decreased, indicating that atrial structural remodeling was occurring. Furthermore, the chronic AF animals, like the study by Marrouche et al., had specific regions within the LA that had more fibrotic remodeling than other regions.

Our findings indicate that during chronic AF, but not in controls, there are sites within the LA that anchor rapid reentrant or focal activity as determined through DF analysis. The controls either did not sustain AF or, in the one case that they did, the high-DF sites were not stable. AF may have terminated spontaneously due to the lack of fibrotic areas providing stability. This finding indicates that the chronic AF substrate may anchor regions of high-DF. Some prior reports disagree about the stability of high-DF sites [34,195]. Salent et al. reported nontemporally stable high dominant frequency by determining whether the dominant frequency in sequential time windows varied by more than ± 0.25 or ± 0.50 Hz [195]. Although our results indicate stable regions of the sites of highest DF, our findings also agree with Salent et al. in that our sites of stable high-DF had a dynamic DF value, however this value was in the highest quartile DF over the 30 minute recording period as compared to other LA regions. This indicates that although the DF value may vary more than 0.50 Hz, these stable sites still have the highest activation frequency and therefore are likely driving the arrhythmia. A study by Jarman et al. also reported temporal and spatial instability of high-DF sites. This study found nonstability by examining sequential 6.8 seconds of data. In 33% of cases a site of high-DF would disappear from a region, and then reappear at a later time (within 1-3 6.8-second time windows) [34]. Our study averaged six 10-second DF windows to have one DF value for each minute of AF. By taking an average DF for each minute of AF we found spatial stability of these high-DF sites over the time course of 30 minutes. This suggest that although sequential 6.8 second windows may have both temporal and spatial instability, during prolonged recording periods, the sites of high-DF tend to occur at specific sites. A recent study by Swarup et al. reported that over the time span of several tens of minutes that they observed spatial temporal stability of rotors or focal sources utilizing phase mapping [35]. The sites of stable high-DF reported in this study may correlate with these sites and detection of these sites with spectral analysis may require these prolonged recording periods.

Our study found that sites of stable high-DF during chronic AF have more organization than other sites within the atrium. Swarup et al. reported that patients in AF have stable rotors or focal sources which are driving the arrhythmia, however it was not clear what

was stabilizing this rapid activity [35]. Recently, Hansen et al. found that fibrosis-insulated atrial bundles could sustain intramural reentry [38]. The high-DF sites found in our study had more regular activations than other sites within the atrium, which suggest that these sites may be the rotors or focal activity found by Swarup and Hansen et al.

The sites of stable high-DF tend to anchor on the border of dense fibrosis. These border regions may cause regions of abrupt conduction slowing, which may predispose these regions to maintain rapid reentrant/focal activity [29, 196]. Cabo et al. reported that inexcitable objects with sharp edges may cause vortex shedding to cause the initiation of high-frequency excitation of the heart [60]. Specific regions of dense fibrosis may cause source sink mismatch and act as an inexcitable object to cause the initiation of stable high-frequency sources. Although our study found that sites of stable high-DF occur on the border of fibrosis, many fibrotic borders zones did not contained stable sites of high-DF. The study by Cabo et al. also reported the requirement of reduced sodium conductance and sharp edges of the inexctiable object. Therefore the formation of stable high-DF sites may require specific sites of fibrosis that have a reduction of sodium conductance and sharpness of edges.

7.5 Limitations

This study was limited to RAP-induced AF models, and although this is similar to AF developed through rapid focal pulmonary vein firing, a human patient population may have a variety of mechanisms of AF development. For these reasons longstanding persistent AF in humans may have different electrophysiological properties than the RAP chronic animal model of AF. Longstanding persistent AF in humans is often entrenched in patients over the time course of many decades. However, such animal models have been used in the past and have provided significant insights into AF mechanisms. Another limitation is the difficulty of merging the EnSite and T1-Mapping MRI geometries by selecting corresponding points between the two models. The effect of selecting incorrect corresponding points was minimized by using several landmarks in the LA, including the pulmonary veins.

7.6 Conclusions

Heterogeneous atrial remodeling, specifically fibrosis, arising from chronic AF provides a substrate that anchors sites of high-DF, and this anchoring of high-frequency sources is not seen in controls. Whole-heart T1-Mapping MRI provides a means to determine these anchor sites noninvasively.

CHAPTER 8

CONCLUSIONS

This dissertation shows that the cardiac substrate helps initiate and/or sustain abnormal cardiac conduction. Novel imaging and electrical recording techniques were used to bridge the domains of cardiac substrate and functional electrical measurements. Although fibrillation is characterized by a disorganization of wavefronts, it is not completely stochastic. Specifically, the results of this dissertation show that the cardiac substrate can manifest in specific electrophysiology properties, which may drive the arrhythmia. Aim 1 measured the activation rate of the conduction system compared to the VM during VF. During short-duration VF, the activation rate of the VM is significantly higher than the His bundle. This finding is consistent with the traditional theory that VF is maintained through rapid reentrant wavefronts within the VM. However, after 1-2 minutes of VF, a transition occurs in which the His bundle activates faster than the VM. The VM activation rate decreases quickly during VF whereas the His bundle activation rate does not significantly decrease. Ischemia changes the electrophysiology of both the conduction system and VM, such that there is a transition of the driver of VF from the VM to the conduction system. Furthermore, the His bundle being a potential driving site is an example of how the cardiac substrate, e.g., differences between the ventricular conduction system and the VM, causes deterministic properties of fibrillation. The next two aims focused on how structural changes that occur during AF relate to increased likelihood of initiation and maintenance of this arrhythmia. Aim 2 found that long strands of fibrosis alter conduction such that the tissue is more arrhythmogenic. Specifically, this aim found that in chronic AF, fibrosis strands located primarily along cells potentially obstruct the transverse connection between cells. The fibrosis strands may result in slowed or blocked transverse conduction. Aim 3 expanded on aim 2 to determine how regions of the most dense fibrosis in the LA relate to the rapid activations in the atrium. The conclusion of aim 3 was that the sites of most rapid activation anchor to the borders of fibrosis. This aim found that even though AF is highly disorganized in its activation, fibrosis can predict where the most rapid sites of activation will be.

8.1 Future Work

Although we found that the cardiac substrate can manifest in certain conduction properties, it is still unclear what effect the substrate has on the properties of fibrillation and whether this information can be used to help patients. The cardiac substrate was shown to manifest in specific electrophysiological properties, but it is still not clear whether fibrillation has a chaotic yet deterministic organization, or whether fibrillation still has more stochastic properties than organized properties. This question becomes central when trying to develop clinical uses for the findings in this dissertation. There are two possible parallel paths for future studies based on the findings of this dissertation. The first is to understand the implications of these findings and to expand the scope of the projects for a more mechanistic understanding of structure and function in fibrillation. The second, parallel path is to develop clinically useful applications of the findings of each aim.

8.1.1 Conduction System and Ventricular Fibrillation

Aim 1 found that the proximal conduction system has a more rapid activation rate than the VM after 1-2 minutes of VF. Even though there is mounting evidence that the conduction system may be a driver of long-duration fibrillation, it is unclear whether this system can be used as a target for low-energy treatment of VF. The conduction system is a promising potential target for terminating VF for two primary reasons. First, it has been implicated in the maintenance of VF, and therefore by pacing this system we may prevent potentially short-lasting, self-terminating VF from progressing into sustained VF. Second, the conduction system structure is electrically connected to the VM at many sites. By pacing the conduction system it may be possible to consistently capture large regions of cardiac tissue to stop VF. To determine whether the conduction system may be a target for pacing during VF, we have to determine whether this system can be paced during VF. The conduction system may be activated as soon as it comes out of refractory. If this is the case, pacing the system will not have an effect during VF. Our preliminary data suggest that the conduction system can be paced during VF. The setup was similar to what is described in Chapter 5, except that the His bundle was paced at 90% of its average cycle length, and a second plaque was placed on the VM to determine whether the pacing reached the distal regions of the conduction system. Fig. 8.1 shows an example in which the His bundle was paced during VF, and the pacing began to capture the distal VM, which resulted in termination of VF.

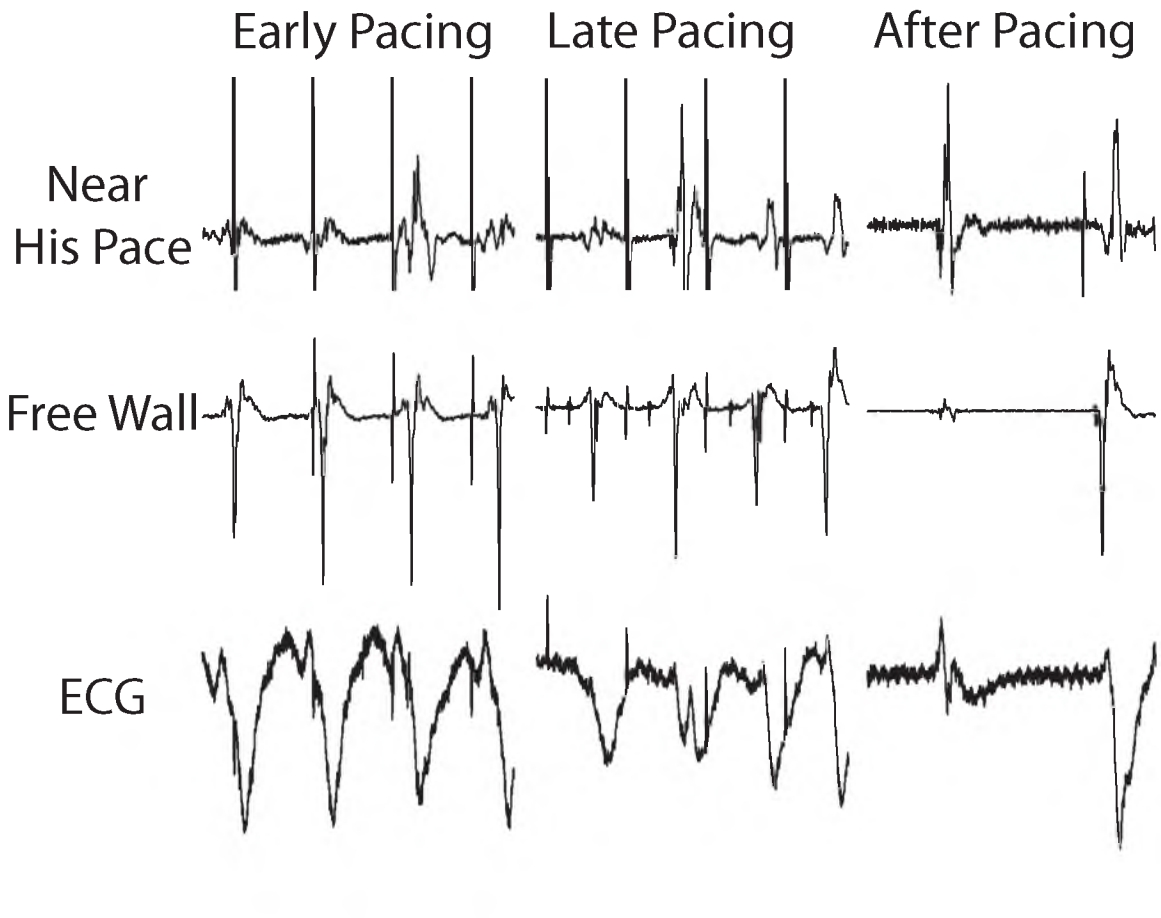

Fig. 8.1: **His bundle paced during VF, resulting in termination of the arrhythmia**. An ECG, an electrogram from the His bundle, and an electrogram from the distal Purkinje fibers are shown. The His bundle was paced at 90% of its cycle length. During early pacing the distal Purkinje fibers and ventricular myocardium are not being captured. However, at the end of the pacing train, of approximately 20 pulses, the His bundle is being captured. Furthermore, the pacing pulses at the His bundle are conducting to and capturing the distal ventricular myocardium. VF no longer was sustained immediately after the pacing.

8.1.2 Structure of Fibrosis and Its Effect on Conduction

This aim found that during chronic AF, conduction slows in the transverse direction, which may be due to the structure of fibrosis. A major limitation is that histology was obtained only from a 4um-thick sample of histology 500um from the epicaridal surface. Therefore, the fibrosis structure was known only on that single plane, and it is not clear what the structure was through the LA wall. An extension of this study would be to visualize and quantify the fibrosis structure transmurally through the LA wall. This three-dimensional structure of fibrosis could be made by sectioning the tissue from epicardium to endocardium, and then reconstructing these sections. Fig. 8.2 shows an example of the three-dimensional structure of fibrosis.

Another limitation of this study that could be studied more is that it is unclear whether the conduction slowing is due to the fibrosis, or whether it is due to electrical remodeling of gap junction due to AF. A potential way to examine whether this transverse conduction slowing is due to electrical or structural remodeling is to repeat these studies in an animal model that has fibrosis but does not have electrical remodeling. Utah State University has such a model, in which goats have been genetically modified to have more atrial fibrosis. These animals can be more easily induced into AF, as compared to controls, but the mechanism is unclear. A potential mechanism is that structural remodeling alone is sufficient to increase the likelihood of AF.

The clinical expansion and implications of this aim are that the architecture of fibrosis may be more important than the overall fibrosis level. There may be patients with substantial levels of diffuse fibrosis who never develop AF because of the architecture of their fibrosis. Of course, there may also be a subset of patients with substantial amounts of obstructive fibrosis (risky substrate) but whose hearts lack a trigger for premature atrial contractions so they do not develop AF. A possible future study would be to determine whether there are differences in fibrosis architecture from patients who respond well to antiarrhythmic drugs or ablation therapy versus those who do not. Quantifying fibrosis on an individual patient basis could lead to patient-specific treatments based on the patient's fibrosis architecture.

8.1.3 Fibrosis Effect on Atrial Fibrillation Conduction

Aim 2 examined how fibrosis may increase the likelihood of AF initiation, and aim 3 examined the role of fibrosis in sustaining AF. This study found that regions of high-frequency activation tend to occur on the border of fibrosis. The stablility of high-frequency activation sites suggest that fibrosis acts as an anchor to driving sites during AF. However,

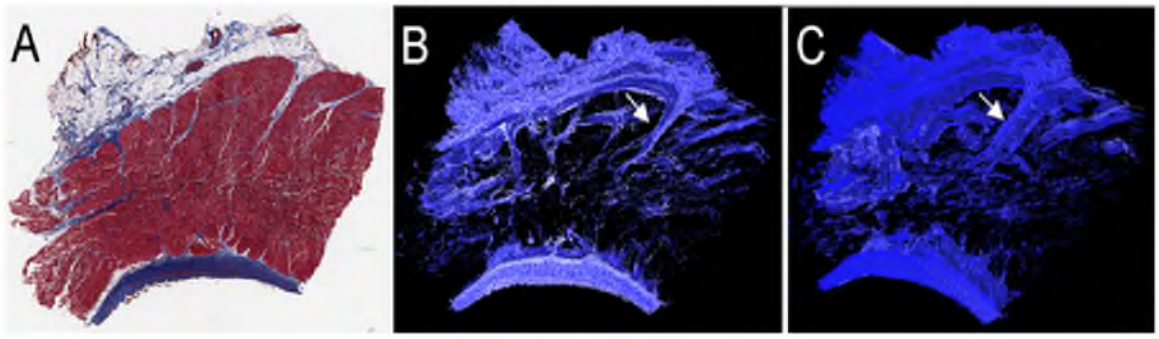

Fig. 8.2: **Reconstruction of three-dimensional collagen bands from LA tissue of an AF dog. A)** Masson trichrome staining shows normal cardiomyocytes and nuclei in red and the extracellular collagen stains in blue. The epicardium is on the top and the endocardium is on the bottom. **B)** Blue stained tissue is shown. The 16 sequential sections are aligned and stacked. A large intramural collagen band is shown with a white arrow. **C)** Rotated image of the three-dimensional stack is shown to demonstrate the three-dimensional structure of collagen bands. The white arrow shows the same collagen band from B) but shows that the collagen band has depth through the entire stack. We anticipate that large collagenous sheaths such as the one marked with the arrow in Panels B and C may be consistent sites of block or conduction slowing.

it is unclear why these sites are more prone to this activity. Specifically, it is unclear whether these driving sites are rotors, or whether they are just regions of multiple wavelets. An example of the possible mechanisms of fibrosis is shown in Fig. 8.3. Future work for this study would be to do more high-density mapping of regions of stable high dominant frequency, with the goal of mapping cardiac waves during fibrillation. This mapping could be done with either a higher density mapping catheter, or in an isolated perfused setup with voltage-sensitive dyes.

Another expansion to Aim 3 is more clinical and is to determine whether ablation of fibrosis sites can result in long-term freedom from AF. If the fibrosis is ablated, there may no longer be the anchor sites available to sustain the arrhythmia. Furthermore, the ablation sites could be preplanned after computing a pixel by pixel T1 map from MRI. Preliminary studies utilizing the canines in aim 3 showed that ablation of fibrosis had promising results with all of the fibrotic target ablation animals not having recurrence after 1 month, and with random ablation being successful in only one third of animals. Furthermore, three out of four of the fibrosis-targeted ablation group could not be induced into AF with burst pacing from three locations. Further studies would need to be done to determine whether T1-Mapping MRI can be used to find ablation targets for humans, which could result in cardiac substrate-guided patient-specific ablation.

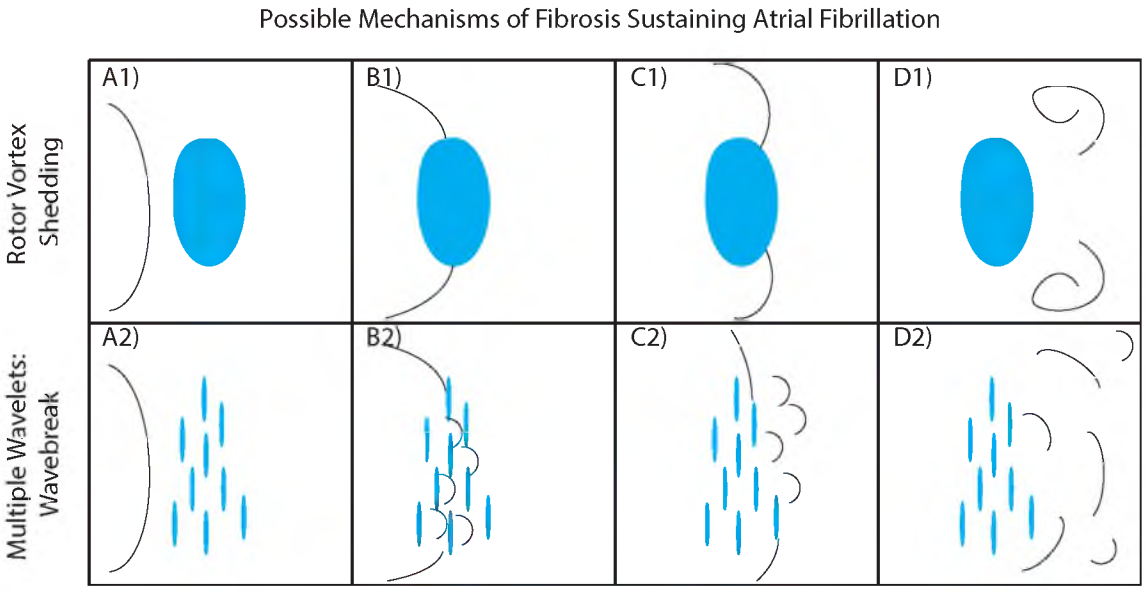

Fig. 8.3: **Schematic of initiation of a rotor due to vortex shedding. A1 and A2)** Cardiac wave shown in black is approaching an inexcitable cardiac tissue shown in blue. **B1)** Cardiac wave interacts with inexcitable cardiac tissue and begins to bypass the tissue. **C1)** When cardiac wave bypass tissue a source sink mismatch forms at the boundary of the object. This causes a convex wave shape at the boundary of the inexcitable object where conduction slows. **D1)** If the curvature of the wave is large enough, the wave can start to rotate around an inexcitable center known as a singularity point. This rotational conduction around an inexcitable core is known as a rotor. **B2)** The broad cardiac wave conducts into the fibrotic region and is broken into many smaller wavelets. **C2)** The many wavelets then conduct out of the fibrotic region. **D2)** The many wavelets then interact with other cardiac wavelets to promote multiple wavelet reentry.

REFERENCES

[1] R. L. Dehaan, "Differentiation of the atrioventricular conducting system of the heart.," *Circulation*, vol. 24, no. August 1961, pp. 458–470, 1961.

[2] F. E. Marchlinski and B. P. Betensky, "Mechanisms of Cardiac Arrhythmias," *Revista Española de Cardiología*, vol. 65, no. 2, pp. 174–185, 2012.

[3] T. J. Wang, M. G. Larson, D. Levy, R. S. Vasan, E. P. Leip, P. a. Wolf, R. B. D'Agostino, J. M. Murabito, W. B. Kannel, and E. J. Benjamin, "Temporal relations of atrial fibrillation and congestive heart failure and their joint influence on mortality: the Framingham Heart Study.," *Circulation*, vol. 107, pp. 2920–5, jun 2003.

[4] D. P. Zipes, "An overview of arrhythmias and antiarrhythmic approaches.," *Journal of cardiovascular electrophysiology*, vol. 10, pp. 267–71, feb 1999.

[5] M. Vaquero, D. Calvo, and J. Jalife, "Cardiac fibrillation: from ion channels to rotors in the human heart," *Heart Rhythm*, vol. 5, no. 6, pp. 872–879, 2008.

[6] M. S. Eisenberg, B. T. Horwood, R. O. Cummins, R. Reynolds-Haertle, and T. R. Hearne, "Cardiac arrest and resuscitation: A tale of 29 cities," *Annals of Emergency Medicine*, vol. 19, no. 2, pp. 179–186, 1990.

[7] C. Marini, F. De Santis, S. Sacco, T. Russo, L. Olivieri, R. Totaro, and A. Carolei, "Contribution of atrial fibrillation to incidence and outcome of ischemic stroke: results from a population-based study.," *Stroke; a journal of cerebral circulation*, vol. 36, pp. 1115–9, jun 2005.

[8] I. Olivotto, F. Cecchi, S. a. Casey, a. Dolara, J. H. Traverse, and B. J. Maron, "Impact of Atrial Fibrillation on the Clinical Course of Hypertrophic Cardiomyopathy," *Circulation*, vol. 104, pp. 2517–2524, nov 2001.

[9] N. Hannon, O. Sheehan, L. Kelly, M. Marnane, A. Merwick, A. Moore, L. Kyne, J. Duggan, J. Moroney, P. M. E. McCormack, L. Daly, N. Fitz-Simon, D. Harris, G. Horgan, E. B. Williams, K. L. Furie, and P. J. Kelly, "Stroke associated with atrial fibrillation - Incidence and early outcomes in the north dublin population stroke study," *Cerebrovascular Diseases*, vol. 29, no. 1, pp. 43–49, 2009.

[10] V. L. Roger, a. S. Go, D. M. Lloyd-Jones, R. J. Adams, J. D. Berry, T. M. Brown, M. R. Carnethon, S. Dai, G. de Simone, E. S. Ford, C. S. Fox, H. J. Fullerton, C. Gillespie, K. J. Greenlund, S. M. Hailpern, J. a. Heit, P. M. Ho, V. J. Howard, B. M. Kissela, S. J. Kittner, D. T. Lackland, J. H. Lichtman, L. D. Lisabeth, D. M. Makuc, G. M. Marcus, a. Marelli, D. B. Matchar, M. M. Mcdermott, J. B. Meigs, C. S. Moy, D. Mozaffarian, M. E. Mussolino, G. Nichol, N. P. Paynter, W. D. Rosamond, P. D. Sorlie, R. S. Stafford, T. N. Turan, M. B. Turner, N. D. Wong, and J. Wylie-Rosett, "Heart Disease and Stroke Statistics–2011 Update: A Report From the American Heart Association," *Circulation*, pp. 1–193, 2010.

[11] P. L. Friedman, J. R. Stewart, and a. L. Wit, "Spontaneous and Induced Cardiac Arrhythmias in Subendocardial Purkinje Fibers Surviving Extensive Myocardial Infarction in Dogs," *Circulation Research*, vol. 33, pp. 612–626, nov 1973.

[12] W. Dun and P. a. Boyden, "The Purkinje cell; 2008 style.," *Journal of molecular and cellular cardiology*, vol. 45, pp. 617–24, nov 2008.

[13] L. Li, X. Zheng, D. J. Dosdall, J. Huang, S. M. Pogwizd, and R. E. Ideker, "Long-duration ventricular fibrillation exhibits 2 distinct organized states.," *Circulation. Arrhythmia and electrophysiology*, vol. 6, pp. 1192–9, dec 2013.

[14] D. J. Dosdall, P. B. Tabereaux, J. J. Kim, G. P. Walcott, J. M. Rogers, C. R. Killingsworth, J. Huang, P. G. Robertson, W. M. Smith, and R. E. Ideker, "Chemical ablation of the Purkinje system causes early termination and activation rate slowing of long-duration ventricular fibrillation in dogs.," *American journal of physiology. Heart and circulatory physiology*, vol. 295, pp. H883–9, aug 2008.

[15] J. Huang, D. J. Dosdall, K.-A. Cheng, L. Li, J. M. Rogers, and R. E. Ideker, "The importance of Purkinje activation in long duration ventricular fibrillation.," *Journal of the American Heart Association*, vol. 3, p. e000495, jan 2014.

[16] M. Haïssaguerre, P. Jaïs, D. C. Shah, a. Takahashi, M. Hocini, G. Quiniou, S. Garrigue, a. Le Mouroux, P. Le Métayer, and J. Clémenty, "Spontaneous initiation of atrial fibrillation by ectopic beats originating in the pulmonary veins.," *The New England journal of medicine*, vol. 339, no. 10, pp. 659–666, 1998.

[17] J. Eckstein, B. Maesen, D. Linz, S. Zeemering, A. van Hunnik, S. Verheule, M. Allessie, and U. Schotten, "Time course and mechanisms of endo-epicardial electrical dissociation during atrial fibrillation in the goat.," *Cardiovascular research*, vol. 89, pp. 816–24, mar 2011.

[18] E. Carmeliet, "Cardiac ionic currents and acute ischemia: from channels to arrhythmias.," *Physiological reviews*, vol. 79, pp. 917–1017, jul 1999.

[19] O. H. Tovar and J. L. Jones, "Electrophysiological Deterioration During Long-Duration Ventricular Fibrillation," *Circulation*, vol. 102, pp. 2886–2891, dec 2000.

[20] J. Andrade, P. Khairy, D. Dobrev, and S. Nattel, "The clinical profile and pathophysiology of atrial fibrillation: Relationships among clinical features, epidemiology, and mechanisms," *Circulation Research*, vol. 114, no. 9, pp. 1453–1468, 2014.

[21] C. McGann, N. Akoum, A. Patel, E. Kholmovski, P. Revelo, K. Damal, B. Wilson, J. Cates, A. Harrison, R. Ranjan, N. S. Burgon, T. Greene, D. Kim, E. V. R. DiBella, D. Parker, R. S. MacLeod, and N. F. Marrouche, "Atrial fibrillation ablation outcome is predicted by left atrial remodeling on MRI," *Circulation: Arrhythmia and Electrophysiology*, vol. 7, no. 1, pp. 23–30, 2014.

[22] J. Pellman, R. C. Lyon, and F. Sheikh, "Extracellular matrix remodeling in atrial fibrosis: mechanisms and implications in atrial fibrillation.," *Journal of molecular and cellular cardiology*, vol. 48, pp. 461–7, mar 2010.

[23] S. Nattel and M. Harada, "Atrial remodeling and atrial fibrillation: Recent advances and translational perspectives," *Journal of the American College of Cardiology*, vol. 63, no. 22, pp. 2335–2345, 2014.

[24] J. Pellman, R. C. Lyon, and F. Sheikh, "Extracellular matrix remodeling in atrial fibrosis: mechanisms and implications in atrial fibrillation.," *Journal of molecular and cellular cardiology*, vol. 48, pp. 461–7, mar 2010.

[25] D. J. Dosdall, R. Ranjan, K. Higuchi, E. Kholmovski, N. Angel, L. Li, R. Macleod, L. Norlund, A. Olsen, C. J. Davies, and N. F. Marrouche, "Chronic atrial fibrillation causes left ventricular dysfunction in dogs but not goats: experience with dogs, goats, and pigs.," *American journal of physiology. Heart and circulatory physiology*, vol. 305, pp. H725–31, sep 2013.

[26] M. Allessie, J. Ausma, and U. Schotten, "Electrical, contractile and structural remodeling during atrial fibrillation.," *Cardiovascular research*, vol. 54, pp. 230–46, may 2002.

[27] R. P. Martins, K. Kaur, E. Hwang, R. J. Ramirez, B. C. Willis, D. Filgueiras-Rama, S. R. Ennis, Y. Takemoto, D. Ponce-Balbuena, M. Zarzoso, R. P. O'Connell, H. Musa, G. Guerrero-Serna, U. M. R. Avula, M. F. Swartz, S. Bhushal, M. Deo, S. V. Pandit, O. Berenfeld, and J. Jalife, "Dominant frequency increase rate predicts transition from paroxysmal to long-term persistent atrial fibrillation," *Circulation*, vol. 129, no. 14, pp. 1472–1482, 2014.

[28] S. Verheule, E. Tuyls, A. Gharaviri, S. Hulsmans, A. van Hunnik, M. Kuiper, J. Serroyen, S. Zeemering, N. H. L. Kuijpers, and U. Schotten, "Loss of continuity in the thin epicardial layer because of endomysial fibrosis increases the complexity of atrial fibrillatory conduction.," *Circulation. Arrhythmia and electrophysiology*, vol. 6, pp. 202–11, feb 2013.

[29] T. Kawara, R. Derksen, J. R. de Groot, R. Coronel, S. Tasseron, a. C. Linnenbank, R. N. Hauer, H. Kirkels, M. J. Janse, and J. M. de Bakker, "Activation Delay After Premature Stimulation in Chronically Diseased Human Myocardium Relates to the Architecture of Interstitial Fibrosis," *Circulation*, vol. 104, pp. 3069–3075, dec 2001.

[30] S. P. J. Krul, W. R. Berger, N. W. Smit, S. C. M. van Amersfoorth, a. H. G. Driessen, W. J. van Boven, J. W. T. Fiolet, a. C. G. van Ginneken, a. C. van der Wal, J. M. T. de Bakker, R. Coronel, and J. R. de Groot, "Atrial Fibrosis and Conduction Slowing in the Left Atrial Appendage of Patients Undergoing Thoracoscopic Surgical Pulmonary Vein Isolation for Atrial Fibrillation," *Circulation: Arrhythmia and Electrophysiology*, vol. 8, no. 2, pp. 288–295, 2015.

[31] T. Kawara, R. Derksen, J. R. de Groot, R. Coronel, S. Tasseron, a. C. Linnenbank, R. N. Hauer, H. Kirkels, M. J. Janse, and J. M. de Bakker, "Activation Delay After Premature Stimulation in Chronically Diseased Human Myocardium Relates to the Architecture of Interstitial Fibrosis," *Circulation*, vol. 104, pp. 3069–3075, dec 2001.

[32] S. P. J. Krul, W. R. Berger, N. W. Smit, S. C. M. van Amersfoorth, a. H. G. Driessen, W. J. van Boven, J. W. T. Fiolet, a. C. G. van Ginneken, a. C. van der Wal, J. M. T. de Bakker, R. Coronel, and J. R. de Groot, "Atrial Fibrosis and Conduction Slowing in the Left Atrial Appendage of Patients Undergoing Thoracoscopic Surgical Pulmonary Vein Isolation for Atrial Fibrillation," *Circulation: Arrhythmia and Electrophysiology*, vol. 8, no. 2, pp. 288–295, 2015.

[33] N. Angel, L. Li, R. S. MacLeod, N. Marrouche, R. Ranjan, and D. J. Dosdall, "Diverse Fibrosis Architecture and Premature Stimulation Facilitate Initiation of

Reentrant Activity Following Chronic Atrial Fibrillation," *Journal of Cardiovascular Electrophysiology*, vol. 26, pp. 1352–1360, 2015.

[34] J. W. E. Jarman, T. Wong, P. Kojodjojo, H. Spohr, J. E. R. Davies, M. Roughton, D. P. Francis, P. Kanagaratnam, M. D. O'Neill, V. Markides, D. W. Davies, and N. S. Peters, "Organizational index mapping to identify focal sources during persistent atrial fibrillation.," *Journal of cardiovascular electrophysiology*, vol. 25, pp. 355–63, apr 2014.

[35] V. Swarup, T. Baykaner, A. Rostamian, J. P. Daubert, J. Hummel, D. E. Krummen, R. Trikha, J. M. Miller, G. F. Tomassoni, and S. M. Narayan, "Stability of Rotors and Focal Sources for Human Atrial Fibrillation: Focal Impulse and Rotor Mapping (FIRM) of AF Sources and Fibrillatory Conduction.," *Journal of cardiovascular electrophysiology*, vol. 25, pp. 1284–92, dec 2014.

[36] S. M. Narayan, D. E. Krummen, K. Shivkumar, P. Clopton, W.-J. Rappel, and J. M. Miller, "Treatment of atrial fibrillation by the ablation of localized sources: CONFIRM (Conventional Ablation for Atrial Fibrillation With or Without Focal Impulse and Rotor Modulation) trial.," *Journal of the American College of Cardiology*, vol. 60, pp. 628–36, aug 2012.

[37] C. Cabo, a. M. Pertsov, J. M. Davidenko, W. T. Baxter, R. a. Gray, and J. Jalife, "Vortex shedding as a precursor of turbulent electrical activity in cardiac muscle.," *Biophysical journal*, vol. 70, pp. 1105–11, mar 1996.

[38] B. J. Hansen, J. Zhao, T. a. Csepe, B. T. Moore, N. Li, L. a. Jayne, A. Kalyanasundaram, P. Lim, A. Bratasz, K. a. Powell, O. P. Simonetti, R. S. D. Higgins, A. Kilic, P. J. Mohler, P. M. L. Janssen, R. Weiss, J. D. Hummel, and V. V. Fedorov, "Atrial fibrillation driven by micro-anatomic intramural re-entry revealed by simultaneous sub-epicardial and sub-endocardial optical mapping in explanted human hearts," *European Heart Journal*, vol. 36, no. 35, pp. 2390–2401, 2015.

[39] J. N. Weiss, Z. Qu, P.-S. Chen, S.-F. Lin, H. S. Karagueuzian, H. Hayashi, A. Garfinkel, and A. Karma, "The dynamics of cardiac fibrillation.," *Circulation*, vol. 112, pp. 1232–40, aug 2005.

[40] J. Eckstein, B. Maesen, D. Linz, S. Zeemering, A. van Hunnik, S. Verheule, M. Allessie, and U. Schotten, "Time course and mechanisms of endo-epicardial electrical dissociation during atrial fibrillation in the goat.," *Cardiovascular research*, vol. 89, pp. 816–24, mar 2011.

[41] A. O. Grant, "Cardiac ion channels," *Circulation: Arrhythmia and Electrophysiology*, vol. 2, no. 2, pp. 185–194, 2009.

[42] K. Collins, "Charge density-dependent strength of hydration and biological structure," *Biophysical Journal*, vol. 72, no. 1, pp. 65–76, 1997.

[43] D. A. Doyle, J. Morais Cabral, R. A. Pfuetzner, A. Kuo, J. M. Gulbis, S. L. Cohen, B. T. Chait, and R. MacKinnon, "The structure of the potassium channel: molecular basis of K+ conduction and selectivity.," *Science (New York, N.Y.)*, vol. 280, no. 5360, pp. 69–77, 1998.

[44] C. G. Nichols and a. N. Lopatin, "Inward rectifier potassium channels.," *Annual review of physiology*, vol. 59, pp. 171–191, 1997.

[45] P. S. Spector, M. E. Curran, a. Zou, M. T. Keating, and M. C. Sanguinetti, "Fast inactivation causes rectification of the IKr channel.," *The Journal of general physiology*, vol. 107, no. 5, pp. 611–619, 1996.

[46] A. O. Grant, "Cardiac ion channels," *Circulation: Arrhythmia and Electrophysiology*, vol. 2, no. 2, pp. 185–194, 2009.

[47] D. Bers, "Cardiac excitationcontraction coupling," *Nature*, vol. 415, no. January, 2002.

[48] P. Comtois, J. Kneller, and S. Nattel, "Of circles and spirals: bridging the gap between the leading circle and spiral wave concepts of cardiac reentry.," *Europace : European pacing, arrhythmias, and cardiac electrophysiology : journal of the working groups on cardiac pacing, arrhythmias, and cardiac cellular electrophysiology of the European Society of Cardiology*, vol. 7 Suppl 2, pp. 10–20, sep 2005.

[49] A. G. KLEBER, "Basic Mechanisms of Cardiac Impulse Propagation and Associated Arrhythmias," *Physiological Reviews*, vol. 84, no. 2, pp. 431–488, 2004.

[50] R. J. Myerburg, K. Nilsson, and H. Gelband, "Physiology of Canine Intraventricular Conduction and Endocardial Excitation," *Circulation Research*, vol. 30, pp. 217–243, feb 1972.

[51] L. Opie, *The Heart: Physiology, from Cell to Circulation.* Philadelphia: Lippincott-Raven, 3rd ed., 1998.

[52] W. R. Giles and Y. Imaizumi, "Comparison of potassium currents in rabbit atrial and ventricular cells.," *The Journal of physiology*, vol. 405, pp. 123–45, 1988.

[53] S. M. Bryant, S. J. Shipsey, and G. Hart, "Regional differences in electrical and mechanical properties of myocytes from guinea-pig hearts with mild left ventricular hypertrophy.," *Cardiovascular research*, vol. 35, no. 2, pp. 315–23, 1997.

[54] J. Jalife, O. Berenfeld, and M. Mansour, "Mother rotors and fibrillatory conduction: A mechanism of atrial fibrillation," *Cardiovascular Research*, vol. 54, no. 2, pp. 204–216, 2002.

[55] P. V. Bayly, B. H. KenKnight, J. M. Rogers, E. E. Johnson, R. E. Ideker, and W. M. Smith, "Spatial organization, predictability, and determinism in ventricular fibrillation.," *Chaos (Woodbury, N.Y.)*, vol. 8, pp. 103–115, mar 1998.

[56] D. E. Krummen, J. Hayase, D. J. Morris, J. Ho, M. R. Smetak, P. Clopton, W.-J. Rappel, and S. M. Narayan, "Rotor Stability Separates Sustained Ventricular Fibrillation From Self-Terminating Episodes in Humans.," *Journal of the American College of Cardiology*, apr 2014.

[57] S. V. Pandit and J. Jalife, "Rotors and the dynamics of cardiac fibrillation.," *Circulation research*, vol. 112, pp. 849–62, mar 2013.

[58] J. J. Fox, "Spatiotemporal Transition to Conduction Block in Canine Ventricle," *Circulation Research*, vol. 90, pp. 289–296, jan 2002.

[59] a. a. Schricker, G. G. Lalani, D. E. Krummen, W.-J. Rappel, and S. M. Narayan, "Human Atrial Fibrillation Initiates via Organized Rather Than Disorganized Mechanisms," *Circulation: Arrhythmia and Electrophysiology*, vol. 7, no. 5, pp. 816–824, 2014.

[60] C. Cabo, a. M. Pertsov, J. M. Davidenko, W. T. Baxter, R. a. Gray, and J. Jalife, "Vortex shedding as a precursor of turbulent electrical activity in cardiac muscle.," *Biophysical journal*, vol. 70, no. 3, pp. 1105–1111, 1996.

[61] P. L. Rensma, M. a. Allessie, W. J. Lammers, F. I. Bonke, and M. J. Schalij, "Length of excitation wave and susceptibility to reentrant atrial arrhythmias in normal conscious dogs," *Circulation Research*, vol. 62, pp. 395–410, feb 1988.

[62] T. J. Wu, M. Yashima, R. Doshi, Y. H. Kim, C. a. Athill, J. J. Ong, L. Czer, a. Trento, C. Blanche, R. M. Kass, a. Garfinkel, J. N. Weiss, M. C. Fishbein, H. S. Karagueuzian, and P. S. Chen, "Relation between cellular repolarization characteristics and critical mass for human ventricular fibrillation.," *Journal of cardiovascular electrophysiology*, vol. 10, pp. 1077–86, aug 1999.

[63] K. R. Laurita, S. D. Girouard, and D. S. Rosenbaum, "Modulation of ventricular repolarization by a premature stimulus. Role of epicardial dispersion of repolarization kinetics demonstrated by optical mapping of the intact guinea pig heart.," *Circulation research*, vol. 79, pp. 493–503, sep 1996.

[64] E. M. Cherry and F. H. Fenton, "Suppression of alternans and conduction blocks despite steep APD restitution: electrotonic, memory, and conduction velocity restitution effects.," *American journal of physiology. Heart and circulatory physiology*, vol. 286, no. 6, pp. H2332–H2341, 2004.

[65] M. L. Riccio, M. L. Koller, and R. F. Gilmour, "Electrical restitution and spatiotemporal organization during ventricular fibrillation.," *Circulation research*, vol. 84, pp. 955–63, apr 1999.

[66] I. Banville, N. Chattipakorn, and R. a. Gray, "Restitution dynamics during pacing and arrhythmias in isolated pig hearts.," *Journal of cardiovascular electrophysiology*, vol. 15, pp. 455–63, apr 2004.

[67] M. L. Koller, M. L. Riccio, and R. F. Gilmour, "Dynamic restitution of action potential duration during electrical alternans and ventricular fibrillation.," *The American journal of physiology*, vol. 275, pp. H1635–42, nov 1998.

[68] B.-S. Kim, Y.-h. Kim, G.-s. Hwang, H.-n. Pak, S. C. Lee, W. J. Shim, D. J. Oh, and Y. M. Ro, "Action potential duration restitution kinetics in human atrial fibrillation.," *Journal of the American College of Cardiology*, vol. 39, no. 8, pp. 1329–1336, 2002.

[69] H. Saitoh, J. C. Bailey, and B. Surawicz, "Action potential duration alternans in dog Purkinje and ventricular muscle fibers. Further evidence in support of two different mechanisms.," *Circulation*, vol. 80, no. 5, pp. 1421–1431, 1989.

[70] M. L. Walker, X. Wan, G. E. Kirsch, and D. S. Rosenbaum, "Hysteresis Effect Implicates Calcium Cycling as a Mechanism of Repolarization Alternans," *Circulation*, vol. 108, no. 21, pp. 2704–2709, 2003.

[71] S. K. Chua, P. C. Chang, M. Maruyama, I. Turker, T. Shinohara, M. J. Shen, Z. Chen, C. Shen, M. Rubart-Von Der Lohe, J. C. Lopshire, M. Ogawa, J. N. Weiss, S. F. Lin, T. Ai, and P. S. Chen, "Small-conductance calcium-activated potassium channel and recurrent ventricular fibrillation in failing rabbit ventricles," *Circulation Research*, vol. 108, no. 8, pp. 971–979, 2011.

[72] Y. C. Hsieh, P. C. Chang, C. H. Hsueh, Y. S. Lee, C. Shen, J. N. Weiss, Z. Chen, T. Ai, S. F. Lin, and P. S. Chen, "Apamin-sensitive potassium current modulates action potential duration restitution and arrhythmogenesis of failing rabbit ventricles," *Circulation: Arrhythmia and Electrophysiology*, vol. 6, no. 2, pp. 410–418, 2013.

[73] J. B. Nolasco and R. W. Dahlen, "A graphic method for the study of alternation in cardiac action potentials.," *Journal of applied physiology (Bethesda, Md. : 1985)*, vol. 25, no. 2, pp. 191–196, 1968.

[74] O. E. Osadchii, E. Soltysinska, and S. P. Olesen, "Na+ channel distribution and electrophysiological heterogeneities in guinea pig ventricular wall.," *American journal of physiology. Heart and circulatory physiology*, vol. 300, no. 3, pp. H989–H1002, 2011.

[75] J. N. Weiss, A. Garfinkel, H. S. Karagueuzian, Z. Qu, and P.-S. Chen, "Chaos and the Transition to Ventricular Fibrillation : A New Approach to Antiarrhythmic Drug Evaluation," *Circulation*, vol. 99, pp. 2819–2826, jun 1999.

[76] M. L. Koller, M. L. Riccio, and R. F. Gilmour, "Dynamic restitution of action potential duration during electrical alternans and ventricular fibrillation.," *The American journal of physiology*, vol. 275, pp. H1635–42, nov 1998.

[77] K. F. Decker, J. Heijman, J. R. Silva, T. J. Hund, and Y. Rudy, "Properties and ionic mechanisms of action potential adaptation , restitution , and accommodation in canine epicardium Properties and ionic mechanisms of action potential adaptation , restitution , and accommodation in canine epicardium," *American journal of physiology. Heart and circulatory physiology*, vol. 296, no. 4, pp. H1017–H1026, 2009.

[78] F. E. Marchlinski and B. P. Betensky, "Mechanisms of Cardiac Arrhythmias," *Revista Española de Cardiología*, vol. 65, no. 2, pp. 174–185, 2012.

[79] P. Wit, L, Boyden, "Triggered Activity and Atrial Fibrillation," *Heart Rhythm*, vol. 4, no. 3, pp. S17–S23, 2007.

[80] G. J. Rozanski and R. C. Witt, "Early afterdepolarizations and triggered activity in rabbit cardiac Purkinje fibers recovering from ischemic-like conditions. Role of acidosis.," *Circulation*, vol. 83, no. 4, pp. 1352–1360, 1991.

[81] A. Burashnikov and C. Antzelevitch, "Late-phase 3 EAD. A unique mechanism contributing to initiation of atrial fibrillation," *PACE - Pacing and Clinical Electrophysiology*, vol. 29, no. 3, pp. 290–295, 2006.

[82] R. Guinamard, M. Demion, A. Chatelier, and P. Bois, "Calcium-Activated Nonselective Cation Channels in Mammalian Cardiomyocytes," *Trends in Cardiovascular Medicine*, vol. 16, no. 7, pp. 245–250, 2006.

[83] A. O. Verkerk, M. W. Veldkamp, L. N. Bouman, and A. C. van Ginneken, "Calcium-activated Cl(-) current contributes to delayed afterdepolarizations in single Purkinje and ventricular myocytes.," *Circulation*, vol. 101, no. 22, pp. 2639–2644, 2000.

[84] A. O. Verkerk, M. W. Veldkamp, A. Baartscheer, C. A. Schumacher, C. Klöpping, A. C. van Ginneken, and J. H. Ravesloot, "Ionic mechanism of delayed afterdepolarizations in ventricular cells isolated from human end-stage failing hearts.," *Circulation*, vol. 104, no. 22, pp. 2728–2733, 2001.

[85] J. Jalife, O. Berenfeld, A. Skanes, and R. Mandapati, "Mechanisms of atrial fibrillation: mother rotors or multiple daughter wavelets, or both?," *Journal of cardiovascular electrophysiology*, vol. 9, pp. S2–12, aug 1998.

[86] D. E. Krummen, J. Hayase, D. J. Morris, J. Ho, M. R. Smetak, P. Clopton, W.-J. Rappel, and S. M. Narayan, "Rotor Stability Separates Sustained Ventricular Fibrillation From Self-Terminating Episodes in Humans.," *Journal of the American College of Cardiology*, apr 2014.

[87] S. M. Narayan, D. E. Krummen, and W. J. Rappel, "Clinical mapping approach to diagnose electrical rotors and focal impulse sources for human atrial fibrillation," *Journal of Cardiovascular Electrophysiology*, vol. 23, no. 5, pp. 447–454, 2012.

[88] J. Ng, A. H. Kadish, and J. J. Goldberger, "Technical considerations for dominant frequency analysis.," *Journal of cardiovascular electrophysiology*, vol. 18, pp. 757–64, jul 2007.

[89] M. Mansour, R. Mandapati, O. Berenfeld, J. Chen, F. H. Samie, and J. Jalife, "Left-to-Right Gradient of Atrial Frequencies During Acute Atrial Fibrillation in the Isolated Sheep Heart," *Circulation*, vol. 103, pp. 2631–2636, may 2001.

[90] G. Moe, W. Rheinboldt, and J. Abildskov, "A computer model of atrial fibrillation," *American heart journal*, vol. 67, no. 2, pp. 200–220, 1964.

[91] R. P. M. Groot, Natasja S, J. L. Smeets, E. Boersma, U. Schotten, M. J. Schalij, H. Crijns, and M. A. Allessie, "Electropathological Substrate of Longstanding Persistent Atrial Fibrillation in Patients With Structural Heart Disease," *Circulation*, vol. 122, no. 17, pp. 1674–1682, 2010.

[92] B. E. Benson, R. Carrick, N. Habel, O. Bates, J. H. T. Bates, P. Bielau, and P. Spector, "Mapping multi-wavelet reentry without isochrones: an electrogram-guided approach to define substrate distribution.," *Europace : European pacing, arrhythmias, and cardiac electrophysiology : journal of the working groups on cardiac pacing, arrhythmias, and cardiac cellular electrophysiology of the European Society of Cardiology*, vol. 16 Suppl 4, pp. iv102–iv109, nov 2014.

[93] J. Tranum-Jensen, M. J. Janse, W. T. Fiolet, W. J. Krieger, C. N. D'Alnoncourt, and D. Durrer, "Tissue osmolality, cell swelling, and reperfusion in acute regional myocardial ischemia in the isolated porcine heart.," *Circulation research*, vol. 49, no. 2, pp. 364–381, 1981.

[94] M. J. Shattock and H. Matsuura, "Measurement of Na(+)-K+ pump current in isolated rabbit ventricular myocytes using the whole-cell voltage-clamp technique. Inhibition of the pump by oxidant stress.," *Circulation research*, vol. 72, no. 1, pp. 91–101, 1993.

[95] K. Clarke, L. C. Stewart, S. Neubauer, J. A. Balschi, T. W. Smith, J. S. Ingwall, J.-F. Nédélec, S. M. Humphrey, A. G. Kléber, and C. S. Springer, "Extracellular volume and transsarcolemmal proton movement during ischemia and reperfusion: A 31P NMR spectroscopic study of the isovolumic rat heart," *NMR in Biomedicine*, vol. 6, no. 4, pp. 278–286, 1993.

[96] K. Kaila and R. D. Vaughan-Jones, "Influence of sodium-hydrogen exchange on intracellular pH, sodium and tension in sheep cardiac Purkinje fibres.," *The Journal of Physiology*, vol. 390, no. 1, pp. 93–118, 1987.

[97] M. L. Wu and R. D. Vaughan-Jones, "Effect of metabolic inhibitors and second messengers upon Na(+)-H+ exchange in the sheep cardiac Purkinje fibre.," *The Journal of Physiology*, vol. 478, no. 2, pp. 301–313, 1994.

[98] J. I. Vandenberg, J. C. Metcalfe, and a. a. Grace, "Mechanisms of pHi recovery after global ischemia in the perfused heart.," *Circulation research*, vol. 72, no. 5, pp. 993–1003, 1993.

[99] S. E. Anderson, E. Murphy, C. Steenbergen, R. E. London, and P. M. Cala, "Na-H exchange in myocardium: effects of hypoxia and acidification on Na and Ca.," *The American journal of physiology*, vol. 259, no. 6 Pt 1, pp. C940–C948, 1990.

[100] M. Pike, S. U. Luo, M. Daniel, M. Pohost, M. Martin, C. S. Luo, M. D. Clark, K. a. Kirk, M. Kitakaze, C. Michael, E. J. Cragoe, and G. M. Pohost, "NMR measurements of Na + and cellular rat heart : role of Na + -H + exchange energy in ischemic," *American Journal of Physiology - Heart and Circulatory Physiology*, vol. 265, no. 6, pp. H2017–H2026, 1993.

[101] W. Fuller, V. Parmar, P. Eaton, J. R. Bell, and M. J. Shattock, "Cardiac ischemia causes inhibition of the Na/K ATPase by a labile cytosolic compound whose production is linked to oxidant stress," *Cardiovascular Research*, vol. 57, no. 4, pp. 1044–1051, 2003.

[102] T. F. McDonald, S. Pelzer, W. Trautwein, and D. J. Pelzer, "Regulation and modulation of calcium channels in cardiac, skeletal, and smooth muscle cells," *Physiol Rev.*, vol. 74, no. 2, pp. 365–507, 1994.

[103] T. Kristián and B. K. Siesjö, "Calcium in ischemic cell death.," *Stroke; a journal of cerebral circulation*, vol. 29, no. 3, pp. 705–718, 1998.

[104] P. Kaplan, M. Hendrikx, M. Mattheussen, K. Mubagwa, and W. Flameng, "Effect of ischemia and reperfusion on sarcoplasmic reticulum calcium uptake.," *Circulation research*, vol. 71, no. 5, pp. 1123–1130, 1992.

[105] L. Li, X. Zheng, D. J. Dosdall, J. Huang, and R. E. Ideker, "Different types of long-duration ventricular fibrillation: can they be identified by electrocardiography.," *Journal of electrocardiology*, vol. 45, no. 6, pp. 658–9, 2012.

[106] N. A. Trayanova, "The long and the short of long and short duration ventricular fibrillation," *Circulation Research*, vol. 102, no. 10, pp. 1151–1152, 2008.

[107] A. A. BAGDONAS, J. H. STUCKEY, J. PIERA, N. S. AMER, and B. F. HOFFMAN, "Effects of ischemia and hypoxia on the specialized conducting system of the canine heart.," *American heart journal*, vol. 61, no. 2, pp. 206–218, 1961.

[108] O. Berenfeld and J. Jalife, "Purkinje-Muscle Reentry as a Mechanism of Polymorphic Ventricular Arrhythmias in a 3-Dimensional Model of the Ventricles," *Circulation Research*, vol. 82, pp. 1063–1077, jun 1998.

[109] R. P. Holland and H. Brooks, "The QRS Complex during Myocardial Ischemia," *The Journal of Clinical Investigation*, vol. 57, no. March, pp. 541–550, 1976.

[110] D. J. Huelsing, K. W. Spitzer, J. M. Cordeiro, and a. E. Pollard, "Modulation of repolarization in rabbit Purkinje and ventricular myocytes coupled by a variable resistance.," *The American journal of physiology*, vol. 276, pp. H572–81, feb 1999.

[111] R. P. Robichaux, D. J. Dosdall, J. Osorio, N. W. Garner, L. Li, J. Huang, and R. E. Ideker, "Periods of highly synchronous, non-reentrant endocardial activation cycles occur during long-duration ventricular fibrillation.," *Journal of cardiovascular electrophysiology*, vol. 21, pp. 1266–73, nov 2010.

[112] L. Li, Q. Jin, D. J. Dosdall, J. Huang, S. M. Pogwizd, and R. E. Ideker, "Activation becomes highly organized during long-duration ventricular fibrillation in canine hearts.," *American journal of physiology. Heart and circulatory physiology*, vol. 298, pp. H2046–53, jun 2010.

[113] S. Deshpande, J. Catanzaro, and S. Wann, "Atrial Fibrillation: Prevalence and Scope of the Problem," *Cardiac Electrophysiology Clinics*, vol. 6, no. 1, pp. 1–4, 2014.

[114] J. Heeringa, D. a. M. van der Kuip, A. Hofman, J. a. Kors, G. van Herpen, B. H. C. Stricker, T. Stijnen, G. Y. H. Lip, and J. C. M. Witteman, "Prevalence, incidence and lifetime risk of atrial fibrillation: the Rotterdam study.," *European heart journal*, vol. 27, pp. 949–53, apr 2006.

[115] P. Di Donna, I. Olivotto, S. D. L. Delcrè, D. Caponi, M. Scaglione, I. Nault, A. Montefusco, F. Girolami, F. Cecchi, M. Haissaguerre, and F. Gaita, "Efficacy of catheter ablation for atrial fibrillation in hypertrophic cardiomyopathy: Impact of age, atrial remodelling, and disease progression," *Europace*, vol. 12, no. 3, pp. 347–355, 2010.

[116] R. A. Winkle, R. H. Mead, G. Engel, and R. A. Patrawala, "Long-term results of atrial fibrillation ablation: the importance of all initial ablation failures undergoing a repeat ablation.," *American heart journal*, vol. 162, pp. 193–200, jul 2011.

[117] R. Weerasooriya, P. Khairy, J. Litalien, L. Macle, M. Hocini, F. Sacher, N. Lellouche, S. Knecht, M. Wright, I. Nault, S. Miyazaki, C. Scavee, J. Clementy, M. Haissaguerre, and P. Jais, "Catheter ablation for atrial fibrillation: are results maintained at 5 years of follow-up?," *Journal of the American College of Cardiology*, vol. 57, pp. 160–6, jan 2011.

[118] M. C. Wijffels, C. J. Kirchhof, R. Dorland, and M. A. Allessie, "Atrial fibrillation begets atrial fibrillation. A study in awake chronically instrumented goats.," *Circulation*, vol. 92, pp. 1954–1968, 1995.

[119] T. Rostock, D. Steven, B. Lutomsky, H. Servatius, I. Drewitz, H. Klemm, K. Müllerleile, R. Ventura, T. Meinertz, and S. Willems, "Atrial fibrillation begets atrial fibrillation in the pulmonary veins on the impact of atrial fibrillation on the electrophysiological properties of the pulmonary veins in humans.," *Journal of the American College of Cardiology*, vol. 51, pp. 2153–60, jun 2008.

[120] M. K. Stiles, B. John, C. X. Wong, P. Kuklik, A. G. Brooks, D. H. Lau, H. Dimitri, K. C. Roberts-Thomson, L. Wilson, P. De Sciscio, G. D. Young, and P. Sanders, "Paroxysmal Lone Atrial Fibrillation Is Associated With an Abnormal Atrial Substrate. Characterizing the "Second Factor"," *Journal of the American College of Cardiology*, vol. 53, no. 14, pp. 1182–1191, 2009.

[121] C. McGann, N. Akoum, A. Patel, E. Kholmovski, P. Revelo, K. Damal, B. Wilson, J. Cates, A. Harrison, R. Ranjan, N. S. Burgon, T. Greene, D. Kim, E. V. R. DiBella, D. Parker, R. S. MacLeod, and N. F. Marrouche, "Atrial fibrillation ablation

outcome is predicted by left atrial remodeling on MRI," *Circulation: Arrhythmia and Electrophysiology*, vol. 7, no. 1, pp. 23–30, 2014.

[122] S. A. Chen, M. H. Hsieh, C. T. Tai, C. F. Tsai, V. S. Prakash, W. C. Yu, T. L. Hsu, Y. A. Ding, and M. S. Chang, "Initiation of atrial fibrillation by ectopic beats originating from the pulmonary veins: electrophysiological characteristics, pharmacological responses, and effects of radiofrequency ablation.," Tech. Rep. 18, 1999.

[123] V. Swarup, T. Baykaner, A. Rostamian, J. P. Daubert, J. Hummel, D. E. Krummen, R. Trikha, J. M. Miller, G. F. Tomassoni, and S. M. Narayan, "Stability of Rotors and Focal Sources for Human Atrial Fibrillation: Focal Impulse and Rotor Mapping (FIRM) of AF Sources and Fibrillatory Conduction.," *Journal of cardiovascular electrophysiology*, vol. 25, pp. 1284–92, dec 2014.

[124] J. W. E. Jarman, T. Wong, P. Kojodjojo, H. Spohr, J. E. R. Davies, M. Roughton, D. P. Francis, P. Kanagaratnam, M. D. O'Neill, V. Markides, D. W. Davies, and N. S. Peters, "Organizational index mapping to identify focal sources during persistent atrial fibrillation.," *Journal of cardiovascular electrophysiology*, vol. 25, pp. 355–63, apr 2014.

[125] U. Schotten, "Electrical and Contractile Remodeling During the First Days of Atrial Fibrillation Go Hand in Hand," *Circulation*, vol. 107, pp. 1433–1439, mar 2003.

[126] R. F. Bosch, X. Zeng, J. B. Grammer, K. Popovic, C. Mewis, and V. Kühlkamp, "Ionic mechanisms of electrical remodeling in human atrial fibrillation.," *Cardiovascular research*, vol. 44, no. 1, pp. 121–131, 1999.

[127] R. Gaspo, R. F. Bosch, E. Bou-Abboud, and S. Nattel, "Tachycardia-Induced Changes in Na+ Current in a Chronic Dog Model of Atrial Fibrillation," *Circulation Research*, vol. 81, no. 6, pp. 1045–1052, 1997.

[128] D. R. Van Wagoner, a. L. Pond, M. Lamorgese, S. S. Rossie, P. M. McCarthy, and J. M. Nerbonne, "Atrial L-type Ca2+ currents and human atrial fibrillation.," *Circulation research*, vol. 85, no. 5, pp. 428–436, 1999.

[129] M. Allessie, J. Ausma, and U. Schotten, "Electrical, contractile and structural remodeling during atrial fibrillation," 2002.

[130] K. T. Konings, C. J. Kirchhof, J. R. Smeets, H. J. Wellens, O. C. Penn, and M. a. Allessie, "High-density mapping of electrically induced atrial fibrillation in humans," *Circulation*, vol. 89, pp. 1665–1680, apr 1994.

[131] W. C. Yu, S. H. Lee, C. T. Tai, C. F. Tsai, M. H. Hsieh, C. C. Chen, Y. A. Ding, M. S. Chang, and S. A. Chen, "Reversal of atrial electrical remodeling following cardioversion of long-standing atrial fibrillation in man," *Cardiovascular Research*, vol. 42, no. 2, pp. 470–476, 1999.

[132] J. Ausma, M. Wijffels, F. Thone, L. Wouters, M. Allessie, and M. Borgers, "Structural Changes of Atrial Myocardium due to Sustained Atrial Fibrillation in the Goat," *Circulation*, vol. 96, no. 9, pp. 3157–3163, 1997.

[133] G. Krenning, E. M. Zeisberg, and R. Kalluri, "The origin of fibroblast and mechanism of cardiac fibrosis," *Journal of cell physiology*, vol. 225, no. 3, pp. 631–637, 2010.

[134] M. S. Spach and J. P. Boineau, "Microfibrosis produces electrical load variations due to loss of side- to-side cell connections: A major mechanism of structural heart disease arrhythmias," *PACE - Pacing and Clinical Electrophysiology*, vol. 20, no. 2 II, pp. 397–413, 1997.

[135] M. S. Spach, P. C. Dolber, and J. F. Heidlage, "Influence of the passive anisotropic properties on directional differences in propagation following modification of the sodium conductance in human atrial muscle. A model of reentry based on anisotropic discontinuous propagation.," *Circulation research*, vol. 62, pp. 811–832, 1988.

[136] S. Verheule, E. Tuyls, A. Gharaviri, S. Hulsmans, A. van Hunnik, M. Kuiper, J. Serroyen, S. Zeemering, N. H. L. Kuijpers, and U. Schotten, "Loss of continuity in the thin epicardial layer because of endomysial fibrosis increases the complexity of atrial fibrillatory conduction.," *Circulation. Arrhythmia and electrophysiology*, vol. 6, pp. 202–11, feb 2013.

[137] N. F. Marrouche, D. Wilber, G. Hindricks, P. Jais, N. Akoum, F. Marchlinski, E. Kholmovski, N. Burgon, N. Hu, L. Mont, T. Deneke, M. Duytschaever, T. Neumann, M. Mansour, C. Mahnkopf, B. Herweg, E. Daoud, E. Wissner, P. Bansmann, and J. Brachmann, "Association of Atrial Tissue Fibrosis Identified by Delayed Enhancement MRI and Atrial Fibrillation Catheter Ablation," *Jama*, vol. 311, p. 498, feb 2014.

[138] A. McLellan, L. Ling, A. Ellims, L. Iles, S. Azzopardi, J. Morton, J. Kalman, A. Taylor, and P. Kistler, "Diffuse Atrial Fibrosis Measured by T1 Mapping on Cardiac MRI Predicts Success of Atrial Fibrillation Ablation," *Heart, Lung and Circulation*, vol. 22, p. S110, jan 2015.

[139] W. J. Manning, D. I. Silverman, S. E. Katz, M. F. Riley, P. C. Come, R. M. Doherty, J. T. Munson, and P. S. Douglas, "Impaired left atrial mechanical function after cardioversion: relation to the duration of atrial fibrillation.," *Journal of the American College of Cardiology*, vol. 23, no. 7, pp. 1535–1540, 1994.

[140] W. J. Manning, D. I. Silverman, S. E. Katz, M. F. Riley, R. M. Doherty, J. T. Munson, and P. S. Douglas, "Temporal dependence of the return of atrial mechanical function on the mode of cardioversion of atrial fibrillation to sinus rhythm.," *The American journal of cardiology*, vol. 75, no. 8, pp. 624–626, 1995.

[141] L. Yue, J. Feng, R. Gaspo, G.-R. Li, Z. Wang, and S. Nattel, "Ionic Remodeling Underlying Action Potential Changes in a Canine Model of Atrial Fibrillation," *Circulation Research*, vol. 81, no. 4, pp. 512–525, 1997.

[142] C. A. Morillo, G. J. Klein, D. L. Jones, and C. M. Guiraudon, "Chronic Rapid Atrial Pacing: Structural, Functional, and Electrophysiological Characteristics of a New Model of Sustained Atrial Fibrillation," *Circulation*, vol. 91, no. 5, pp. 1588–1595, 1995.

[143] T. Rostock, D. Steven, B. Lutomsky, H. Servatius, I. Drewitz, H. Klemm, K. Müllerleile, R. Ventura, T. Meinertz, and S. Willems, "Atrial fibrillation begets atrial fibrillation in the pulmonary veins on the impact of atrial fibrillation on the electrophysiological properties of the pulmonary veins in humans.," *Journal of the American College of Cardiology*, vol. 51, pp. 2153–60, jun 2008.

[144] S. M. Narayan, M. R. Franz, P. Clopton, E. J. Pruvot, and D. E. Krummen, "Repolarization alternans reveals vulnerability to human atrial fibrillation.," *Circulation*, vol. 123, pp. 2922–30, jun 2011.

[145] C. Cabo, a. M. Pertsov, J. M. Davidenko, W. T. Baxter, R. a. Gray, and J. Jalife, "Vortex shedding as a precursor of turbulent electrical activity in cardiac muscle.," *Biophysical journal*, vol. 70, pp. 1105–11, mar 1996.

[146] M. Mansour, R. Mandapati, O. Berenfeld, J. Chen, F. H. Samie, and J. Jalife, "Left-to-Right Gradient of Atrial Frequencies During Acute Atrial Fibrillation in the Isolated Sheep Heart," *Circulation*, vol. 103, pp. 2631–2636, may 2001.

[147] P. Zimetbaum, "Antiarrhythmic drug therapy for atrial fibrillation," *Circulation*, vol. 125, no. 2, pp. 381–389, 2012.

[148] C. T. January, L. S. Wann, J. S. Alpert, H. Calkins, J. C. Cleveland, J. E. Cigarroa, J. B. Conti, P. T. Ellinor, M. D. Ezekowitz, M. E. Field, K. T. Murray, R. L. Sacco, W. G. Stevenson, P. J. Tchou, C. M. Tracy, and C. W. Yancy, *2014 AHA/ACC/HRS guideline for the management of patients with atrial fibrillation: A report of the American college of cardiology/American heart association task force on practice guidelines and the heart rhythm society*. 2014.

[149] D. Dosdall, J. Huang, and R. Ideker, "Mechanisms of defibrillation," *Annual review of biomedical engineering*, vol. 12, pp. 233–260, 2009.

[150] A. R. J. Mitchell, P. A. R. Spurrell, L. E. Boodhoo, and N. Sulke, "Long-term care of the patient with the atrial defibrillator," *American Heart Journal*, vol. 147, no. 2, pp. 210–217, 2004.

[151] T. M. Hurst, M. Hinrichs, C. Breidenbach, N. Katz, and B. Waldecker, "Detection of myocardial injury during transvenous implantation of automatic cardioverter-defibrillators.," *Journal of the American College of Cardiology*, vol. 34, pp. 402–8, aug 1999.

[152] A. J. Moss, H. Greenberg, R. B. Case, W. Zareba, W. J. Hall, M. W. Brown, J. P. Daubert, S. McNitt, M. L. Andrews, and A. D. Elkin, "Long-term clinical course of patients after termination of ventricular tachyarrhythmia by an implanted defibrillator.," *Circulation*, vol. 110, pp. 3760–5, dec 2004.

[153] J. B. van Rees, C. J. W. Borleffs, M. K. de Bie, T. Stijnen, L. van Erven, J. J. Bax, and M. J. Schalij, "Inappropriate implantable cardioverter-defibrillator shocks: incidence, predictors, and impact on mortality.," *Journal of the American College of Cardiology*, vol. 57, pp. 556–62, feb 2011.

[154] H.-N. Pak, Y.-B. Liu, H. Hayashi, Y. Okuyama, P.-S. Chen, and S.-f. Lin, "Synchronization of ventricular fibrillation with real-time feedback pacing: implication to low-energy defibrillation.," *American journal of physiology. Heart and circulatory physiology*, vol. 285, pp. H2704–11, dec 2003.

[155] C. M. Ambrosi, C. M. Ripplinger, I. R. Efimov, and V. V. Fedorov, "Termination of sustained atrial flutter and fibrillation using low-voltage multiple-shock therapy.," *Heart rhythm : the official journal of the Heart Rhythm Society*, vol. 8, pp. 101–8, jan 2011.

[156] W. Li, A. H. Janardhan, V. V. Fedorov, Q. Sha, R. B. Schuessler, and I. R. Efimov, "Low-energy multistage atrial defibrillation therapy terminates atrial fibrillation with less energy than a single shock.," *Circulation. Arrhythmia and electrophysiology*, vol. 4, pp. 917–25, dec 2011.

[157] M. S. Wathen, M. O. Sweeney, P. J. DeGroot, a. J. Stark, J. L. Koehler, M. B. Chisner, C. Machado, and W. O. Adkisson, "Shock Reduction Using Antitachycardia Pacing for Spontaneous Rapid Ventricular Tachycardia in Patients With Coronary Artery Disease," *Circulation*, vol. 104, pp. 796–801, aug 2001.

[158] A. H. Janardhan, W. Li, V. V. Fedorov, M. Yeung, M. J. Wallendorf, R. B. Schuessler, and I. R. Efimov, "A novel low-energy electrotherapy that terminates ventricular tachycardia with lower energy than a biphasic shock when antitachycardia pacing fails.," *Journal of the American College of Cardiology*, vol. 60, pp. 2393–8, dec 2012.

[159] J. M. Miller and D. P. Zipes, "Catheter Ablation of Arrhythmias," *Circulation*, vol. 106, no. 25, pp. e203–e205, 2002.

[160] M. Haïssaguerre, P. Jaïs, D. C. Shah, a. Takahashi, M. Hocini, G. Quiniou, S. Garrigue, a. Le Mouroux, P. Le Métayer, and J. Clémenty, "Spontaneous initiation of atrial fibrillation by ectopic beats originating in the pulmonary veins.," *The New England journal of medicine*, vol. 339, no. 10, pp. 659–666, 1998.

[161] H. Oral, "Pulmonary Vein Isolation for Paroxysmal and Persistent Atrial Fibrillation," *Circulation*, vol. 105, pp. 1077–1081, feb 2002.

[162] V. Swarup, T. Baykaner, A. Rostamian, J. P. Daubert, J. Hummel, D. E. Krummen, R. Trikha, J. M. Miller, G. F. Tomassoni, and S. M. Narayan, "Stability of Rotors and Focal Sources for Human Atrial Fibrillation: Focal Impulse and Rotor Mapping (FIRM) of AF Sources and Fibrillatory Conduction.," *Journal of cardiovascular electrophysiology*, vol. 25, pp. 1284–92, dec 2014.

[163] J. Ng, A. I. Borodyanskiy, E. T. Chang, R. Villuendas, S. Dibs, A. H. Kadish, and J. J. Goldberger, "Measuring the complexity of atrial fibrillation electrograms.," *Journal of cardiovascular electrophysiology*, vol. 21, pp. 649–55, jun 2010.

[164] A. S. Jadidi, H. Cochet, A. J. Shah, S. J. Kim, E. Duncan, S. Miyazaki, M. Sermesant, H. Lehrmann, M. Lederlin, N. Linton, A. Forclaz, I. Nault, L. Rivard, M. Wright, X. Liu, D. Scherr, S. B. Wilton, L. Roten, P. Pascale, N. Derval, F. Sacher, S. Knecht, C. Keyl, M. Hocini, M. Montaudon, F. Laurent, M. Haïssaguerre, and P. Jaïs, "Inverse relationship between fractionated electrograms and atrial fibrosis in persistent atrial fibrillation: combined magnetic resonance imaging and high-density mapping.," *Journal of the American College of Cardiology*, vol. 62, pp. 802–12, aug 2013.

[165] D. H. Lau, B. Maesen, S. Zeemering, S. Verheule, H. J. Crijns, and U. Schotten, "Stability of complex fractionated atrial electrograms: a systematic review.," *Journal of cardiovascular electrophysiology*, vol. 23, pp. 980–7, sep 2012.

[166] J. Kalifa, K. Tanaka, A. V. Zaitsev, M. Warren, R. Vaidyanathan, D. Auerbach, S. Pandit, K. L. Vikstrom, R. Ploutz-Snyder, A. Talkachou, F. Atienza, G. Guiraudon, J. Jalife, and O. Berenfeld, "Mechanisms of wave fractionation at boundaries of high-frequency excitation in the posterior left atrium of the isolated sheep heart during atrial fibrillation.," *Circulation*, vol. 113, pp. 626–33, feb 2006.

[167] J. L. Salinet, J. H. Tuan, A. J. Sandilands, P. J. Stafford, F. S. Schlindwein, and G. André Ng, "Distinctive Patterns of Dominant Frequency Trajectory Behavior in Drug-Refractory Persistent Atrial Fibrillation: Preliminary Characterization of Spatiotemporal Instability," *Journal of Cardiovascular Electrophysiology*, vol. 25, pp. 371–379, apr 2014.

[168] J. W. E. Jarman, T. Wong, P. Kojodjojo, H. Spohr, J. E. Davies, M. Roughton, D. P. Francis, P. Kanagaratnam, V. Markides, D. W. Davies, and N. S. Peters, "Spatiotemporal behavior of high dominant frequency during paroxysmal and persistent atrial fibrillation in the human left atrium.," *Circulation. Arrhythmia and electrophysiology*, vol. 5, pp. 650–8, aug 2012.

[169] R. Tung, E. Buch, and K. Shivkumar, "Catheter Ablation of Atrial Fibrillation," *Circulation*, vol. 126, no. 2, pp. 223–229, 2012.

[170] P. Benharash, E. Buch, P. Frank, M. Share, R. Tung, K. Shivkumar, and R. Mandapati, "Quantitative Analysis of Localized Sources Identified by Focal Impulse and Roter Modulation Mapping in Atrial Fibrillation," *Circulation: Arrhythmia and Electrophysiology*, 2015.

[171] R. Coronel, F. J. Wilms-Schopman, J. R. de Groot, M. J. Janse, F. J. van Capelle, and J. M. de Bakker, "Laplacian electrograms and the interpretation of complex ventricular activation patterns during ventricular fibrillation.," *Journal of cardiovascular electrophysiology*, vol. 11, pp. 1119–28, oct 2000.

[172] B. B. Punske, Q. Ni, R. L. Lux, R. S. MacLeod, P. R. Ershler, T. J. Dustman, M. J. Allison, and B. Taccardi, "Spatial Methods of Epicardial Activation Time Determination in Normal Hearts," *Annals of Biomedical Engineering*, vol. 31, pp. 781–792, jul 2003.

[173] A. S. Jadidi, H. Cochet, A. J. Shah, S. J. Kim, E. Duncan, S. Miyazaki, M. Sermesant, H. Lehrmann, M. Lederlin, N. Linton, A. Forclaz, I. Nault, L. Rivard, M. Wright, X. Liu, D. Scherr, S. B. Wilton, L. Roten, P. Pascale, N. Derval, F. Sacher, S. Knecht, C. Keyl, M. Hocini, M. Montaudon, F. Laurent, M. Haïssaguerre, and P. Jaïs, "Inverse relationship between fractionated electrograms and atrial fibrosis in persistent atrial fibrillation: combined magnetic resonance imaging and high-density mapping.," *Journal of the American College of Cardiology*, vol. 62, pp. 802–12, aug 2013.

[174] L. Iles, H. Pfluger, A. Phrommintikul, J. Cherayath, P. Aksit, S. N. Gupta, D. M. Kaye, and A. J. Taylor, "Evaluation of diffuse myocardial fibrosis in heart failure with cardiac magnetic resonance contrast-enhanced T1 mapping.," *Journal of the American College of Cardiology*, vol. 52, pp. 1574–80, nov 2008.

[175] T. A. Treibel, S. K. White, and J. C. Moon, "Myocardial Tissue Characterization: Histological and Pathophysiological Correlation.," *Current Cardiovascular Imaging Reports*, vol. 7, no. 3, p. 9254, 2014.

[176] A. S. Flett, M. P. Hayward, M. T. Ashworth, M. S. Hansen, A. M. Taylor, P. M. Elliott, C. McGregor, and J. C. Moon, "Equilibrium contrast cardiovascular magnetic resonance for the measurement of diffuse myocardial fibrosis: preliminary validation in humans.," *Circulation*, vol. 122, pp. 138–44, jul 2010.

[177] M. Fitts, E. Breton, E. G. Kholmovski, D. J. Dosdall, S. Vijayakumar, K. P. Hong, R. Ranjan, N. F. Marrouche, L. Axel, and D. Kim, "Arrhythmia insensitive rapid cardiac T1 mapping pulse sequence.," *Magnetic resonance in medicine : official journal of the Society of Magnetic Resonance in Medicine / Society of Magnetic Resonance in Medicine*, vol. 70, pp. 1274–82, dec 2013.

[178] S. Chemla and F. Chavane, "Voltage-sensitive dye imaging: Technique review and models," *Journal of Physiology Paris*, vol. 104, no. 1-2, pp. 40–50, 2010.

[179] T. J. Herron, P. Lee, and J. Jalife, "Optical imaging of voltage and calcium in cardiac cells & tissues," *Circulation Research*, vol. 110, no. 4, pp. 609–623, 2012.

[180] M. Potse, A. Vinet, T. Opthof, and R. Coronel, "Validation of a simple model for the morphology of the T wave in unipolar electrograms.," *American journal of physiology. Heart and circulatory physiology*, vol. 297, no. 2, pp. H792–H801, 2009.

[181] R. E. Ideker, W. M. Smith, S. M. Blanchard, S. L. Reiser, E. V. Simpson, P. D. Wolf, and N. D. Danieley, "The Assumptions of Isochronal Cardiac Mapping," *Pacing and Clinical Electrophysiology*, vol. 12, no. 3, pp. 456–478, 1989.

[182] F. Ravelli and M. Masè, "Computational mapping in atrial fibrillation: how the integration of signal-derived maps may guide the localization of critical sources.," *Europace*, vol. 16, pp. 714–23, may 2014.

[183] P. Gal, A. C. Linnenbank, A. Adiyaman, J. Jan, J. Smit, A. R. Ramdat, P. Paul, H. M. Delnoy, J. M. T. D. Bakker, and A. Elvan, "Correlation of atrial fi brillation cycle length and fractionation is associated with atrial fi brillation free survival," *International Journal of Cardiology*, vol. 187, pp. 208–215, 2015.

[184] A. Elvan, A. C. Linnenbank, M. W. van Bemmel, A. R. R. Misier, P. P. H. M. Delnoy, W. P. Beukema, and J. M. T. de Bakker, "Dominant frequency of atrial fibrillation correlates poorly with atrial fibrillation cycle length.," *Circulation. Arrhythmia and electrophysiology*, vol. 2, pp. 634–44, dec 2009.

[185] K. Umapathy, K. Nair, S. Masse, S. Krishnan, J. Rogers, M. P. Nash, and K. Nanthakumar, "Phase mapping of cardiac fibrillation.," *Circulation. Arrhythmia and electrophysiology*, vol. 3, pp. 105–14, feb 2010.

[186] R. A. Gray, A. M. Pertsov, and J. Jalife, "Spatial and temporal organization during cardiac fibrillation," *Nature*, vol. 392, pp. 75–78, mar 1998.

[187] C. Marini, F. De Santis, S. Sacco, T. Russo, L. Olivieri, R. Totaro, and A. Carolei, "Contribution of atrial fibrillation to incidence and outcome of ischemic stroke: results from a population-based study.," *Stroke; a journal of cerebral circulation*, vol. 36, pp. 1115–9, jun 2005.

[188] R. Weerasooriya, P. Khairy, J. Litalien, L. MacLe, M. Hocini, F. Sacher, N. Lellouche, S. Knecht, M. Wright, I. Nault, S. Miyazaki, C. Scavee, J. Clementy, M. Haissaguerre, and P. Jais, "Catheter ablation for atrial fibrillation: Are results maintained at 5 years of follow-up?," *Journal of the American College of Cardiology*, vol. 57, no. 2, pp. 160–166, 2011.

[189] T. Rostock, D. Steven, B. Lutomsky, H. Servatius, I. Drewitz, H. Klemm, K. Müllerleile, R. Ventura, T. Meinertz, and S. Willems, "Atrial fibrillation begets

atrial fibrillation in the pulmonary veins on the impact of atrial fibrillation on the electrophysiological properties of the pulmonary veins in humans.," *Journal of the American College of Cardiology*, vol. 51, pp. 2153–60, jun 2008.

[190] U. Schotten, "Electrical and Contractile Remodeling During the First Days of Atrial Fibrillation Go Hand in Hand," *Circulation*, vol. 107, pp. 1433–1439, mar 2003.

[191] L. Iles, H. Pfluger, A. Phrommintikul, J. Cherayath, P. Aksit, S. N. Gupta, D. M. Kaye, and A. J. Taylor, "Evaluation of diffuse myocardial fibrosis in heart failure with cardiac magnetic resonance contrast-enhanced T1 mapping.," *Journal of the American College of Cardiology*, vol. 52, pp. 1574–80, nov 2008.

[192] M. Koopmann, K. Hong, E. G. Kholmovski, E. C. Huang, N. Hu, J. Ying, R. Levenson, S. Vijayakumar, D. J. Dosdall, R. Ranjan, and D. Kim, "Post-contrast myocardial T1 and ECV disagree in a longitudinal canine study.," *NMR in biomedicine*, vol. 27, pp. 988–95, aug 2014.

[193] S. K. White, D. M. Sado, M. Fontana, S. M. Banypersad, V. Maestrini, A. S. Flett, S. K. Piechnik, M. D. Robson, D. J. Hausenloy, A. M. Sheikh, P. N. Hawkins, and J. C. Moon, "T1 mapping for myocardial extracellular volume measurement by CMR: bolus only versus primed infusion technique.," *JACC. Cardiovascular imaging*, vol. 6, pp. 955–62, sep 2013.

[194] D. M. Sado, A. S. Flett, and J. C. Moon, "Novel imaging techniques for diffuse myocardial fibrosis," *Future Cardiology*, vol. 7, pp. 643–650, sep 2011.

[195] J. L. Salinet, J. H. Tuan, A. J. Sandilands, P. J. Stafford, F. S. Schlindwein, and G. André Ng, "Distinctive Patterns of Dominant Frequency Trajectory Behavior in Drug-Refractory Persistent Atrial Fibrillation: Preliminary Characterization of Spatiotemporal Instability," *Journal of Cardiovascular Electrophysiology*, vol. 25, pp. 371–379, apr 2014.

[196] S. M. Narayan, M. R. Franz, P. Clopton, E. J. Pruvot, and D. E. Krummen, "Repolarization alternans reveals vulnerability to human atrial fibrillation.," *Circulation*, vol. 123, pp. 2922–30, jun 2011.